INCIPIENT FAULT DETECTION USING HIGHER-ORDER STATISTICS

APPROVED BY
SUPERVISORY COMMITTEE:

Georgia-Ann Klutke

Michael J. Fl

Kenneth W. Ca

K. Joe Thornhill

J. W. Barnes

Samuel A. Powers

REPORT DOCUMENTATION PAGE

Form Approved
OMB No 0704-0188

1. AGENCY USE ONLY (Leave blank)	2. REPORT DATE	3. REPORT TYPE AND DATES COVERED
	August 1991	THESIS/DISSERTATION

4. TITLE AND SUBTITLE
Incipient Fault Detection Using Higher-Order Statistics

5. FUNDING NUMBERS

6. AUTHOR(S)
Richard William Barker, Major

7. PERFORMING ORGANIZATION NAME(S) AND ADDRESS(ES)
AFIT Student Attending: University of Texas

8. PERFORMING ORGANIZATION REPORT NUMBER
AFIT/CI/CIA-91-023D

9. SPONSORING / MONITORING AGENCY NAME(S) AND ADDRESS(ES)
AFIT/CI
Wright-Patterson AFB OH 45433-6583

10. SPONSORING / MONITORING AGENCY REPORT NUMBER

11. SUPPLEMENTARY NOTES

12a. DISTRIBUTION / AVAILABILITY STATEMENT
Approved for Public Release IAW 190-1
Distributed Unlimited
ERNEST A. HAYGOOD, Captain, USAF
Executive Officer

12b. DISTRIBUTION CODE

13. ABSTRACT *(Maximum 200 words)*

14. SUBJECT TERMS

15. NUMBER OF PAGES
175

16. PRICE CODE

17. SECURITY CLASSIFICATION OF REPORT	18. SECURITY CLASSIFICATION OF THIS PAGE	19. SECURITY CLASSIFICATION OF ABSTRACT	20. LIMITATION OF ABSTRACT

Dedicated to the Memory of My Dad

Havelock William Barker

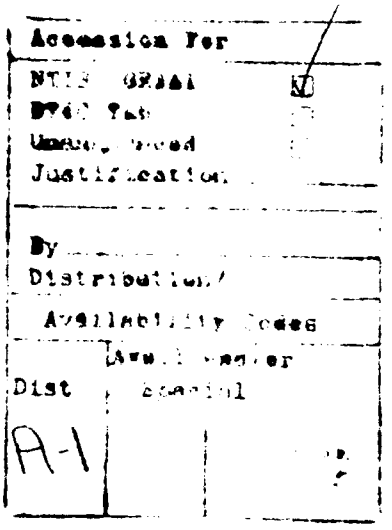

INCIPIENT FAULT DETECTION USING HIGHER-ORDER STATISTICS

by

RICHARD WILLIAM BARKER, B.S., M.B.A., M.S.

DISSERTATION

Presented to the Faculty of the Graduate School of

The University of Texas at Austin

in Partial Fulfillment

of the Requirements

for the Degree of

DOCTOR OF PHILOSOPHY

THE UNIVERSITY OF TEXAS AT AUSTIN

August 1991

Preface

Richard W. Barker
The University of Texas at Austin, 1991

Supervising Professors: Melvin J. Hinich and Georgia-Ann Klutke

This study balances the development of theory and its application to real and simulated incipient fault data from systems which have cyclostationary properties. The study's theoretical contribution reveals the advantages of approaching estimation of time series in a general framework where estimation of the cumulant spectrum can reveal implications for three classes of stochastic processes: stationary, cyclostationary, and nonstationary. The developed cumulant spectrum estimation capability provides estimates for feature construction in addition to bispectrum and power spectrum estimates of stochastic process data. Actual experimental data is obtained to study the incipient wear process of manufacturing drill bits cutting through epoxy-glass composite material used for construction of electronic semiconductor panels. The fluctuating vibrations caused by the drill bits cutting through the epoxy-glass composite are not subject to precise prediction, nor are the external noise, measurement errors, and other disturbances in the transmission of the vibration signal to three accelerometers mounted on the drilling machine considered to have the same characteristic of unpredictability. Even though there is some element of determinism in the generated signal data due to the common periodic excitation of the rotating drill spindle, the vibration signals and

noises do vary with time. The randomness which exists from sample function to sample function throughout a complete ensemble (inherent sampling variability) is a characteristic of any stochastic process. But there is also a randomness from time instant to time instant from an object sample function to the same sample function as the object wears over time. This is the other element of randomness that is of primary focus in this research. The application portion of the study consists of pattern recognition analyses of simulated and actual experimental data to determine the incipient fault discrimination and classification ability of classifiers using features with and without higher-order statistical (HOS) information. Exploitation of probabilistic and statistical concepts has led to a new incipient fault detection approach for rotating physical systems.

Acknowledgements

First, I thank my wife Judy for all her support and love. I thank Doctor's Hinich and Klutke, my co-supervising professors, for their guidance, insight, and encouragement during this conducted research. The dissertation was given a "real world flavor" with the IBM drill wear application data provided by Dr. Ramirez and Dr. Thornhill. I thank both of them for their sharing of the data and assistance in understanding the wear experiment.

INCIPIENT FAULT DETECTION USING HIGHER-ORDER STATISTICS

Publication No._____

Richard William Barker, Ph.D.
The University of Texas at Austin, 1991

Supervising Professors: Melvin J. Hinich and Georgia-Ann Klutke

A new analytical approach is developed for detecting incipient faults of rotating machinery whose periodical characteristics generate time series data representable as cyclostationary processes. The new approach is a higher-order statistical (HOS) method as nonstationary time series estimation, in addition to stationary and nonlinear estimation, provide the basis for enhanced feature information of the random fault mechanisms under study. An algorithm selects and combines different transformed estimates of the raw time series, second-order cumulant spectrum (nonstationary), power spectrum (stationary), and bispectrum (nonlinear), for investigation of incipient fault discrimination and classification power of multivariate classifiers using different extracted feature information sets. The HOS approach (cumulant spectrum, bispectrum, and power spectrum), is tested and evaluated against a traditional power spectrum approach with simulated

and actual experimental data. Robustness of the HOS approach is first investigated in simulated time series signals with amplitude and phase modulation indices and differing levels of additive Gaussian noise as parameters. Simulations show that use of HOS features improves incipient fault detection capability of a linear classifier and is less sensitive to Gaussian noise within the signal environment. Actual vibration signals from a rotating drill wear monitoring study are also analyzed. The drills are used in the manufacturing of electronic circuit cards from epoxy-glass composite. Combining HOS features with power spectrum features improved the overall classification performance of parametric and non-parametric classifiers. Additionally, the HOS approach is less sensitive to changes in drilling process parameters such as circuit card construction and chip load. The pattern recognition analyses performed in this research provide strong statistical evidence that HOS estimation and feature extraction is beneficial for discrimination and classification of incipient failures of rotating tools, a difficult mechanical system monitoring problem.

Table of Contents

List of Tables

List of Figures

Chapter 1

Introduction

1.1 Introduction

This dissertation is concerned with the problem of detecting incipient faults of rotating machinery. Because of their periodic nature, these types of physical systems are mathematically represented as *cyclostationary* processes. Rotating machine research studies have proposed various monitoring methods (Micheletti, 1976, and Jetly, 1984) but for reasons such as instrumentation difficulties in obtaining measurements at or near the cutting surface of rotating tools, implementation of most monitoring methods in industry is limited. Some of the better monitoring techniques appear within the vibration analysis literature (Braun, 1986, and Shives and Mertaugh, 1986) where vibration monitoring is shown to significantly reduce the cost of maintenance, increase reliability, and decrease the probability of catastrophic failure of rotating machinery. Milner (1988) lists *bispectrum analysis*, a particular higher-order statistical (HOS) method, as a possible approach for monitoring vibration of small rotating machines in a NASA spacecraft. However, he did not investigate bispectrum analysis due to the lack of adequate computational methods. HOS methods are defined in this study as statistical approaches which analyze stochastic processes and their generated time series data associated with *nonlinear* and also *nonstationary* phenomena. The bispectrum provides a first glimpse at nonlinear effects as it is the Fourier transform of the third-order moment

function of a stochastic process while the power spectrum, the Fourier transform of the second-order moment, is most useful in problems estimating linear processes. Recent findings (Dan and Mathew, 1990) conclude that no single condition monitoring method appears suitable for all machine operations and material combinations. Consequently, condition monitoring research is better directed towards improving instrumentation effectiveness, collecting better data on the functional relationship between wear and measured parameters, and developing *sensor fusion* methods which *combine* data from different sensors and features to improve system monitoring accuracy.

There are many examples of models using a combination of sensors and signal features for monitoring rotating tool wear. A vector autoregressive moving average model developed by Yao (1990) used three axis tool force measurements to estimate tool wear in turning of steel. Spindle vibration, cutting torque, and force in monitoring of milling were input to power spectrum analyses to extract peak values which were then input to a linear classifier (Elbestawi, 1989). A linear classifier was also used for detecting crankshaft drill wear (Liu and Wiu, 1990) using thrust force and axial acceleration amplitude signals. Acoustic emission spectrum features and cutting force signals input to a neural network classifier demonstrated the applicability of neural networks for noise suppression and also that there are an optimal number of features (Rangwala and Dornfeld, 1990) for classification purposes. Time and frequency domain characteristics of drilling forces for carbon steel (Braun and Lenz, 1986) used a feature based on probability distribution moments of intensities and times of occurrences of a single oscillating signal pattern. Braun and Lenz (1986) also stated that the choice of appropriate features, whether single or combined, need to be based on test results or experimental databases.

These studies are a few examples of recent sensor fusion techniques in milling, drilling of metals, and turning operations. Significantly with regard to this research, feature construction of sensor signals in these recent studies is limited to the *power spectrum* rather than any *higher-order* forms of spectra.

However, one study using bispectrum analysis as a HOS technique to diagnose abnormal states of a machine from the normal one was conducted on gear noise signal data (Sato et al., 1977). Its results showed that the gear noise signals were almost periodical under proper loading and normal operating conditions. But when *heavy* load conditions scored the gear surfaces, the periodic signal characteristics were reduced and the signals appeared more random. This change in randomness caused the modulus of the bicoherence function, defined as the normalized bispectrum with respect to power spectra, to decrease significantly. The more exact diagnosis which considered the *nonstationary* properties of the noises was left as future work, and an experimental design strategy with an associated statistical classification approach also was *not* evident in this first HOS monitoring approach. This first HOS approach also investigated *severe* faults rather than *incipient* faults. Incipient faults are those failures which are just beginning to appear in the mechanical system.

To overcome the deficiencies of this first HOS monitoring study this research developed time series estimation procedures based on a *nonstationary* or *cumulant spectrum* representation of the stochastic process under study. An experimental design strategy and statistical pattern recognition framework was implemented to allow strong inferences from the data analyses. Furthermore, the developed HOS approach is evaluated for its ability to detect *incipient*, rather than *severe*, faults. Thus, the types of monitoring problems addressed in this research

are more difficult than those previously studied. The developed HOS approach combines different forms of spectrum measurements (power, second-order cumulant, and bispectrum) from sensors in a statistical classification scheme not only to *improve* a monitoring system's classification performance, but also to *reduce* its sensitivity to variables other than machine condition. These variables include, but are not limited to, process environment parameters such as workpiece material construction, cutting conditions, and noise. The developed HOS approach is a new type of sensor fusion technique which Dan and Mathew (1990) state as one of the most important open areas in condition monitoring research.

1.2 Problem Statement and Scope

The goal of this study was development of a new analytical approach for detecting *incipient* faults in physical systems which have a periodic driving force mechanism generating potential signature data. The approach is the first to incorporate *nonstationary* (second-order cumulant spectrum) in addition to *nonlinear* (bispectrum) and *linear* (power spectrum) characteristics of *signature* time series for use as feature sets to improve the discriminatory power of a multivariate classifier. Signature denotes signal patterns which characterize a specific system state.

Investigation of *bispectrum* analysis as a fault detection approach is motivated by the fact that fault processes of rotating mechanical structures are known to generate highly nonlinear time series data through the generation of sum and difference frequencies (Braun, 1986). Nonlinearity is a result of intermodulation between the frequency components of the driving process and produces spectra with *sideband* structure. Without phase information, the presence of nonlinearities is not

detectable. The bispectrum captures this relative phase information among frequency components. Investigation of *cumulant spectrum* analysis is motivated by the fact that the signal data generated by faults in physical systems under study is not only nonlinear, but also *nonstationary* due to the modulation effects of the random fault mechanisms.

A good condition monitoring approach is insensitive to parameter changes, noise disturbances, and nonlinearities which are intrinsic to the random processes under study. So evaluation of the developed HOS approach includes *marginal* and *sensitivity* studies of both *simulated* and *actual* experimental databases. Marginal analyses determined the incremental value of HOS features to power spectrum features for discrimination and classification tasks. Sensitivity analyses determined the impact of different classification algorithms, stochastic process parameters, and noise on classification performance of classifiers utilizing spectral feature sets *with*, and *without*, HOS information.

Simulation experiments of modulated signals explored potential robustness properties of the new HOS approach. Single tone amplitude and phase modulation indices of a cosine-wave carrier signal (representing the periodic driving force of a rotating machine system) and standard deviation of Gaussian noise are the simulation parameters. Incipient faults such as initial wear of rotating machinery can appear as amplitude and phase modulation changes. More emphasis is directed to changes in phase modulation as amplitude modulation changes are assumed related more directly to deviations in the process environment such as differences in workpiece properties and cutting parameters rather than *slight* changes in process state. Single tone modulation and the values chosen for the modulation index parameters should not limit the applicability of the simulation study results. In-

creasing the complexity of the signal modulation simulations would generate additional frequency interactions and modulations and consequently provide more frequency support in each of the higher-order spectral principal domain regions. Hence, the possibility of strengthening, rather than weakening, the value of the HOS approach is afforded by increasing the complexity of the modulation simulation experiments. Analyses of simulated data provide a first step in developing estimates of *actual* classification error rates and also allow an evaluation of the impact of Gaussian noise on classification using feature sets with and without HOS information.

Since not much condition monitoring research addresses high-speed circuit card drilling of epoxy-glass composite, IBM (Austin) conducted an experimental drill wear study. Ramirez (1991) discusses the IBM circuit card manufacturing process and drilling mechanics which generated the experimental drill wear data. An indirect online wear monitoring approach using drill spindle acceleration, displacement, and speed responses was investigated. A major conclusion of the Ramirez (1991) study was particular vibration power spectrum harmonics from the thrust axis accelerometer were the most useful responses for drill wear monitoring. Also, since circuit card material composition plays a key role in generating vibration, variations in card construction can mask the effects of wear of vibration power spectra. The developed HOS approach is investigated for its potential use in the industrial environment by analyzing IBM experimental drill wear data of three factors: drill bit age, circuit card stack material, and chip load cutting condition. Accelerometer data obtained were from three axial positions (X,Y, and Z) gathered on two types of bits defined by their number of circuit card holes drilled (0 and 8000), two types of stack materials (NIP and 6S2P), and two types of chip

load (3 and 4 mil/rev). Chip load is the amount of axial distance travelled by the drill bit tip in a single revolution or rotation. Actual wear data analyses will demonstrate the marginal contribution of HOS features to power spectrum features for detecting incipient faults of manufacturing drill bits. Actual wear data analyses will also add supportive evidence for further investigation and possible implementation of the new HOS approach in an industrial environment.

Both simulated and actual time series data represent incipient failure conditions rather than new and definitely worn conditions of a rotating machine process. Intuitively, it should be harder to detect *slight* or moderate wear than *advanced* wear of rotating machinery. This is logical as signals used to characterize advanced wear are usually more pronounced than those signals characterizing slight wear. Wear condition of drill bits from the IBM experimental study were optically checked under a microscope to accurately classify wear states. Because time series waveforms are already grouped for their "similarity", cluster analyses are not needed. Simulated and actual experimental data analyzed in this study are highly non-Gaussian and nonlinear based on the Hinich (1982) bispectrum statistical tests. Hence, feature extraction rather than an optimality approach (Shumway, 1982) is the technique used for time series discrimination and classification.

Both background noise and signal propagation media interfere with signature signals. Although there is some determinism due to the rotating machine's periodic driving force mechanism, each of the signal types (noise, propagation, and signature) is characterized by an element of unpredictability. Hence, an ensemble of signals for different states of cyclostationary processes are analyzed to ensure an effective study of alternative classification approaches. Probability of false alarm and probability of detection are the main performance measures. These measures

are averaged over the signal ensembles to decrease the variability of these performance estimates.

1.3 General Research Approach and Presentation

This research focused on the development of two new methodologies: cumulant spectrum estimation (second-order) and HOS feature extraction. In Chapters 3 and 4, the new methodological developments are discussed which build upon the background material given in Chapter 2. The HOS approach developed in this work is tested with both simulated and actual physical phenomena to investigate and quantify the benefits of HOS estimation and feature extraction for incipient fault detection. New estimation code to perform second-order and third-order cumulant estimation of time series is developed. So besides the bispectrum, the second-order cumulant spectrum is investigated and employed in discrimination and classification tasks. Presentation of results to just the second-order cumulant spectrum is due to time constraints and some technical problems. Because a large number of measurements result from the spectral transformations of the raw time series, a HOS feature extraction algorithm is developed to combine the most useful spectral measurements for incipient fault identification. Appropriate measures of effectiveness to evaluate the relative merit of spectral feature sets, with and without HOS information, are devised for both simulated and actual experimental studies. These measures of effectiveness are in the results section of Chapter 5 after each experiment description.

Chapter 2

Background

2.1 Introduction

Detailed information on the major methodologies investigated to develop a new analytical approach to the research problem is given in this chapter. First is a description of existing incipient fault detection techniques for rotating machinery using *vibration* signals. Second is an examination of the statistical theory and models which permit interpretation of multivariate or group differences. Some special considerations for use of multivariate approaches for *time series* discrimination and classification are discussed. Third, different types of stochastic processes and the mathematical functions used to describe them are defined. Existing theory related to *higher-order* statistics (HOS) concludes the chapter.

2.2 Existing Incipient Fault Detection Techniques

Although many types of signals are used for diagnostic monitoring of rotating machinery, there are more examples of the demonstrated use and success of *vibration* monitoring for significantly reducing the cost of maintenance, increasing reliability, and decreasing the probability of catastrophic failure of rotating machinery (Braun, 1986, and Shives and Mertaugh, 1986). One success is TRACOR Applied Science's (Austin) vibration monitoring program for the United States

Navy to improve the reliability and maintainability of the rotating machines on their TRIDENT submarines and surface ships (Milner, 1990). They use signature analysis of the accelerometer outputs, a common vibration monitoring technique. Other incipient fault detection techniques using vibration signal monitoring include demodulation of high frequency acceleration signals, statistical analysis of acceleration amplitude, process modelling or parametric approaches such as autoregressive moving average (ARMA) time series models, phase-locked processing, cepstrum analysis, transient analysis, Hilbert transforms, and general pattern recognition. These major techniques are summarized for a general understanding of their strengths and weaknesses. Braun (1986) and Shives and Mertaugh (1986) have complete discussions of these methods including schemes that combine some of them.

Signature analysis of acceleration outputs is used in many commercial applications in addition to TRACOR's use for the Navy. Specific topics of analysis bands, resolution, accelerometer type and its placement, instrumentation, and presentation of accelerometer output are peculiar to the particular application. However, a common thread among all applications is the reliance on association of a particular failure mode with *features* of the vibration power spectrum. Tones and other power spectral features present in rotating machinery vibration are generally due to predictable causes. There are many published relationships of faults versus power spectral features for many different types of machines and their components. Braun (1986) contains the theory and applications of many different methods within the field known as *mechanical signature analysis*. Signature analysis is a very common technique as it has general applicability and proven success for a large variety of machine types. Also, the computation of the spectral amplitude

at selected frequencies and the association of amplitude increases with specific faults is a necessary first step of several other techniques (general pattern recognition, trend analysis and process modelling at key frequencies, transient and cepstrum analysis).

High frequency demodulation of acceleration signals extracts relatively low frequency information from a high frequency signal that has been amplitude modulated by a mechanical defect. It is mostly applied for bearing fault detection. At the very early stages of a bearing fault, impulses due to the rolling element passing over the fault will be very short in duration and can extend as high as 300 kHz (Bell et al., 1985). The impulses excite resonant modes of the machine and the envelope of the resulting time signal is the amplitude modulated component of the defect signal. The envelope signal will contain discrete peaks with periodicities determined by the input rate of the defect. After effectively bandpassing the signal, power spectral analysis of the envelope will produce a harmonic series with a fundamental frequency that is related to the bearing frequencies. Other general areas of application of this technique include fault detection of gears and fluid film bearings, and seal rub analysis (Darlow et al., 1975 and Drago, 1979). Because of the high frequency range used with this technique, there is a high defect signal-to-noise ratio which is often stated as an advantage. However, an associated disadvantage is the requirement that the particular frequency within the high range must be predetermined before filtering and demodulation is performed.

Weighted likelihood ratio processing and kurtosis are two statistical techniques used to process amplitude signals. Weighted likelihood ratio processing is described later in this chapter so only kurtosis processing is described here. A "universal" behavior noticed in wear-induced failures is that localized defects ap-

pear first and distributed types of defects follow. Hence, induced vibrations often have an impulsive character with the appearance of a localized defect, changing to a more continuous function over time. The sharp peaks at the onset of defects affect the tails of a probability density function (pdf), and moments of the distribution such as kurtosis can enhance the sensitivity to changes occurring at the pdf tail. Kurtosis is the normalized fourth moment of a probability density function and emphasizes the peakness of a particular signal pattern. Normalization is accomplished by removing the mean from the data and dividing by the fourth power of the standard deviation. Kurtosis as a statistic is considered as an indication of Gaussian versus non-Gaussian densities as it is equal to *three* for all Gaussian densities. One example of the practical use of kurtosis is in the area of rolling element bearing fault condition (Dyer and Stewart, 1978). The kurtosis value for good bearings followed the Gaussian distribution value of three while significantly degraded bearings had large variations in the normalized acceleration distribution. These large variations led to kurtosis values significantly different from three. The authors stated more tests including simulation results for performance evaluation are needed before conclusive remarks can be made on kurtosis as a fault indicator.

Process models are methods of detecting changes in expected waveform structure. This technique generally involves mathematically modelling the system outputs to determine if abnormalities exist in the signatures by statistically comparing them to normal model output. The extraction of features from the parametric spectrum can mimic the methods applied to non-parametric spectra. Another feature extraction approach is directly using system identified parameters that describe the data (ie. AR, MA, ARMA). Classification of automobile engine faults in a production assembly-line using a nearest neighbor classifier was based

on this latter type of feature extraction approach (Gersch, 1986). The Kullback-Leibler measure of dissimilarity was employed which assumes the time series are Gaussian-distributed (Kullback, 1959).

An approach related to Kalman filtering methods is based on analysis of residuals after fitting of the parametric model to data. Variations in residual magnitude, or statistical distributions different from normal meaning the fitted model is no longer appropriate, can indicate a change in signal patterns. Specifically, an approach called the Dynamic Data System (DDS) uses operational data from a mechanical system and applies ARMA mathematical models to extract features from the data with a high degree of sensitivity. The DDS model is combined with statistical quality control chart concepts to monitor for abnormalities with a very limited amount of data (Wu, 1977).

Phase-locked processing describes a general class of special processing techniques that efficiently extract and filter periodic signals. Use of phase-locking gives equivalent results in both time and frequency domains. This technique uses encoders to give an integer number of pulses per revolution (Braun and Seth, 1979). The number of pulses from the encoder should be equal to two to the power of the number of pulses per revolution as the discrete Fourier transform (DFT) is usually computed with a Radix 2 fast Fourier transform. The rotationally locked components are located at multiple points in the DFT indexed by $p = N/M$ where N is the number of pulses analyzed per revolution and M is the number of points in one period. By employing a filter whose response is set to zero for all $p \neq N/M$ the extraction of the periodic signal from additional non-coherent interferences is achieved. If additional signals non-coherent with the rotational frequency of the

machine exist, windowing is employed to minimize errors in the signal extraction process due to possible leakage problems.

Cepstrum analysis is used in echo detection and deconvolution problems. Braun (1986) has a detailed discussion of the use and problems in the computation of cepstra. A common signal processing problem is the analysis of signals which are composed of a wavelet and one or more echoes which may overlap. A simple form of this composite signal is $x(t) = s(t) + a_0 s(t - t_0)$. Distortional effects such as noise, overlapping of echoes and the wavelet, and different transmission paths obscure the echo arrival time and basic wavelet shape. The signal plus echo may be modelled as the convolution of $s(t)$ with a time function $\delta(t) + a_0\delta(t - t_0)$ and the separation of these two convolved signals is performed with operations in the power cepstrum analysis. For example, if $x(t) = s(t) \times h(t)$, then $\ln |X(\omega)|^2 = \ln |S(\omega)|^2 + \ln |H(\omega)|^2$. There is also *complex* cepstrum analysis which is more general than the power cepstrum as inverse operations can recover the original time signal. Both the power and complex cepstrum methods are impacted by smoothness and bandwidth of the wavelet. Additive noise is another major degrading influence in the effectiveness of cepstral methods. A wide bandwidth and smooth wavelet spectrum is necessary for a less erratic wavelet cepstrum which subsequently helps distinguish echo spikes from the wavelet cepstrum. A majority of rotating machinery applications using cepstrum analysis are on gear faults (Randall, 1982). Generally, it has been determined that gears in good condition normally contain frequency sidebands of nearly constant amplitude over time in the power spectrum. Changes in the number and amplitude of the sidebands are proposed as indicative of a deterioration of a gear's condition and the cepstrum is able to detect this change with an increase in amplitude of a single line. Thus, an

advantage of using a cepstrum approach is not being confounded by several sets of periodicities in the power spectrum causing difficulty with a visual interpretation of the data. However, Braun (1986) states this method is an interesting approach to analysis of convolved signals, but it must be treated with caution and care for the interpretation of its application to machinery diagnostic problems.

Because of their origins, transient signals usually have different durations, peak amplitudes, repetition rates, frequencies, and bandwidths. Transient signal detection schemes exploit varying degrees of *a priori* waveform structural information. Most transient processors perform two primary functions: event capture and transient analysis (Owsley and Quazi, 1970). Event capture involves continuous loop data recording with a trigger signal that causes transfer to permanent data storage. The trigger signal is driven by a simple detector of energy increases. Transient analysis depends on the application and so varies significantly. Fourier analysis is used to select key features such as the center frequency of a narrowband transient and its bandwidth to classify the transient. Other extracted features include pulse duration and repetition rate (Nolte, 1968).

Hilbert transforms are another way to easily extract envelope information from a modulated time signal. The Hilbert transform differs from the Fourier transform because it leaves the signal in its original domain. It shifts the value of a time signal by 1/4 wavelength or a 90° phase shift in frequency domain. Bell et al. (1985) use the Hilbert transform for incipient fault detection of rolling element bearings.

Many examples of machinery monitoring systems in the literature can be categorized as a general pattern recognition approach. One excellent commercial example is the statistically based system developed at Oak Ridge National Labora-

tory for continuous, on-line, unattended surveillance of dynamic reactor signals (Smith, 1983). Their monitoring system is based on identification of changes in the power spectrum of measured variables where change is detected by using discriminant functions formulated to emphasize relevant features. Discriminants were constructed to detect the following: (1) a fluctuation in the integral power of the spectrum; (2) spectral shape changes; (3) deviations in the magnitude of individual spectral estimates at a given frequency; and (4) shifts in the frequency of spectral peaks. Their system, typical of most pattern recognition systems, used classification functions based on Bayesian estimation decision theory preceded by a *heuristic feature extraction process* to transform the raw time series data. Whatever features are used, the determination of thresholds is usually determined by experience where monitoring systems are fine-tuned as more information on the process is obtained. Features are used for classification purposes and their statistical properties affect monitoring performance. However, few references or studies describe monitoring systems based on formal statistical aspects because of the difficulty of acquiring information and databases from sufficiently large sample populations (Paul, 1977). Statistical pattern recognition is the general framework of this research and simulation and *actual* time series databases are from sufficiently large sample populations. The statistical approach employed in this research is unique for constructed features are not restricted to power spectrum estimates, but also include estimates of two higher-order spectrum forms.

2.3 Measuring Differences Among Multivariate Populations

Since the developed monitoring approach is described and evaluated from

formal statistical aspects, this background section first discusses the types of analysis questions that arise when confronted with the problem of measuring differences among multivariate populations. Decision theory definitions introduce the theoretical basis underlying discrimination and classification tasks. Estimation of class-conditional probability density functions (pdfs) or discriminant functions under various levels of assumption are discussed and compared. Performance assessment issues of the developed feature extraction sets input to multivariate classifiers using *design* and *test* sets are discussed. Mathematical details that address the partitioning of the *total sample variance*, a fundamental step in the development of techniques which separate multivariate populations and statistical considerations in measuring population differences, conclude the background section.

Several analysis questions are postulated when investigating multivariate group differences. *First*, are the groups significantly different with respect to their multivariate descriptions? This is a multivariate equivalent to the sample (univariate) t-test on population means. A sample mean vector, or *centroid*, for each population is formed, and the null hypothesis of equal population centroids is tested using Hotelling's T^2 statistic, or equivalently, Wilks' Λ statistic when considering only *two* groups. If more than two groups or populations are involved, multivariate analysis of variance looks for differences among population centroids. *Second*, what role do the measurement variables play in separating the groups? A discriminant function which can be a linear, quadratic or some other transformation of the measured variables answers this question. Its evaluation objective is to yield similar values for cases from the same population and different values for cases from different populations. Examining the discriminant function provides insight on which measurement or feature variables are most important in separating the

groups. The population separation problem using only information about one of the variables at a time usually is not very efficient and is suboptimal. For example, two individual variables may not be good discriminators by themselves, but when combined they may be highly effective. Developing a discriminant function corresponds to the search for a vantage point which provides a view with maximum group or population separation. This underlies the motivation for performing HOS estimation and feature extraction in addition to traditional power spectrum methods. It is conjectured that higher-order forms of spectra combined with power spectra will provide a better vantage point. Moreover, HOS features will just simply be better discriminators than power spectrum features. Discriminant functions can be constructed using stepwise selection of variables similar to stepwise selection of variables used in multiple regression. When there are more than two groups, multiple discriminant functions can be developed (beyond this study's scope). *Third*, if responses or measurements of the variables are known for a new observation, to which group does the case belong? This is the multivariate *classification problem* while the first two questions concerned multivariate *discrimination*. In many applications of discriminant analysis, classification is the major objective. For example, if there is a description of new drill bits and slightly used drill bits in terms of spectral features calculated at times of different wear states, these spectral features can then be used in classification rules which would specify whether another drill bit is a member of one of the wear categories. Thus, classification rules are developed from the discriminant functions.

Consider definitions from decision theory to explain the basis underlying discrimination and classification. A decision rule partitions a space into regions Ω_i, $i = 1, \ldots, N$ where N is the number of classes. An object, or time series, is

classified as coming from class ω_k if its corresponding vector representation, $\mathbf{x}$ lies in region Ω_k. The vector representation $\mathbf{x}$ can either represent direct time series measurements or features, $\phi(\mathbf{x}_i)$, which are functions of the $\mathbf{x}_i$. The boundaries between regions are called decision surfaces. Assume that *prior* probabilities, $P(\omega_i)$ are known that an object comes from class ω_i $(i = 1, \ldots, N)$. Information in the form of a vector, $\mathbf{x}$, is then determined for an object to be classified. The Bayes minimum error rule is formed by comparing the *posterior* probabilities of belonging to each class using the information vector and classify according to whichever is larger:

$$P(\omega_k \mid \mathbf{x}) > P(\omega_j \mid \mathbf{x}) \text{ for all } j \neq k \rightarrow \mathbf{x} \in \Omega_k.$$

Since the posterior probabilities are rarely known, they need to be estimated from samples of known classification. Another formulation of the Bayes minimum error rule is obtained through application of Bayes Theorem to determine the class membership probabilities:

$$P(\omega_i \mid \mathbf{x}) = \frac{p(\mathbf{x} \mid \omega_i) P(\omega_i)}{p(\mathbf{x})}$$

which results with

$$p(\mathbf{x} \mid \omega_k)\, P(\omega_k) > p(\mathbf{x} \mid \omega_j)\, P(\omega_j), \text{ for all } j \neq k \rightarrow \mathbf{x} \in \Omega_k. \qquad [1]$$

If $p(\mathbf{x} \mid \omega_i)$, the class-conditional pdfs are known, the problem is solved by substitution of $\mathbf{x}$ into [1] for the time series being classified and finding the largest value of $p(\mathbf{x} \mid \omega_i)\, P(\omega_i)$. But similar to $P(\omega_i \mid \mathbf{x})$, the $p(\mathbf{x} \mid \omega_i)$ are probably unknown and require estimation from a set of classified samples.

Bayes minimum error rule for the two case situation is:

$$\frac{p(\mathbf{x} \mid \omega_1)}{p(\mathbf{x} \mid \omega_2)} \gtrless \frac{P(\omega_2)}{P(\omega_1)} \rightarrow \mathbf{x} \in \begin{Bmatrix} \Omega_1 \\ \Omega_2 \end{Bmatrix}.$$

This rule minimizes the overall error assuming *equal* misclassification costs but for industrial manufacturing situations where misclassifying a worn tool may be more serious than misclassifying a new tool, a different criterion which considers the different misclassification costs (Bayes minimum risk) may be more appropriate. Additionally, if the *prior* probabilities of a new time series are unknown, a minimax rule designed to minimize the maximum possible risk is used. Hand (1981) develops all three rules expressed as functions of $\mathbf{x}$ using the class-conditional pdfs $p(\mathbf{x} \mid \omega_i)$. Considering the absolute values of the probabilities not as relevant as their relative magnitudes allows more general rules. For the two-class situation the general rule is:

$$h(\mathbf{x}) \gtrless \text{constant} \rightarrow \mathbf{x} \in \begin{Bmatrix} \Omega_1 \\ \Omega_2 \end{Bmatrix}$$

where h is called a *discriminant* function. As before, the discriminant function will require estimation from classified samples. Estimation procedures are categorized by the level of assumptions used for the likelihood function: *parametric* and *non-parametric*. Non-parametric approaches estimate the class-conditional pdfs or the discriminant functions without any knowledge about their parametric form. In parametric approaches, assumptions are made about the form of the class-conditional pdfs or discriminant functions and estimation of the unknown functional parameters are performed with the classified samples. Parametric and

non-parametric estimation methods applied in this research study are discussed next.

2.3.1 Estimation Methods

If the class-conditional pdfs or discriminant functions forms are known, then the tasks of discrimination and classification are simplified as likelihood function ratios with various risk thresholds are compared for its solution. Unfortunately, this knowledge rarely exists but the general parametric form may be known from some theoretical knowledge or from a study of the sampling distributions. In this situation, samples are used to give estimates of parameters of the class-conditional pdfs or more generally, sample distributions are used to estimate the parameters of the discriminant functions. However, when simplifying assumptions are not defendable, non-parametric methods are also applied. Lachenbruch (1975) and Hand (1981) outline and compare various parametric and non-parametric pdf estimation methods. After preliminary experimentation and application of several of these estimation methods, three were chosen for their consistent classification performance of the experimental data described in Chapter 5. The k-nearest-neighbor (k-NN) method was the non-parametric method applied to actual time series data. Two parametric approaches, linear and quadratic discriminant functions, were also applied to the actual data. Linear discriminant functions were constructed for the simulated experiments.

Assuming a multivariate normal distribution for the spectral features of each time series class resulted in discriminant rules based on the pooled covariance matrix (yielding a linear function) or the individual within-group covariance matri-

ces (yielding a quadratic function). Feature measurements are placed in the class from which it has the smallest generalized squared distance or the largest posterior probability.

The squared distance from feature vector $\mathbf{x}$ to class ω is

$$d_{\omega}^{2}(\mathbf{x}) = (\mathbf{x} - \bar{\mathbf{x}}_{\omega})' \mathbf{V}_{\omega}^{-1} (\mathbf{x} - \bar{\mathbf{x}}_{\omega})$$

with $\mathbf{V}_{\omega}$ being the pooled or within-class covariance matrix and $\bar{\mathbf{x}}_{\omega}$ being the feature variable means in class ω. The class specific density at $\mathbf{x}$ from class ω is:

$$f_{\omega}(\mathbf{x}) = (2\pi)^{-p/2} | V_{\omega} |^{-1/2} \exp(-.5 d_{\omega}{}^{2}(\mathbf{x}))$$

and posterior probability of x belonging to class ω is computed by applying Bayes Theorem:

$$p(\omega \mid \mathbf{x}) = \frac{P_{\omega} f_{\omega}(\mathbf{x})}{\sum_{\Omega} P_{\Omega} f_{\Omega}(\mathbf{x})}$$

where the summation is over all the classes.

Now, the generalized square distance from x to class ω is

$$D_{\omega}{}^{2}(\mathbf{x}) = d_{\omega}{}^{2}(\mathbf{x}) + g_{1}(\omega) + g_{2}(\omega)$$

with $g_{1}(\omega) = \log_{e} | V_{\omega} |$ if within-class covariances are used (quadratic function), $g_{1}(\omega) = 0$ if pooled covariance matrix is used (linear function), $g_{2}(\omega) = -2 \log_{e}(q_{\omega})$ if prior probabilities are unequal, and $g_{2}(\omega) = 0$ if prior probabilities are equal. The posterior probability of x belonging to class ω is then

$$p(\omega \mid x) = \frac{\exp(-.5D_{\omega}^{2}(\mathbf{x}))}{\sum_{\Omega}\exp(-.5D_{\Omega}^{2}(\mathbf{x}))}.$$

Thus, an observation, or feature variable set, is classified into class Ω if setting ω equal to Ω produces the *largest* posterior probability or *smallest* value of $D_{\omega}^{2}(\mathbf{x})$. The difference between the generalized squared distances of the class means is the squared Mahalanobis distance measure.

Non-parametric estimates of class-specific probability densities of feature sets are computed with a k-nearest neighbor approach. Squared Mahalanobis distance calculated from the pooled covariance matrices is used to determine proximity. The k-nearest neighbor does not have a complicated approach to its selection of the smoothing parameter, k, as it is based on which gives the best classification performance. Following Hand (1981), consider the probability that a point will fall in a local neighborhood L of $\mathbf{x}$ for the multivariate pdf $p(\mathbf{x} \mid \omega_m)$ as

$$\theta = \int_{L} p(\mathbf{y} \mid \omega_m)\, d\mathbf{y}.$$

The following approximation is made if L is small and has volume V:

$$\theta \simeq p(\mathbf{x} \mid \omega_m) \cdot V$$

which yields

$$p(\mathbf{x} \mid \omega_m) \simeq \theta / V.$$

A pdf estimator for θ is then computed by the proportion of the n_m sample points falling in the local neighborhood L. Assign k to denote the number of sample points falling in and obtain $\hat{\theta} = k/n_m$ which then leads to the estimator defined as:

$$\hat{p}(\mathbf{x} \mid \omega_m) = \frac{k}{n_m V}.$$

The volume V is made dependent on the data by fixing k and determining V needed to enclose the k nearest points to **x**. Next, combine all the classes' sample points into one set of n points such that $\sum_m n_m = n$. The hypersphere of volume V which just encloses k points from this combined set is found. Now consider that among the k points, k_m occur from class ω_m. Thus, a k-NN estimator for class ω_m is defined:

$$\hat{p}(\mathbf{x} \mid \omega_m) = \frac{k_m}{n_m V}.$$

There are also the estimators $\hat{P}(\omega_m) = \frac{n_m}{n}$ and $\hat{p}(\mathbf{x}) = \frac{k}{nV}$. Application of Bayes Theorem gives:

$$\hat{P}(\omega_m \mid \mathbf{x}) = \frac{\hat{p}(\mathbf{x} \mid \omega_m)\hat{P}(\omega_m)}{\hat{p}(\mathbf{x})} = \frac{\left\{ \frac{k_m}{n_m V} \cdot \frac{n_m}{n} \right\}}{\frac{k}{nV}} = \frac{k_m}{k}.$$

So, the following classification rule is generated: classify **x** as belonging to class i if $k_i = \max_m(k_m)$.

2.3.1.1 Advantages and Disadvantages of Applied Estimation Methods

A disadvantage of k-nearest neighbor is distances from the feature vector to all of the sample points must be determined. Hence, all of the sample points must be retained and this can increase the amount of computer time for classification. However, there are branch and bound techniques to reduce the amount of data required so quicker computation is possible (Hand, 1981). It also has the theoretical disadvantage of not being a pdf (Hand, 1981). Assuming parametric forms for the class-conditional pdfs allows *quicker* classifications of new samples and no large databases of training set points are necessary to retain. However, an incorrect distributional assumption will incur an associated cost in terms of an increased misclassification error rate, but this cost may be acceptable if computational advantages outweigh it.

2.3.2 Other Estimation Approaches Considered

Several other estimation approaches investigated during the study were weighted likelihood ratio and logistic discrimination. These methods were not used to generate final study results for their results were not as good as the others. However, weighted likelihood ratio processing is described here as it was applied to data proposed as a future application for the developed HOS approach. Logistic discrimination is described because of its similarity to the linear discriminant approach.

Milner (1988) found that a likelihood ratio weighting technique of vibration power spectra to be superior in detection performance for a wide range of problems

in pump and fan data. This approach assumes a Gaussian density function of the logarithmic amplitude of the power spectrum. The binary test hypotheses, (a) power spectrum indicates new object (K_1), or (b) power spectrum indicates slightly used object (K_0), alter this Gaussian density in mean level only, and the power estimates of each bin or frequency are assumed independent. Given the definition of the natural logarithm of the likelihood ratio derived from the Bayes criterion for binary hypotheses, the log likelihood ratio is:

$$ln(S_i) = \frac{1}{2}\left[\sum_{i=1}^{M}\left(\frac{(-S_i - m_{0i})^2}{\sigma_i^2}\right) - \sum_{i=1}^{M}\left(\frac{(-S_i - m_{1i})^2}{\sigma_i^2}\right)\right] \quad [2]$$

where S_i is amplitude of the object vibration power spectrum in decibels (dB) at frequency i, m_{1i} is average log amplitude of frequency i of new object vibration power spectrum, m_{0i} is average log amplitude of frequency i of slightly used object vibration power spectrum, and M is the number of useful frequency tones. Completing the square and canceling common terms [2] becomes:

$$\ln(S_i) = \sum_{i=1}^{M}\frac{S_i(M_{1i} - M_{0i})}{\sigma_i^2}. \quad [3]$$

If [3] is greater than zero, the object is classified as slightly used. If [3] is less than or equal to zero, then the object is classified as new. Implementation of this test

first computes power spectra for the set of new objects and for the set of slightly used objects. Then values for m_{1i} and m_{0i} are computed, and the bins with the largest mean shift as compared to their stability receive the largest weights. These weights are consequently indicators of the relative importance of specific frequencies as indicators of object wear. A weighted sum over all useful frequency information for the particular time series is computed to detect the worn condition.

Weaknesses of this approach outweighed any advantage of incorporating global spectral characteristics. The weaknesses are assuming the class distributions are different in mean level only, and that power estimates at each frequency are independent so a diagonal covariance matrix can be used. These assumptions were not appropriate for the actual experimental data analyzed in this study.

Logistic discrimination is a partial distribution classification method as it assumes the log-likelihood ratio is linear in the measured parameter vectors:

$$\ln \left\{ \frac{L(\mathbf{x} \mid K_1)}{L(\mathbf{x} \mid K_2)} \right\} = \beta_0' + \beta' \mathbf{x}, \qquad [4]$$

where $\beta' = (\beta_1, \ldots, \beta_p)$. Anderson and Richardson (1979) show three advantages for using logistic discrimination versus a fully distributional or distribution-free classification approach. First, the model given at [4] gives a simple form for the posterior probabilities:

$$(k \mid \mathbf{x}) = \exp \frac{\beta_0' + \ln C + \beta' \mathbf{x}}{(1 + \exp(\beta_0' + \ln C + \beta' \mathbf{x}))},$$

where $C = \Pi_1/\Pi_2$, and Π_s is the proportion of sample from K_s with (s = 1,2). Second, once the parameters (β_0', β and C) are estimated, the allocation of a new observation or feature vector set requires only a linear function calculation:

$$\beta_0' + C + \beta'\mathbf{x}.$$

Third, this same estimation procedure is applicable with either continuous or discrete predictor variables.

2.3.3 Mathematical Development of Analysis of Variance

A fundamental step in the development of statistical techniques based on separation of multivariate populations is the partitioning of the total sample variance into components representing *within* class variation (variance of individual observations about their class's centroid), and *among* class variation (variance of individual observations around the centroid for the combined sample). This partitioning process is the multivariate equivalent of the partitioning sum-of-squares accomplished in the univariate analysis of variance (ANOVA) model. In univariate problems, hypotheses concerning equality of means can be tested using the two sample t-test when two groups are involved, or F-tests using statistics derived from one-way ANOVA when multiple groups are considered. In multivariate analysis, equality of mean vectors or centroids across groups or populations are tested. For the two population case, Hotelling's T^2 provides the multivariate equivalent to the two sample t-test and test statistics derived from one-way multivariate analysis of variance (MANOVA) provide the appropriate hypothesis tests for the multiple population situation. When there are only two groups or classes as in this research

study, the one-way MANOVA is equivalent to the two-sample Hotelling's T^2 test and this is the presented approach.

2.3.3.1 Partitioning of Variance

Consider developed expressions representing the partitioning of an arbitrary *linear* combination of measurement variables into *within* and *among* class components. Notation is defined:

x_{ijk} $i = 1,2, \ldots, n_k$; $j = 1, 2, \ldots, g$ represents the observed value on the j^{th} variable from the i^{th} case in the k^{th} class. There are g groups or classes and p measured variables. Class k includes n_k observations.

$\underline{x}_{ik} = [x_{i1k} \ldots x_{ipk}]'$ is a p-element column vector representing the complete multivariate observation for the i^{th} sample in the k^{th} class.

$\underline{\bar{x}}_k = [\bar{x}_{1k} \ldots \bar{x}_{pk}]'$ is a p-element column vector representing the centroid of the k^{th} class.

The elements of $\underline{\bar{x}}_k$ are the sample means for each variable computed for observations in the k^{th} class, and denoted $\bar{x}_{jk}$; $j = 1, 2, \ldots, p$.

$\underline{\bar{x}} = (\frac{1}{n}) \sum_{k=1}^{g} n_k \, \underline{\bar{x}}_k$ is a p-element column vector representing the combined class centroid.

The elements of $\underline{\bar{x}}$ are the sample means of each variable computed for observations from all g classes, and n is the total sample size: $n = \sum_{k=1}^{g} n_k$.

Consider a special vector representation of the matrix of sums-of-squares and crossproducts of deviations from the mean. This matrix, when divided by (n-1) for n total observations, is the sample covariance matrix. Also consider the fol-

lowing product of the vector of deviations from the combined class centroid for a specific observation and its transpose:

$$(\underline{x}_{ik} - \underline{\bar{x}})(\underline{x}_{ik} - \underline{\bar{x}})' = \begin{bmatrix} x_{i1k} - \bar{x}_1 \\ x_{i2k} - \bar{x}_2 \\ \cdot \\ x_{ipk} - \bar{x}_p \end{bmatrix} [(x_{i1k} - \bar{x}_1),(x_{i2k} - \bar{x}_2), \ldots ,(x_{ipk} - \bar{x}_p)]$$

$$= \begin{bmatrix} (x_{i1k} - \bar{x}_1)^2 & (x_{i1k} - \bar{x}_1)(x_{i2k} - \bar{x}_2) \ldots & (x_{i1k} - \bar{x}_1)(x_{ipk} - \bar{x}_p) \\ \cdot & (x_{i2k} - \bar{x}_2)^2 \ldots & (x_{i2k} - \bar{x}_2)(x_{ipk} - \bar{x}_p) \\ \cdot & \cdot & (x_{ipk} - \bar{x}_p)^2 \end{bmatrix}. \qquad [5]$$

The matrix which results from this multiplication of a column times a row vector is a p x p matrix of squares and crossproducts of the deviations of the observation for each variable from the corresponding sample mean. If these vector products are calculated for each observation in the k^{th} class and the results are summed, the following square matrix will result:

$$\sum_{i=1}^{n_k} (\underline{x}_{ik} - \underline{\bar{x}})(\underline{x}ik - \underline{\bar{x}})'$$

$$= \begin{bmatrix} \sum (x_{i1k} - \bar{x}_1)^2 & \ldots \ldots \ldots \ldots & \sum (x_{i1k} - \bar{x}_1)(x_{ipk} - \bar{x}_p) \\ \cdot & \sum (x_{i2k} - \bar{x}_2)^2 & \cdot \\ \cdot & \cdot & \sum (x_{ipk} - \bar{x}_p)^2 \end{bmatrix}. \qquad [6]$$

Summing [6] across g classes results in another symmetric matrix which looks like [6] except for the double summations which accumulate results for all observations across the g classes has the sums-of-squared deviations of each variable from its mean on the diagonal. The off-diagonal elements are sums of crossproducts of deviations from the mean for all pairs of variables. If this matrix is scalar multiplied by $1/(n-1)$, the sample covariance matrix for the combined class (*total* covariance matrix) is obtained. The summation of [6] across all classes is the total sums-of-squares and crossproducts, and is denoted by T:

$$T = \sum_{k=1}^{g} \sum_{i=1}^{n_k} (\underline{x}_{ik} - \bar{\underline{x}})(\underline{x}_{ik} - \bar{\underline{x}})'. \qquad [7]$$

The total covariance matrix is:

$$S = \frac{1}{(n-1)} T \text{ and } n = \sum_{k=1}^{g} n_k. \qquad [8]$$

A similar computation, performed by substituting the centroid for the k^{th} class for the overall centroid and summing only over the observation subscript (i), yields the within class sums-of-squares and crossproducts matrix denoted by W_k for the k^{th} class:

$$W_k = \sum_{i=1}^{n_k} (\underline{x}_{ik} - \bar{\underline{x}}_k)(\underline{x}_{ik} - \bar{\underline{x}}_k)'. \qquad [9]$$

If W_k is scalar multiplied by $1/(n_k - 1)$, the *sample* covariance matrix for the k^{th} class is obtained.

For the discriminant analysis problem, the T matrix is partitioned into matrices attributable to the within class (W) and among class (A) differences. This partitioning process is analogous to the partitioning of the total sum-of-squares in the univariate ANOVA model except this is working with vector rather than scalar quantities. If the W matrix is multiplied by $1/\sum(n_k - 1) = 1/(n - g)$, the result is a pooled estimate of the covariance matrix or within class covariance matrix (multivariate analogy of the pooled estimate of variance used in univariate two-sample t-test and the pooled estimate of the error variance used in univariate ANOVA). This matrix is denoted by S_w where $S_w = \frac{1}{n-g} W$.

There are different ways to manipulate combinations of time series measurement or feature deviations from their centroids in the development of discriminant functions and statistical tests for centroid differences. In a discussion restricted to only linear discriminant functions, g, computational advantages will result from a g that is linear in the components of the observation measurements x_i or features which are functions of the x_i. Considering only manipulating linear combinations of feature vector deviations from their centroids, scores like the following are calculated:

$$f_{ik} = \sum_{j=1}^{p} a_j(x_{ijk} - \bar{x}_j) \qquad [10]$$

where a_j is a coefficient, i represents an observation index or i^{th} time series, and j is a feature variable index. In matrix terms, [10] is:

$$f_{ik} = \underline{a}'(\underline{x}_{ik} - \bar{\underline{x}}) \text{ where } \underline{a} = \begin{bmatrix} a_1 \\ a_2 \\ \cdot \\ a_p \end{bmatrix}. \qquad [11]$$

The partitioning of the total sum-of-squares of the f_{ik} scores into within and among class components is required for developing the discriminant function. Since

$$\sum_{k=1}^{g}\sum_{i=1}^{n_k} f_{ik}^2 = \sum_{k=1}^{g}\sum_{i=1}^{n_\omega}[\underline{a}'(\underline{x}_{ik} - \bar{x})][(\underline{x}_{ik} - \bar{\underline{x}})'\underline{a}]$$

$$= \underline{a}' T \underline{a} \qquad [12]$$

and recalling the partitioning of the T matrix:

$$\underline{a}' T \underline{a} = \underline{a}' \sum_{i=1}^{n_k} W_k \underline{a} + \underline{a}' A \underline{a} = \underline{a}' W \underline{a} + \underline{a}' A \underline{a}. \qquad [13]$$

[13] is an equation with scalar terms as pre and post multiplication of the p x p matrices by $\underline{a}'$ and $\underline{a}$ results in 1 x 1 matrix products. Pre and post multiplication by $\underline{a}$ results with the first term of [13] representing the sum-of-square values of the linear function defined by the coefficients in $\underline{a}$ evaluated for deviations of each feature vector observation from its class mean. The final term of [13] is a weighted sum-of-squared values of the linear function evaluated for deviations of class centroids from the combined class centroid. Thus, [13] is used to partition the total

variance in discriminant function scores into the between and within groups components as $\underline{a}'W\underline{a}$ represents the within group sum-of-squares, $\underline{a}A\underline{a}$ the among group sum-of-squares, and $\underline{a}'T\underline{a}$ the total sum-of-squares. Considering $\underline{a}$ as a vector of discriminant function coefficients obtained using the Lagrange multiplier solution technique to the maximization problem:

$$\text{Find} : \frac{\underline{a}'A\underline{a}}{\underline{a}'W\underline{a}}$$
$$\text{Subject to} : \underline{a}'W\underline{a} = n - g,$$

also obtains $\underline{a}'A\underline{a} = \lambda(n-g)$. The restriction $\underline{a}'W\underline{a} = n - g$ imposed to finding the optimal discriminant function allows [13] to be rewritten:

$$\underline{a}'T\underline{a} = (n-g) + \lambda(n-g) = (n-g)(1+\lambda). \qquad [14]$$

Since $\underline{a}'A\underline{a} = \lambda(n-g)$ is the among group sum-of-squares, or the group separation "explained" by the specific discriminant function which $\underline{a}$ defines, a reasonable measure of the power of this discriminant function is the fraction of sum-of-squares "explained":

$$\frac{\lambda(n-g)}{(1+\lambda)(n-g)} = \frac{\lambda}{(1+\lambda)}. \qquad [15]$$

The square root of [15] is the canonical correlation coefficient and is an indicator of the power of a specific discriminating function. Another evaluation of discriminant function effectiveness can be obtained by examining its statistical significance. Tests for significance based on properties of the within and among groups matrices is examined next.

2.3.3.2 One-Way ANOVA and MANOVA

Consider the univariate one-way ANOVA model:

$$x_{ik} = \mu + \alpha_k + \varepsilon_{ik} \quad i = 1, \ldots, n_k; \quad k = 1, \ldots, g \qquad [16]$$

where x_{ik} is the observed value of an interval scaled criterion variable, μ is the overall mean, α_k is an effect due to the presence of the k^{th} treatment or experimental condition, and ε_{ik} is an error term analogous to the ε_i term in the multiple regression model. In this model, i indexes a specific observation in one of the g groups of observations collected using the various experimental conditions. By letting $\mu_k = \mu + \alpha_k$, where μ_k represents the k^{th} group mean, [16] is

$$x_{ik} = \mu_k + \varepsilon_{ik}. \qquad [17]$$

If the random errors are independent normally distributed with common variance, statistical tests for the significance of the α_k's are performed. The hypothesis tested is:

$$H_0 : \mu_1 = \mu_2 = \ldots = \mu_g$$
$$H_1 : \text{at least two } \mu_k\text{'s differ.}$$

The significance of the differences among group means is interpreted by partitioning the total sum-of-squares of x_{ik} deviations from their sample mean into the within groups component which represents an estimate of error variance, and the among groups component which measures deviations from the null hypothesis of no group differences. Let $\bar{x}_k$ represent the sample mean for the k^{th} group, and $\bar{x}$ the overall sample mean. The partitioning is then:

$$\sum_{k=1}^{g}\sum_{i=1}^{n_k}(x_{ik}-\bar{x})^2 = \sum_{k=1}^{g}\sum_{i=1}^{n_k}[(x_{ik}-\bar{x}_k)+(\bar{x}_k-\bar{x})]^2$$

which equals:

$$\sum_{k=1}^{g}\sum_{i=1}^{n_k}(x_{ik}-\bar{x})^2 = \sum_{k=1}^{g}\sum_{i=1}^{n_k}(x_{ik}-\bar{x}_k)^2 + \sum_{k=1}^{g}\sum_{i=1}^{n_k}(\bar{x}_k-\bar{x})^2 \qquad [18]$$

where the term on the LHS of [18] stands for the *total* sum-of-squares (SS_T), the first term of the RHS of [18] is the *within* groups sum-of-squares (SS_w), and the second term of the RHS of [18] is the *among* groups sum-of-squares (SS_A). If the null hypothesis of no group mean differences is true, the among group sum-of-squares should be very small with most variation due to the within groups component. If the error terms, ε_{ik} are independent and normally distributed with common variance and zero mean, the following statistic tests the group difference hypothesis:

$$F_o = \frac{SS_A/(g-1)}{SS_W/(n-g)}.$$

The statistic F_o is distributed as an F-statistic with g-1 and n-g degrees of freedom. Large values of F_o lead to the rejection of the hypothesis that all group means are identical.

In the multivariate equivalent to the one-way ANOVA, scalar elements are simply replaced by vectors so $\underline{x}_{ik}$ is a p-element observation vector with elements

x_{ijk}, $\underline{\mu}$ is a p-element centroid for the overall population centroid, $\underline{\alpha}_k$ is the effect of the k^{th} treatment, and $\underline{\varepsilon}_{ik}$ is an error vector. Hence, the tested hypothesis is:

$$H_0 : \underline{\mu}_1 = \underline{\mu}_2 = \ldots = \underline{\mu}_g$$
$$H_1 : \text{at least two } \underline{\mu}_{k's} \text{ differ.}$$

Rejecting the null hypothesis leads to the conclusion that there is a difference among some of the group centroids.

Similar to the univariate case, the significance of the difference among centroids is investigated by partitioning the sum-of-squared deviations of the observation vectors, $\underline{x}_{ik}$, from the combined sample group centroid denoted by $\bar{\underline{x}}$. This is the same problem where the partitioning process results in expressing the total sum-of-squares and crossproducts matrix, T, as the sum of within and among groups components, W and A, or $T = W + A$. If the null hypothesis is true, matrix W will be similar to matrix T. The evaluation of the relative magnitude of within and among groups sum-of-squares is complicated by the fact that they are p x p matrices. However, Wilks (1963) developed a test based on the determinants of the W and T matrices. His procedure represents a likelihood ratio test of the hypothesis that all groups have identical centroids and the Wilks' lambda statistic, Λ, is:

$$\Lambda = \frac{|W|}{|A + W|} = \frac{|W|}{|T|}.$$

Thus, it is seen that small values of Λ lead to rejection of the null hypothesis of no group centroid differences. The sampling distribution of Λ is complex because the number of groups (g), observations (n), and variables (p), are all parameters, but

various approximations for evaluating Λ are available. One is the F-statistic for the one-way MANOVA model developed by Rao (Tatsuoka, 1971):

$$F_o = 1 - \frac{\Lambda^{1/s}}{\Lambda^{1/s}} ms - p(g-1)/2 + \frac{1}{p(g-1)}$$

where p is the number of variables, g is the number of groups or treatments, $m = n - 1 - (p+g)/2$ and

$$s = \sqrt{p^2(g-1)^2 - \frac{4}{p^2 + (g-1)^2 - 5}}$$

where s = 1 if the numerator and denominator equals zero. The statistic F_o is distributed as $F_{v1,v2}$ where $v_1 = p(g-1)$ and $v_2 = ms - p(g-1)/2 + 1$. The critical region for the test is:

$$\text{Reject } H_o : \underline{\mu}_1 = \ldots = \underline{\mu}_k$$

if $F_o > F_{\alpha, v1, v2}$ where α is the significance level for the test, and v_1 and v_2 are the numerator and denominator degrees of freedom, respectively.

2.3.4 Classifier Performance Measurement Criteria

A critical aspect for comparing alternative feature extraction approaches input to several classification algorithms is a fair and consistent estimation of their total misclassification error rates. Lachenbruch (1975) discusses the leaving-one-out, or *jacknife*, method for computing error rate estimates. This method estimates the discriminant rule omitting one sample time series and then applies that rule to classify the remaining observational time series. Misclassifications are tallied after

the jackknife process is iteratively done for all observations. The various types of error rates are discussed in the next section. Another measure of classifier performance is the total cost of misclassification. Stated from a decision theory perspective, a Type I error, or lower probability of detection, is worse than a Type II error, or higher probability of false alarm. An actual total classification cost can be computed for alternative classification approaches if the respective misclassification costs are known.

The easiest way of estimating a classifier's misclassification rate is calculating how many of the *design* or *training* set observations are misclassified. Early work in pattern recognition research implemented this approach but it was discovered that the estimated error rates underestimated the *actual* error rate of the classifier. This is because the classifier or decision rule is optimized on the design set and unless this set perfectly represents the population distribution, a new set, which is random sample drawn from the same distribution, will be different and so the classifier will not be optimal. The error rate calculated by reclassifying the *design* set is called the *apparent* error rate. This is distinguishable from the *actual* error rate which is the expected error rate of the constructed classifier on *future* samples from the same population distribution as the training set.

The simple approach of reclassifying the design set has an optimistic bias so researchers investigated methods for estimating the actual error rate from a design set (Hills, 1966). However, problems with still optimistically biasing the estimation of actual error rate caused researchers to concentrate on estimating the *expected actual* error rate. One way to estimate the expected actual rate, the leaving-one-out method, gives an *unbiased* estimate and works well with non-Gaussian observations (Lachenbruch, 1975). This is the method for computing

classification error rate estimates for the experimental data in this research. But another research strategy was not to restrict feature performance comparisons by constructing a classifier and estimating its error rate from only a *design* set of data. In simulation experiments, other independent time series were generated and used as *test* sets so application of a designed classifier to these new sets yielded a straightforward estimate of the *actual* error rates for the various feature extraction/classification approaches. Special considerations are now discussed about discrimination and classification of data that are in time series form.

2.4 Discrimination and Classification of Time Series

There are two major approaches for viewing, analyzing, and interpreting time series--one based on the time domain and another based on the frequency or spectral domain. The theoretical development of time series methodology has exhibited a leader-follower pattern, first emphasizing one domain, then the other. Spectral (Fourier) analysis decomposes functions representing fluctuating phenomena in space or time into sinusoidal components that have varying frequencies, amplitudes, and phases. Several texts specify the necessary mathematical conditions for the existence of the Fourier transform (Brigham, 1974 and Bracewell, 1978). Here, let it suffice that the Fourier transform does exist for waveforms physically observed in nature (Bracewell, 1978). For a given random process, $\mathbf{x} = \{x(t), t \in R\}$, the continuous Fourier transform (CFT) definition $X(f)$, is:

$$X(f) = \int_{-\infty}^{\infty} x(t)e^{-i2\pi ft}dt,$$

and the inverse Fourier transform definition $x(t)$ is:

$$x(t) = \int_{-\infty}^{\infty} X(f)e^{i2\pi ft}df.$$

The inverse Fourier transform shows how the x random time function can be described by a superposition of complex sinusoids $e^{i2\pi ft}$, with the amplitude and phase of those sinusoids lying in the spectral band between f and $f + df$ defined by $X(f)df$. Hence, $X(f)$ is a complex amplitude spectral density function. For example, if x has the dimensions of volts, then $X(f)$ has the dimensions of volts/Hz. In addition to the Fourier transform being a function that represents the amplitude and phase at each frequency, it is an effective tool mathematically, statistically, and computationally. It is of great mathematical use because the convolution operation occurs so often and is greatly simplified by the Fourier transform. Statistically, the large sample properties of the Fourier transform are much simpler than those of the corresponding time domain quantities. Computationally, fast Fourier algorithms allow evaluation of interested parameters more rapidly with smaller round-off error than by direct time domain evaluation. Spectral analysis has an inherent consistency and efficiency in its application because the power spectrum and all higher-order spectrum density functions use the estimates provided by the direct discrete

Fourier transform (DFT) of the raw time series. For these reasons, spectral analysis is the time series processing method implemented for feature development and subsequent input to a classifier. The decision for employing a feature extraction approach rather than an optimality approach is discussed next.

Consider the time series discrimination problem where the observation of a discrete parameter time series x at each of T points in time is given and the standard objective is to classify the observed time series into one of k mutually exclusive and exhaustive classes with an overall low misclassification error rate. The univariate sample time series can be represented as $\mathbf{x} = (x(0), \ldots, x(T-1))$ and so the classification problem concerns finite dimensional random vectors where standard multivariate approaches are applied. However, Neyman-Pearson likelihood or Bayes criterion rules are usually applied to classifying multivariate vectors where T is small, and the learning population is adequate for estimating the unknown parameters. Generally, this is *not* the case for time series data. For example, the simulated time series analyzed in this study have T of approximately 1200, and the learning populations contain a maximum of 250 time series. Furthermore, the actual time series data analyzed in this study have T of approximately 2500, and the learning populations contain a maximum of 60 time series. Thus, the computations for discriminant function calculation and performance evaluation will involve inversion of large covariance matrices which are also not of full rank. Hence, the numerical difficulties of time domain calculations motivated investigation of other approaches for time series discrimination.

Shumway (1982) gives two distinct alternative approaches of spectral time series discrimination. The first, or optimality approach, assumes very specific Gaussian models and solutions are developed to satisfy definitive minimum error

criteria. This approach generally requires prior knowledge of the time series or signal waveforms so that either linear or quadratic discriminant functions can be constructed. Shumway discusses the use of the frequency domain discriminant analysis approach where matrix inverses can be replaced by simple sums involving discrete Fourier transforms (DFT) and spectral density functions. Since the DFT of a weakly stationary process produces nearly uncorrelated random variables and variances approximately equal to the power spectrum, estimation and hypothesis testing problems are formulated in terms of sample spectral densities with simple approximate distributions. Shumway (1982) gives results which make discriminant analysis in the frequency domain framework a very promising approach. But Shumway noted the danger or limitation of the optimal approach (either time or frequency domain) is the fact that inappropriate assumptions of time series distribution structure can cause an "optimum" solution to be only a rough approximation to the actual problem. In fact, the time series measurements within the experimental databases in this research were found to be highly non-Gaussian and nonlinear based on the Hinich bispectrum-based statistical tests (Hinich, 1982). Thus, feature extraction, the other distinct approach to time series discrimination and classification, was the approach followed in this study. A HOS feature extraction algorithm developed to combine various types of spectral features of the simulated and actual time series is discussed in Chapter 4. Time series are most often realizations from a stochastic process and mathematical representations called covariance functions used to characterize its behavior are defined next.

2.5 Stochastic Processes and Their Covariance Functions

A stochastic process $\mathbf{x} = \{x(t), t \in T\}$ is a collection of random variables that describes the evolution through time of some physical process. The index set of the process, T, is usually the set of integers (discrete) or the set of real numbers (continuous). Consider here stochastic processes which are discrete-time processes so $\mathbf{x} = \{x(t_n)\ n \in \mathrm{N}\}$ is a sequence of random variables. Let the means of $\{x(t_n)\}$ be represented by μ_n. The n^{th}-order covariance of $\mathbf{x}$ is:

$$\begin{aligned}
R_n(t_1, t_2, \ldots, t_n) &= E\{x(t_1 - \mu_1)x(t_2 - \mu_2) \ldots x(t_n - \mu_n)\} \\
&= E\{x(t_1)x(t_2) \ldots x(t_n) - \mu_n x(t_{n-1}) - \cdots - \mu_2 x(t_1) \\
&\quad - \mu_1 x(t_2) - \ldots - \mu_{n-1} x(t_n) + \mu_1 \mu_2 \ldots \mu_n\} \\
R_n(t, \tau) &= E\{x(t_1)x(t_1 + \tau) \ldots x(t_{n-1} + \tau)\} - \mu_n E\{x(t_{n-1})\} - \cdots - \mu_2 E\{x(t_1)\} \\
&\quad - \cdots \mu_{n-1} E\{x(t_n + \tau)\} - \mu_1 E\{x(t_1 + \tau)\} + \mu_1 \mu_2 \ldots \mu_n \\
&= E\{x(t_1) \ldots x(t_{n-1} + \tau)\} - \mu_1 \mu_2 \ldots \mu_n \\
&= E\{x(t_1) \ldots x(t_{n-1} + \tau)\}.
\end{aligned}$$

where the marginal terms all vanish as it is always assumed in this discussion that random variable means are zero and that $\mathbf{x}$ has finite order moments. Clearly, there are many possible orders (number of random variables in the joint probability distribution) that are used for describing $\mathbf{x}$, but concern is presently with the covariance of *two* random time variables or the second-order covariance function. Let the means of $x(t_1)$ and $x(t_2)$ be represented by μ_1 and μ_2 respectively. The second-order covariance is:

$$
\begin{aligned}
R_{xx}(t_1, t_2) &= E\{x(t_1 - \mu_1)x(t_2 - \mu_2)\} \\
&= E\{x(t_1)x(t_2) - \mu_2 x(t_1) - \mu_1 x(t_2) + \mu_1\mu_2\} \\
R_{xx}(t, \tau) &= E\{x(t_1)x(t_1 + \tau)\} - \mu_2 E\{x(t_1)\} - \mu_1 E\{x(t_1 + \tau)\} + \mu_1\mu_2 \qquad [19] \\
&= E\{x(t_1)x(t_1 + \tau)\} - \mu_1\mu_2 \\
&= E\{x(t_1)x(t_1 + \tau)\}.
\end{aligned}
$$

where the second term vanishes as random variable means are zero. The second-order covariance is thus a bivariate expected value which provides a summary of the degree which two random time variables are associated.

When [19] is a function of only the time difference or lag parameter, τ, with $\tau = t_2 - t_1$, so that

$$R_{xx}(t_1, t_2) = R_{xx}(\tau),$$

the x process is known as a wide-sense or weakly stationary stochastic process. Requiring all marginal and joint density functions of a random process to be time independent, or strictly stationary, is frequently too restrictive an assumption in practice as it is hard to find a strictly stationary random process. But there are physical situations in which the process does not change appreciably during the time it is being observed. Hence, wide sense or weak stationarity is adequate to guarantee that the covariance of any pair of random variables are constants independent of the choice of time origin. In these cases, the relaxed wide sense stationary assumption leads to a convenient mathematical model to closely approximate reality. However, it is the mathematical convenience when assuming weak stationarity which tends to prevent the proper investigation and applicability of other forms of joint random variable distributions of a particular stochastic process under study. Even if nonlinearity of a stochastic process is addressed

through HOS analysis, these studies also frequently assume stationarity of the random process.

For stationary time series, there exists a uniquely defined decomposition into a deterministic and a purely nondeterministic component which are mutually orthogonal (Wold, 1954). This decomposition forms the basis of a *time-domain* analysis of a given stochastic process generalizing the well known properties of stationary processes. Also, *spectral* analysis, rather than the time domain, provides the powerful methods of harmonic analysis (Wiener and Masani, 1957). Harmonic analysis is possible for stationary processes because spectral representations in the form of Fourier-Stieltjes integrals exist for the process variable and the associated covariance functions:

$$x(t_n) = \int_{n=-\infty}^{\infty} e^{i2\pi fn} dA_x(f)$$

where $A_x(f)$ is a stochastic process with orthogonal increments. Cramer (1960) considers certain classes of nonstationary processes having similar spectral representations. He shows that without requiring $A_x(f)$ to have orthogonal increments, one is led to a class of stochastic processes called *harmonizable* or *cyclostationary* processes.

A process is strictly cyclostationary if:

$$E\{x(t_1) \ldots x(t_n)\} = E\{x(t_1 + kT) \ldots x(t_n + kT)\}$$

for $k \in \mathbf{N}$, for all n, and T denotes the period. When [19] is periodic in t with period T for a fixed time difference or lag parameter, τ, the second-order covariance is:

$$\begin{aligned} R_{xx}(t_1, t_2) &= E\{x(t_1)x(t_2)\} \\ &= E\{x(t_1 + T)x(t_1 + T + \tau)\}, \end{aligned}$$

and the **x** process is known as a weakly cyclostationary stochastic process. Cyclostationary processes are processes whose joint distributions vary over time, and are thus nonstationary, but whose parameters vary according to periodic functions. Cyclostationary processes are a class of stochastic processes which appear in the physical world via a mechanism that provides some deterministic structure in the observed time series. These processes are therefore appropriate models for phenomena involving cycles or when there exists some underlying periodicity to the data-generating mechanism.

To successfully deal with problems of statistical inference connected with stochastic processes, it is crucial to have an appropriate and convenient type of analytical representation for the particular class of processes under study. This analytical representation should express in mathematical form the essential features of the random mechanism assumed to generate the process. This ensures accurate assessments are made on the various statistical questions arising from process generation. Consequently, HOS in addition to power spectrum, representations were used and developed in this research so that the *intermodulation* and *nonlinear* effects of random fault mechanisms of cyclostationary processes such as rotating machine systems are captured in the physical process representations. Background information on existing HOS theory is given next.

2.6 Higher-Order Statistical (HOS) Theory

For single time series, the idea of polyspectra, or higher-order spectra, was originated by Blanc-Lapierre (1953). Algebraic and analytic detail was provided by Leonov and Shiryaev (1959) and Shiryaev (1960), who also considered the spectral representation for a cumulant, rather than for a product moment. Shiryaev attributed this idea to Kolmogorov. Brillinger (1965) generalizes the definitions of these earlier papers by considering k-dimensional time series. Brillinger (1965) also developed a theorem which explained the importance of cumulants rather than product moments. The actual term, polyspectrum, is due to Tukey who began the development of a calculus relating polynomial operations to higher-order spectra.

The power spectrum is a complex-valued function of frequency and is defined as the Fourier transform of the second-order stationary covariance function, $c_2(\tau) = E[X(t)X(t+\tau)]$:

$$P(f) = \int_{-\infty}^{\infty} c_2(\tau) e^{-i2\pi f} d\tau.$$

Now, a specific case of polyspectra is the third-order spectrum, or bispectrum, a complex-valued function of two frequencies and defined as the *double* Fourier transform of the third-order stationary covariance function, $c_3(\tau_1, \tau_2) = E[X(t)X(t+\tau_1)X(t+\tau_2)]$:

$$B(f_1, f_2) = \int_{-\infty}^{\infty} \int_{-\infty}^{\infty} c_3(\tau_1, \tau_2) e^{-i2\pi(f_1\tau_1 + f_2\tau_2)} d\tau_1 \, d\tau_2.$$

From examining each spectrum's Parseval relations:

$$E[y^2(t)] = \frac{1}{2\pi}\int_{-\infty}^{\infty} P(f)\,df, \text{ and}$$

$$E[y^3(t)] = \frac{1}{(2\pi)^2}\int_{-\infty}^{\infty}\int_{-\infty}^{\infty} B(f_1,f_2)\,df_1\,df_2,$$

it is clear that the power spectrum represents the contribution to the *second* moment over a particular *range* of frequency, and the bispectrum represents the contribution to the *third* moment over of a particular *pair* of frequencies. Nikias and Raghuveer (1987) list a wide range of bispectrum applications. Specific examples of nonlinear structure detected in a variety of time series using bispectral analysis include: nonlinear interaction of ocean waves in shallow water (Hasselman et al., 1963), analysis of acoustic gear noise (Sato et al., 1977), and nonlinear energy transfers in plasma (Kim and Powers, 1978). More sophisticated statistical applications of the bispectrum are within studies of nonlinear spectral transfer of energy in turbulence (Lii et al., 1976, Van Atta, 1979, and Helland et al., 1979). Proceedings from the 1989 Workshop on Higher Order Spectral Analysis (Nikias and Mendel, 1989) contain some recent developments of bispectrum theories and applications of processing signals to extract information based on cumulants. The latest developments of HOS theory and its various applications are in the IEEE Proceedings from the 1991 International Signal Processing Workshop on Higher Order Statistics (Georgel, 1991). In this research, in addition to the bispectrum, the second-order cumulant spectrum not constrained by stationarity, is investigated for

providing feature information to a multivariate classifier to detect incipient failures of rotating machinery.

2.6.1 Moments and Cumulants

Following Rosenblatt (1983), consider the random variables $(X_1, \ldots, X_k)$. Let $\phi(t_1, \ldots, t_k)$ be the joint characteristic function of the random variables

$$\phi(t_1, \ldots, t_k) = E \exp\left\{ i \sum_{j=1}^{k} t_j X_j \right\} = \phi(t). \qquad [20]$$

If mixed moments $E X^{\nu} = E(X v_1^1 \ldots X v_k^k) = m_{\nu}$,

$$\nu = (\nu_1, \ldots, \nu_k),\ \nu_j \geq 0,\ |\nu| = \sum_{j=1}^{k} \nu_j,\ \nu! = \prod_{j=1}^{k} \nu_j!$$

exist up to a certain order $|\nu| \leq k$, they are the coefficients in the Taylor expansion of ϕ about zero

$$\phi(t) = \int \left\{ \sum_{|\nu| \leq k} (it)^{\nu} \frac{x^{\nu}}{\nu!} + o(|t|^k) \right\} dG(x) = \sum_{|\nu| \leq k} (it)^{\nu} \frac{m_{\nu}}{\nu!} + o(|t|^k). \qquad [21]$$

The joint cumulants $c_v = \text{cum}(Xv_1^1, \ldots, Xv_k^k)$ are the coefficients in the Taylor expansion of log ϕ about zero

$$\log \phi(t) = \sum_{|v| \leq k} (it)^v \frac{c_v}{v!} + o(|t|^k). \qquad [22]$$

Kendall and Stuart (1958) has formulas relating cumulants of order k or less to the moments of order k or less, and Leonov and Shiryaev (1959) has formulas for the inverse relationship. The relationship of zero mean cumulants to moments up to order six are shown on the next page. Rectangular brackets are used to enclose cumulants, and curly brackets to enclose expectations. The curly brackets with subscripted numbers are used to replace the enclosed term with the sum of all distinct terms in a combinatorial fashion (all permutations of the indices). The subscript value denotes how many terms are obtained from the index permutation operation.

$$[X_1] = \{X_1\} = 0$$

$$[X_1X_2] = \{X_1X_2\}$$

$$[X_1X_2X_3] = \{X_1X_2X_3\}$$

$$[X_1X_2X_3X_4] = \{X_1X_2X_3X_4\} - \{\{X_1X_2\}\{X_3X_4\}\}_3$$

$$[X_1X_2X_3X_4X_5] = \{X_1X_2X_3X_4X_5\} - \{\{X_1X_2X_3\}\{X_4X_5\}\}_{10}$$

$$[X_1X_2X_3X_4X_5X_6] = \{X_1X_2X_3X_4X_5X_6\} - \{\{X_1X_2X_3X_4\}\{X_5X_6\}\}_{15} - \{\{X_1X_2X_3\}\{X_4X_5X_6\}\}_{10}$$

$$+ \{\{X_1X_2\}\{X_3X_4\}\{X_5X_6\}\}_{15}$$

These relationships show that cumulants are expectations with lower order statistical dependence removed. If the cumulant of n random variables is desired, the expectation of the product of all n random variables is constructed, and additional terms are added so the net result will completely vanish if any subset of the variables is independent of any other subset. For the simple case of n = 2,

$$[X_1X_2] = \{X_1X_2\} - \{X_1\}\{X_2\}, \qquad [23]$$

the RHS of [23] vanishes if X_1 and X_2 are independent. For $n = 3$,

$$\begin{aligned}[X_1X_2X_3] = {} & \{X_1X_2X_3\} \\ & - \{X_1\}\{X_2\}\{X_3\} - [X_1X_2]\{X_3\} - [X_1X_3]\{X_2\} - [X_2X_3]\{X_1\}.\end{aligned} \qquad [24]$$

In the zero mean case, the last four terms of the RHS of [24] are zero, and so the third-order cumulant and third-order moment are the same. If X_1 and X_2 and X_3 are independent, the entire RHS of [24] is zero.

Rosenblatt (1983) showed that the existence of all moments up to order k is equivalent to the existence of all cumulants up to order k. Nevertheless, the bispectrum is defined as the Fourier transform of the *cumulant* sequence rather than the moment sequence. Brillinger (1965) gives three reasons for this definition. First, cumulants have better independence properties than moments as they are constructed so each order cumulant has the dependence on lower order cumulants removed. Second, for ergodic stationary stochastic processes, Fourier transforms of cumulants are mathematically better behaved than Fourier transforms of moments. The third justification for the use of cumulants is if the process is stationary

Gaussian, then all of its k^{th}-order moments for $k \geq 3$ do *not* provide any additional information about the process. However, the cumulant function *does* provide additional information as for $k \geq 3$, cumulants are *zero* for Gaussian processes. Hence, the cumulant, rather than the moment, is the function needed to detect departures from a Gaussian structure or linearity.

2.6.2 Mathematical Properties of The Bispectrum

Mathematical properties of the bispectrum are discussed in many HOS literature references but Hinich and Patterson (1989) emphasize the concepts of linearity, Gaussianity, and stationarity. Consider a time series, x(t) generated by the linear model:

$$x(t) = \sum_{n=-\infty}^{\infty} a(n)\varepsilon(t-n) \qquad [25]$$

where $\{\varepsilon(t)\}$ is a purely random series. The weighting function, or impulse response, a(n), is real for physically realizable systems, and from causality, is zero for negative n. If the series $\{\varepsilon(t)\}$ is Gaussian, then the original process $\{x(t)\}$ is also Gaussian, and has a zero bispectrum. But if the series $\{\varepsilon(t)\}$ is pure noise and non-Gaussian, then $\{x(t)\}$ is non-Gaussian, and has a nonzero bispectrum. Also, [25] can be nonlinear if $\{\varepsilon(t)\}$, the input process, and a(n) are dependent and $\{x(t)\}$ will be nonlinear even if $\{\varepsilon(t)\}$ is Gaussian, and the bispectrum will be nonzero.

Let $\{x(t)\}$ be a stationary time series with zero mean, and assume that all expected values and sums used exist. The power spectrum of [25] is the Fourier transform of the autocovariance function $C_{xx}(t) = E[x(t+n)x(t)]$.

$$S(f) = \sum_{n=0}^{\infty} C_{xx}(t) \exp\{-i2\pi fn\}.$$

If $S(f)$ is constant, then $\{x(t)\}$ is serially uncorrelated on a white noise process.[1] The bispectrum of [25] is defined as the two-dimensional Fourier transform of the bicovariance function $C_{xxx}(n,m) = E[x(t+n)\,x(t+m)\,x(t)]$ which does not depend on t because the process is stationary:

$$B(f_1,f_2) = \sum_{m}\sum_{n} C_{xxx}(n,m) \exp\{-i2\pi f_1 n - i2\pi f_2 m\}.$$

The two frequency notation hides the three frequency interaction which is important in bispectral estimation applications so three frequency notation $B(f,g,-f-g)$ and the Cramer representation of [25] was introduced by Brillinger and Rosenblatt (1967a):

$$x(t) = \int_{n=-\infty}^{\infty} exp\,[i2\pi fn]\,dA_x(f) \qquad [26]$$

where $\{dA_x(f)\}$ is a complex stochastic orthogonal increments process, and the integral defined in [26] is in Stieltjes sense. Now, because [25] is real, $dA_x(-f)$ is

---

[1] Whiteness of a series does not imply the series is purely random. This is important as some time series techniques do stop fitting a model when the residual errors appear to be white noise. The assumption of Gaussian residuals is made for the sake of convenience as zero correlation does imply independence in the Gaussian case, but if the series is non-Gaussian, this assumption can lead to wrong inferences.

the complex conjugate of $dA_x(f)$. The spectral density at f of [25] is $S(f)df = E\{dA_x(f)\,dA_x(-f)\}$, and the bispectral density for $h = -f - g$ is

$$B(f, g, h)\,df\,dg = E\{dA_x(f)\,dA_x(g)\,dA_x(h)\}. \qquad [27]$$

Because of stationarity, [27] is invariant to time translations so for $B(f, g, h)\,df\,dg$ to equal $B(f,g)\,df\,dg$ for all f and g, the sum f + g + h *must* be zero.

When $\{x(t)\}$ is linear, [27] is shown by Brillinger (1975) to be

$$B(f, g, h)\,df\,dg = \mu_3 A(f)A(g)A(h) \qquad [28]$$

where $A(f)$ is the transfer function of the impulse response a(t), $\mu_3 = E\{\varepsilon^6(t)\}$, and $\{\varepsilon(t)\}$ is the innovation process. The spectrum of the linear process [25] is

$$S(f) = \sigma_\varepsilon^2 A(f)A(-f) \qquad [29]$$

where σ_ε^2 is the innovation process variance.

The right hand side of [28] is invariant to permutations of the frequency indices $f, g,$ and $h = -f - g$. Thus, the bispectrum's symmetry lines are as shown in Figure 2.1 on page 56. Symmetry means that if values of the bispectrum are known at all points in one region about a symmetry relation, values in the other region can be determined through either a permutation and/or conjugation operation.

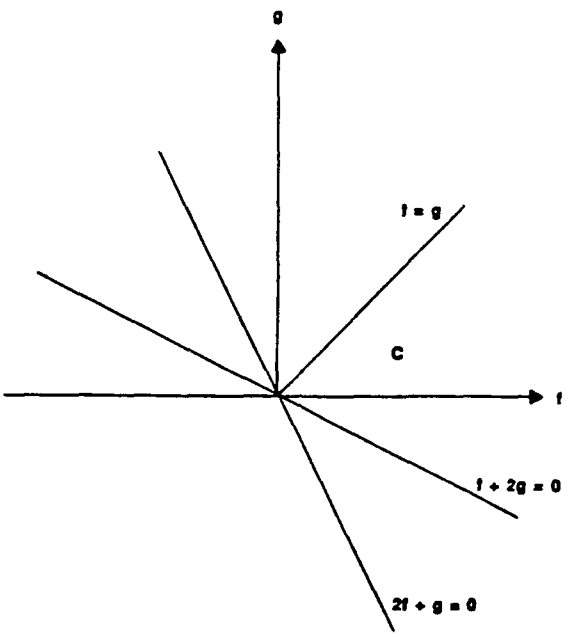

Figure 2.1: Symmetries of Bispectrum

Because $dA_x(-f) = dA_x^*(f)$, $B(-f, -g, -h)\,df\,dg = B^*(f, g, h)\,df\,dg$. This skew symmetry gives another three symmetry lines:

$$g = -f, h = -f (g = 0), \text{ and } h = -g\,(f = 0).$$

Thus, the cone,

$$C = \{f,g:\ 0 \le f, 0 \le g \le f\},$$

is the principal domain region of the continuous-time bispectrum in the (f,g) plane. Principal domain is the minimum region or frequency space which estimates are computed.

In physical reality, a continuous-time process is always sampled for some finite period, so investigated processes are band limited at some cutoff frequency

f_c. Contribution of frequencies above the cutoff frequency to the process variance is therefore zero, and so the continuous-time bispectrum is cut off at $f = \pm f_c$, $g = \pm f_c$, and $f+g = \pm f_c$. Thus, the continuous-time set of positive support for absolute value of [28] is the right isosceles triangle

$$IT = \{f,g : 0 \le f \le f_c, 0 \le g \le f, f+g = f_c\}$$

shown at Figure 2.2 on page 58. But there is also a discrete-time bispectrum where Hinich (1989) shows the discrete-time bispectral density with τ as the sampling interval:

$$\begin{aligned} B_\tau(f,g,h)\,df\,dg &= E\{d_\tau A_x(f)\, d_\tau A_x(g)\, d_\tau A_x(h)\} \\ &= \sum_k \sum_m \sum_n B\left(f+\frac{k}{\tau}, g+\frac{m}{\tau}, h+\frac{n}{\tau}\right) df\,dg \end{aligned}$$

for $f+g+h+\frac{(k+m+n)}{\tau} = 0$, with signed integers k,m,n restricted to keep the indices in the bispectrum's principal domain (Brillinger and Rosenblatt, 1967a). But since there is band limitation at f_c, the summation is restricted to k,m, and n such that

$$0 \le f+\frac{k}{\tau} \le f_c, \quad 0 \le g+\frac{m}{\tau} \le f_c,$$

and

$$0 \le h+\frac{n}{\tau} = \frac{(k+m)}{\tau} - f - g \le f_c.$$

Sampling actually causes an infinite number of parallel symmetry lines defined by $2f+g = \frac{n}{\tau}$ and $f+2g = \frac{n}{\tau}$. The cone C in Figure 2.1 on page 56 is cut by

both of these symmetry relations, but for a particular n^*, the line $f + 2g = \frac{n^*}{\tau}$ is at least to the line $2f + g = \frac{n^*}{\tau}$ when both lines are within C. Hence, the principal domain of the the discrete-time bispectrum, B_r is the triangle

$$\left\{f, g:\ 0 \le f \le \frac{1}{2\tau},\ 0 \le g \le f,\ 2f + g = \frac{1}{\tau}\right\},$$

which is a proper subset of C. This triangle is the union of the sets IT and OT in Figure 2.2. Statistical tests for Gaussianity and linearity (Hinich, 1982) and aliasing (Hinich and Wolinsky, 1988) of time series data use estimates calculated over this discrete-time bispectrum principal domain region.

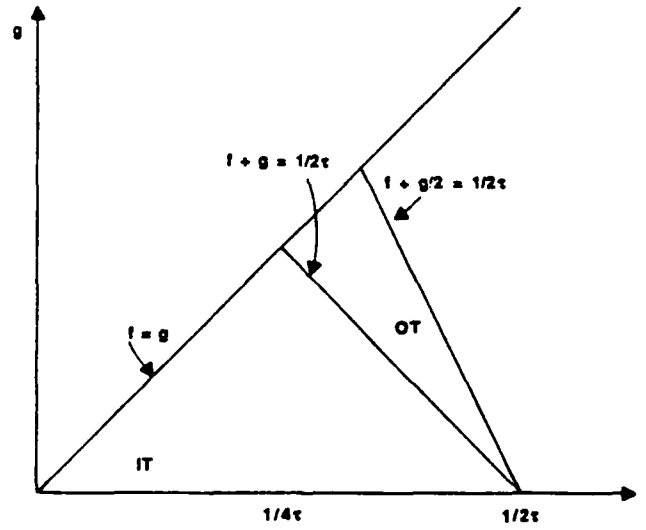

Figure 2.2: Discrete-Time Bispectrum Principal Domain

2.6.3 Bispectrum-Based Statistical Tests

Ashley et al. (1986) showed the Hinich bispectrum-based statistical tests (Hinich, 1982) to have substantial detection power for many common forms of nonlinear serial dependence (bilinear, nonlinear and threshold autoregressive, nonlinear moving average). Also demonstrated was that the bispectral linearity test can be applied to raw source data as well as to the fitting errors of an estimated linear model. Consider now the development of these statistical tests.

If the mechanism generating a time series has non-zero terms in the third-order cumulant function, then the bispectrum will be nonzero and vary with frequency. This fact is the basis for the linearity and Gaussianity statistical tests developed by Subba Rao and Gabr (1980) and Hinich (1982). Even though Rao and Gabr first implemented Brillinger's (1965) method for measuring the departure of a process from linearity and Gaussianity by using bispectrum estimates of the observed time series, their tests do not use the asymptotic properties of the bispectrum developed by Rosenblatt and Van Ness (1965), Shaman (1965), and Brillinger and Rosenblatt (1967a,b). There are two approaches to smoothing sample bispectra to obtain consistent and asymptotic Gaussian estimators with known sampling properties for large samples. Rao and Gabr (1980) use a lag window kernal to multiply the sample third-order covariance, or bicovariance, array computed from a sample of the time series; this weighted covariance is then Fourier transformed to yield a bispectral estimator. Hinich (1982) applies a fast Fourier transform to the data array, computes triple products of the discrete complex Fourier coefficients, and then uses a two dimensional smoothing filter in the

bifrequency domain to obtain a bispectral estimator with known sampling properties. This allows for the tradeoff between variance and bias of the estimator. The Hinich FFT approach uses fewer arithmetic steps than Gabr and Rao's lagged covariance products approach. Another element of Hinich's faster computational approach is the breaking of the data record into intervals and then averaging the sample bispectra for the record blocks. Additionally, Rao and Gabr (1980) did not develop test statistics for the significance of individual bispectral estimates. On the other hand, the Hinich statistical tests give chi-squared statistics for testing the significance of the bispectra. For these reasons, the Hinich bispectral-based statistical tests to detect departures from nonlinearity and non-Gaussianity are applied to time series data in this research.

With a finite impulse response and two-frequency index notation, [25] is

$$B_x(f_1,f_2) = \mu_3 \Lambda(f_1)\Lambda(f_2)\Lambda^*(f_1+f_2), \qquad [29]$$

where $\mu_3 = E\,\varepsilon^6(t)$, $\Lambda(f) = \sum_{n=0}^{\infty} a(t)\exp(-i2\pi fn)$, and Λ^* is the complex conjugate of Λ. From [25] and [29] a functional relationship called the *squared-skewness function* of $\{x(t)\}$ is defined and is the basis of the Hinich linearity and Gaussianity tests:

$$\frac{|B(f_1,f_2)|^2}{S(f_1)S(f_2)S(f_1+f_2)} = \frac{\mu_3^2}{\sigma_\varepsilon^6} = \psi^2(f_1,f_2). \qquad [30]$$

Hence, [30] is a standardized third-order cumulant spectral function as it is the square of the bispectrum normalized by the power spectrum product of each corresponding frequency. The degree of dependence between two frequencies is measured by [30]. If [25] is linear then [30] is constant over all frequency pairs

(f_1, f_2) in the bispectrum principal domain. The test for Gaussianity of the time series $\{x(t)\}$ involves testing that [30] is zero. Since $\mu_3 = 0$ for the Gaussian case, a non-zero value of the bispectrum rejects Gaussianity. Brockett et al. (1987) has a more complete discussion of these tests and Hinich (1982) has the precise formulas and proofs concerning the test for linearity and the derivation of an asymptotically normal test statistic based on [30].

2.6.4 Cyclostationary Processes and Higher-Order Spectra

HOS research studies show that nonlinear phenomena can be studied by computing higher-order spectrum estimates. Nonstationary phenomena can also be studied by computing higher-order spectrum estimates which are not constrained by the assumptions of stationarity. For example, there may be situations where it is beneficial to compute estimates of the second-order cumulant spectrum and the third-order cumulant spectrum rather than the power spectrum and the bispectrum, respectively. This HOS study conducted a time series estimation approach which computed linear (power spectrum), nonstationary (second-order cumulant spectrum), and nonlinear (bispectrum) estimates of cyclostationary processes for construction of feature information. Of interest in this research is mechanical vibration monitoring and diagnosis for rotating machinery. In this situation, the periodicity arises from rotation, revolution, or reciprocation of mechanical structures such as shafts, gears, pistons, or propellers. This work presents evidence that frequency support in the second-order cumulant spectrum principal domain (2-CSPD) region provides additional and significant feature information to bispectrum and power spectrum features for wear signal characterization of rotating machinery. Devel-

opment of the principal domain regions for the second and third-order random variable cases is contained in the next chapter.

2.7 Summary

Pertinent details of the major methodologies investigated to develop a new approach to the research problem were given in this chapter. Reviews of existing incipient fault detection techniques show an approach which employs HOS concepts needs investigation. Measuring differences in multivariate populations, and particularly time series, from a statistical perspective was discussed. Feature extraction is the time series discrimination method employed as the Gaussianity assumption for an optimality approach does not apply to the highly non-Gaussian and nonlinear time series data analyzed in this research. Even though different assumptions are made about the form of the class-conditional probability density functions (pdfs) used to characterize population differences, explanations in a Bayesian decision theory framework show that the class-conditional pdf is estimated in a way so similar values result when the function is evaluated for features from the same class, and widely differing values result when evaluated from different classes. Statistical tests of the null hypothesis that the centroids of different classes are equal are used. These tests are based on the partitioning of the matrix of squared deviations of observational feature sets from the sample centroid into matrices representing within and among class components. Closely related to discrimination is classification which applies the decision rule to assign a multivariate feature set with unknown class membership to its proper class. This research applied linear, quadratic, and 4-nearest-neighbor classifiers. An unknown time series

observation generated by a cyclostationary process, defined by "optimum" discriminant feature sets, will be assigned to the class which has the highest classification function, or posterior probability value. Applying classification rules to simulated and actual experimental time series data of known categories will result in measures of the classification power of the rules and their respective extracted feature sets. Major concepts of existing HOS theory emphasize the importance of justifying the use of certain limiting assumptions such as linearity, Gaussianity, and stationarity of the stochastic process under study. Use of proper spectral estimation procedures which include cumulant spectrum estimation are investigated to provide improvement to extracted feature information for cyclostationary time series discrimination and classification. The development of this new analytical approach is contained in the next two chapters.

Chapter 3

Cumulant Spectrum Estimation

3.1 Introduction

This chapter discusses the approach to cumulant spectrum estimation of periodic time series data generated by physical systems such as rotating machinery. Cyclostationary models are used to represent these physical systems as they contain both deterministic and random components. The deterministic component is due primarily to the constant periodic force of the machine. The random component is due to various sources such as the randomness of the process under study (ie. the process of wear), different operating and maintenance conditions (process environment), and randomness of the machine manufacturing process (no two machines are exactly the same).

In the time domain, various orders of covariance functions can be used to describe random processes. Alternatively, random processes can be characterized by the Fourier transforms of these various covariance functions. This chapter presents the key ideas underlying second-order cumulant spectrum estimation for a single time series. Second-order cumulant spectrum estimation is a new procedure that provides information beyond the bispectrum and power spectrum estimation of the experimental time series data described in Chapter 5. The spectral estimation approach describes the estimation of stationary, cyclostationary, and nonstationary processes in an integrated manner. It has the potential with further development

for use as tests for stationarity and periodicity of the observed time series but the primary interest in this research is the use of second-order cumulant spectrum estimates for feature extraction and incipient fault characterization of cyclostationary processes.

This work is different from the previous HOS monitoring study (Sato, 1977) and other treatments of cyclostationary processes (Gladyshev, 1961 and Ogura, 1971 and Hurd, 1969, 1989a, 1989b, and Gardner, 1989) in that it incorporates estimation concepts of several classes of stochastic processes (nonstationary, stationary, and cyclostationary) in terms of spectral correlation functions calculated over a second-order cumulant spectrum principal domain (2-CSPD) region. The 2-CSPD is derived from symmetry properties of the Fourier transform. There are several important properties of the 2-CSPD region. *First*, the support of the 2-dimensional cumulant spectral measure for purely stationary processes is constrained to a diagonal line defined by $f_1 = -f_2$ in the fourth quadrant of the 2-CSPD space. Cramer (1960) and Brillinger (1965) state this property so this idea is not new. *Second*, the support for strongly harmonizable periodically correlated processes (Gardner and Franks, 1975 and Hurd, 1989a, 1989b) or purely cyclostationary processes (PCS) is constrained to a set of equally spaced parallel lines to this stationary support set where the Euclidean line separation distance between correlated spectral components indicates the period or cycle exhibited in the data set. However, the new result demonstrated in this research is that calculated second-order cumulant spectrum estimates *not* on a purely periodic support grid are those of concern and increased interest when studying incipient wear of rotating machinery. The estimated frequency support not restricted to the fundamental periodic components and their harmonics for both stationary and

cyclostationary support sets in the 2-CSPD represent *intermodulations* of the stochastic process. These modulated frequency components are proposed to provide *additional* and *better* feature information for incipient wear signal characterization than periodic spectrum components.

3.2 Cumulant Spectra and Their Estimation

Let $x(t_1) \ldots, x(t_N)$ be N observations from a random time series sampled on $\mathrm{M} = \{n : n = 0,1,-1,2,-2, \ldots\}$. The $\{x(t_n), n \in \mathrm{M}\}$ are random variables and this notation is equivalent to $X(1), \ldots, X(N)$ with N jointly distributed random variables with a common marginal distribution and zero mean, but lower case x is used in time series literature. Consider the vector of time points

$$\vec{t} = (t_1, \ldots, t_N) \varepsilon \mathrm{M}^N$$

where $\mathrm{M}^N = \mathrm{M} \times \mathrm{M} \times \mathrm{M} \times \cdots \mathrm{M}$. Let $cum(\vec{t}/N)$ denote the Nth-order cumulant of the time series sample of any N dimensional subset $\{x(t_1), x(t_2), \ldots, x(t_N)\}$ of the jointly distributed random variables. In this notation, $cum(t/1) = E[X(t)] = E[x(t)] = 0$ for each t because common marginal distributions have zero mean. Strictly stationary processes have $cum(\vec{t}/N)$ depending only on the N-1 time points denoted by the vector $\vec{d} = (t_2 - t_1, \ldots, t_N - t_1)$. Strictly periodically correlated or cyclostationary processes have $cum(\vec{t}/N)$ depending only on the N/T time points where T denotes the period or cycle and denoted by the vector $\vec{p} = (t_1, \ldots, t_{N/T})$.

Consider the general nonstationary case and transform a vector of time points, $\vec{t}$ to its spectral representation, $\vec{f} = (f_1, \ldots, f_N)$. The Nth-order *cumulant spectrum* is now defined:

$$Cum\, S_x(\vec{f}/N) = \sum_{\vec{t}\,\varepsilon \mathbf{M}^N} cum\,(\vec{t}/N)\exp[-i2\pi(\vec{t}'\vec{f}\,)]. \qquad [31]$$

A strictly stationary process has the Nth-order cumulant spectrum replaced by the N-1th order *polyspectrum* definition:

$$S_x(\vec{f}/N-1) = \sum_{\vec{d}\,\varepsilon \mathbf{M}^{N-1}} cum\,(\vec{d}/N)\exp[-i2\pi(\vec{d}'\vec{f}_{N-1})]. \qquad [32]$$

A strictly periodically correlated process has the the Nth-order cumulant spectrum replaced by the Nth-order *periodically correlated* spectrum:

$$PC\, S_x(\vec{f}/N) = \sum_{\vec{p}\,\varepsilon \mathbf{M}^N} cum\,(\vec{p}/N)\exp[-i2\pi(\vec{p}'\vec{f}\,)]. \qquad [33]$$

Applying [32] to [31], the general relationship between cumulant spectra and polyspectra can be expressed as:

$$Cum\, S_x(\vec{f}/N) = \delta(f_1 + \cdots + f_N)\, S_x(\vec{f}/N-1), \qquad [34]$$

where $\delta(f)$ is the Dirac delta function. The RHS of [34] is zero for $f_1 + f_2 + \ldots f_N \neq 0$ due to the sifting property of delta functions. Therefore,

[34] states that correlated polyspectral components that do *not* sum to zero are represented only in the cumulant spectrum principal domain.

Similarly, applying [33] to [31], a general relationship between cumulant spectra and periodic correlated spectra can be expressed as:

$$Cum\, S_x(\vec{f}/N) = \delta(\alpha f_1 + \cdots + \alpha f_N)\, PC\, S_x(\vec{f}/N), \qquad [35]$$

where $\delta(\alpha f)$ is the Dirac delta function and $\alpha = \frac{1}{T}$ denotes the period. Again, since the RHS of [35] is zero for $\alpha f_1 + \alpha f_2 + \ldots + \alpha f_N \neq 0, \pm 1, \pm 2, \ldots$ due to the sifting property of delta functions, [35] implies that correlated periodic spectral components whose values do *not* sum to zero or any integral multiple of the periodicity are represented only in the cumulant spectrum principal domain.

Hence, periodically correlated spectra and polyspectra are both *subsets* of cumulant spectra. Stated differently, purely periodic correlated spectra are constrained to a spectral support set that is constrained to equally spaced manifolds defined by cycle frequencies that sum to zero or integral multiples of the period. Polyspectra are constrained to a spectral support set where the individual frequency variates sum to zero. In a practical approach to demonstrate these relationships different orders of stationarity, cyclostationarity, and nonstationarity are investigated. Consider first the covariance structure for the two random time variable case and its corresponding second-order cumulant spectrum domain representation.

3.2.1 Second-Order Cumulant Spectrum

Consider a zero-mean second-order continuous-time stochastic process $\mathbf{x} = \{x(t), i \in \mathbf{N}\}$ with

$$E\{x(t_1)x(t_2)\} = E\{x(t_1)x(t_1+\tau)\} = cum_2(t_1, t_2) = R_{xx}(t, \tau).$$

Assume the process is such that the expected value exists for all t and τ with $\tau = t_2 - t_1$, is not identically zero, and is continuous to avoid anomalous behavior. If the second-order cumulant is a function of the time difference, τ:

$$cum_2(t_1, t_2) = R_{xx}(t_2 - t_1) = R_{xx}(\tau)$$

then the random process **x** is weakly stationary. Now, if $R_{xx}(t, \tau)$ is periodic in t with period T for a fixed τ, then **x** is wide sense cyclostationary or periodically correlated, and the second-order cumulant function is:

$$\begin{aligned} cum_2(t_1, t_2) &= R_{xx}(t_1 + T, t_2 + T) \\ &= R_{xx}(t_1 + T, t_1 + T + \tau) \\ &= R_{xx}(\alpha t, \alpha t + \tau) \end{aligned}$$

with $\alpha t = t + T$ denoting the period.

This expectation or second-order cumulant *time* function has the following second-order cumulant *spectrum* representation:

$$\sum_{\alpha} \sum_{k=0}^{N-1} \sum_{l=0}^{N-1} E[X_k X_l] e^{i2\pi f_k(\alpha t)} e^{i2\pi f_l(\alpha t + \tau)}.$$

Using the properties of exponentiation and summing α over all possible integral multiples of the fundamental period:

$$= \lim_{T \to \infty} \sum_{\alpha = \frac{1}{T}} \sum_{k=0}^{N-1} \sum_{l=0}^{N-1} E[X_k X_l] e^{i2\pi(\alpha f_k + \alpha f_l)t} e^{i2\pi f_l \tau}$$

Now, break the triple sum into two parts, $\alpha f_k = -\alpha f_l$ and $\alpha f_k \neq -\alpha f_l$ to obtain:

$$\begin{aligned} &= \lim_{T \to \infty} \sum_{\alpha = \frac{1}{T}} \sum_{k=0}^{N-1} E\left[|X_k|^2\right] e^{i2\pi f_k \tau} + \\ &\lim_{T \to \infty} \sum_{\alpha = \frac{1}{T}} \sum_{k=0}^{N-1} \sum_{l=0}^{N-1} E[X_k X_l] e^{i2\pi(\alpha f_k + \alpha f_l)t} e^{i2\pi f_l \tau}. \end{aligned} \qquad [36]$$

Close inspection of the spectral representation of [36] reveals some important implications:

1. If **x** is a wide-sense *stationary* random process, the spectral correlation is only a function of the time shift parameter, τ. It is independent of the time parameter, t, and also the period parameter, α, so the second term of [36] vanishes or is zero. Furthermore, the period parameter does not exist in the spectral correlations. This is possible only if the random complex amplitudes, X_k and X_l are uncorrelated or $E[X_k X_l] = 0$ for *all* $f_k \neq -f_l$. Thus, stationary processes will have spectral correlation support in the second-order cumulant spectrum principal domain (2-CSPD) region constrained to $f_k = -f_l$.
2. If **x** is *cyclostationary*, spectral correlations are non-zero at integral multiples of α. This first implies that different random complex amplitudes are constrained to specific portions of the diagonal stationary support line in the 2-CSPD defined by $\alpha f_k = -\alpha f_l$. This correlation is defined as the first term of

[36] and has stationary characteristics. Periodic correlation components are also created from the second term. These are a function of αt and are *off* the support set defined by $\alpha f_k = -\alpha f_l$, but rather are constrained to a support grid in the 2-CSPD defined by: $\alpha f_k \neq -\alpha f_l$. So, cyclostationary processes also have nonstationary characteristics and provide a "bridge" between stationary and nonstationary processes. In fact, cyclostationary processes are tractable with generalizations of the tools used to study stationary processes (Cramer, 1960, Gardner and Franks, 1975, and Hurd, 1989a and 1989b).

3. If x is *nonstationary*, non-zero spectral correlation may occur not only at integral multiples of αt but rather for *any* t. Note that this general class includes cyclostationary and stationary processes as a subset. Also, only the general second-order cumulant spectrum representation captures spectral correlations beyond the various support sets defined by $f_k = -f_l$, $\alpha f_k = -\alpha f_l$, and $\alpha f_k \neq -\alpha f_l$. Correlated frequency components that are a function of any t represent modulations of the purely periodic interacting components. Also, the second term of [36] which has the periodic frequency components multiplied by the sinusoid $e^{i2\pi f_l t}$ also represent modulations and has support off the purely cyclostationary grid (see Figure 3.1 on page 72). These modulated dependent frequencies are proposed as more useful than single or coupled harmonic tones in characterizing random incipient wear processes of rotating machinery.

It is shown how cyclostationary processes have both stationary and nonstationary characteristics. More importantly, the investigation of a more powerful feature characterization of periodic signal data for wear discrimination and classification *requires* cumulant spectrum estimation. The 2-CSPD region on which estimates are computed for the joint random complex amplitude distribution is now developed.

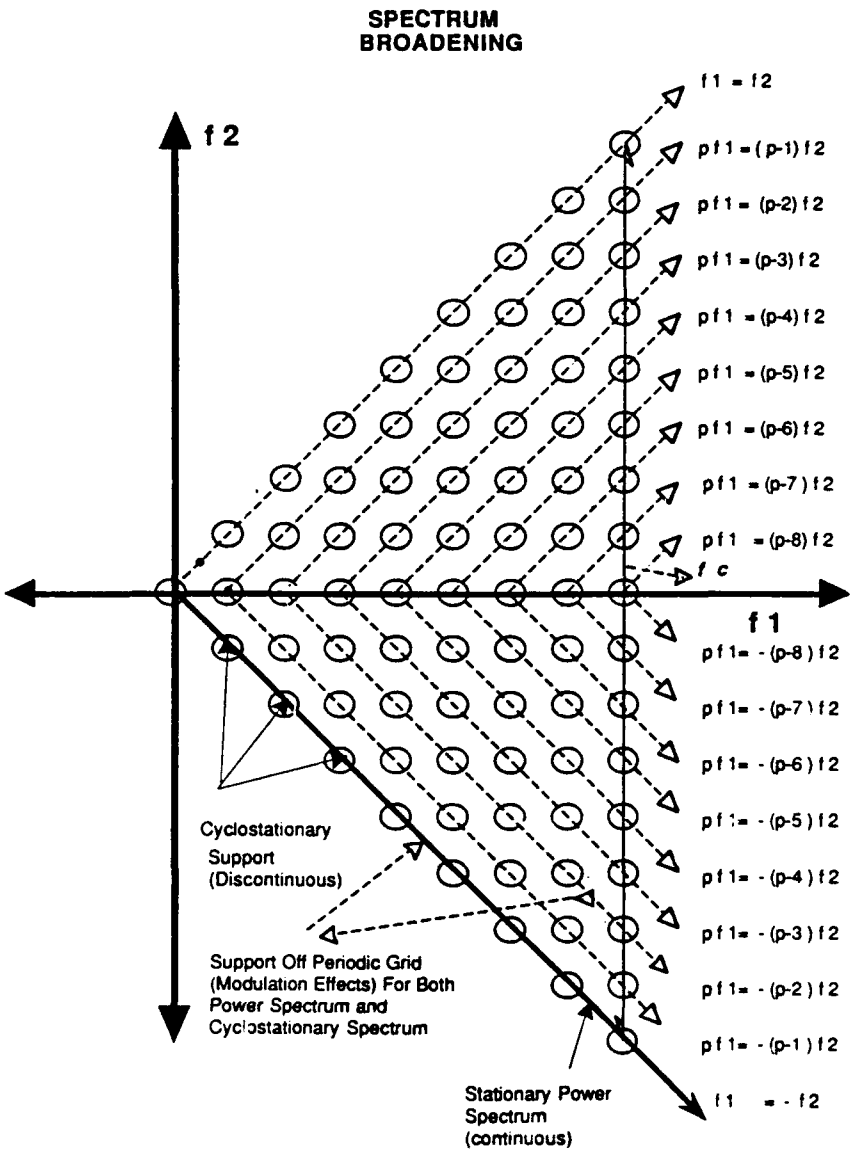

Figure 3.1: Spectrum Broadening Due to Modulation -- "Sidebands"

3.2.1.1 Principal Domain Development

Without assuming weak stationarity the continuous, second-order cumulant spectral representation of a stochastic process is:

$$Cum\, S\,(f_1, f_2) = \int_{-\infty}^{\infty}\int_{-\infty}^{\infty} c_2(t_1, t_2) e^{-i2\pi\,(t_1 f_1 + t_2 f_2)}\, dt_1\, dt_2. \qquad [37]$$

This cumulant spectrum equation defines each estimated quantity over the entire (f_1, f_2) planar region. However, it is not necessary to compute the second-order cumulant spectrum over this entire frequency plane as the Fourier transform possesses two important symmetry properties: *permutation* and *conjugation*. The 2-CSPD is defined as the minimum space on which second-order cumulant spectrum estimates are computed. The following four step process can describe the PD development for any order:

1. Apply permutation symmetry of Fourier transform (complex variates).
2. Apply conjugation symmetry of Fourier transform (real variates).
3. Combine permutation and conjugation symmetry operations.
4. Bandlimit and properly sample the process.

The 2-CSPD is now developed with a corresponding graphical depiction.

Consider $Cum\hat{S}_{xx}(f_1, f_2)$ as an estimate of the *true* second-order cumulant spectrum which is based on the continuous Fourier transform of a large but finite record length, T, of the process **x**:

$$Cum\hat{S}_{xx}(f_1, f_2) = \frac{1}{T} E\{X(f_1)\, X(f_2)\}. \qquad [38]$$

Now consider $Cum\hat{S}_{xx}(f_2, f_1)$:

$$\begin{aligned} Cum\hat{S}_{xx}(f_2, f_1) &= \frac{1}{T} E\{X(f_2) X(f_1)\} \\ &= \frac{1}{T} E\{X(f_1) X(f_2)\} \\ Cum\hat{S}_{xx}(f_2, f_1) &= Cum\hat{S}_{xx}(f_1, f_2). \end{aligned}$$

Because of this *permutation* symmetry, a 45° line divides the entire (f_1, f_2) plane into two equivalent half-planes. See Figure 3.2.

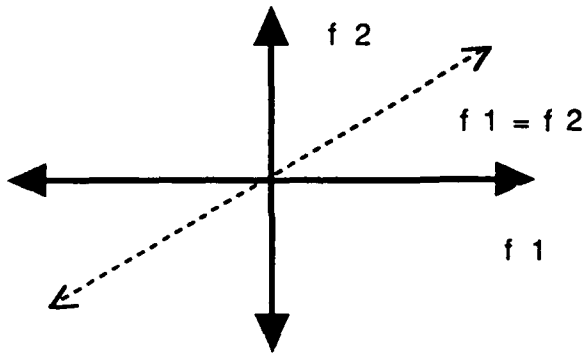

Figure 3.2: Complex Second-Order Cumulant Spectrum Principal Domain

Consider only the right half-plane. The *complex* 2-CSPD is:

$$\{f_1, f_2 : -\infty \le f_1 \le \infty, f_2 \le f_1\}.$$

Now consider $Cum\hat{S}_{xx}(-f_1, -f_2)$:

$$\begin{aligned} \hat{Cum}S_{xx}(-f_1,-f_2) &= \frac{1}{T}E\{X(-f_1)X(-f_2)\} \\ &= \frac{1}{T}E\{X^*(f_1)X^*(f_2)\} \\ \hat{Cum}S_{xx}(-f_1,-f_2) &= \hat{Cum}S^*_{xx}(f_1,f_2). \end{aligned}$$

where $*$ denotes the conjugate operation. This is the *conjugation* symmetry property. It exists because for x a real-valued stochastic process, $X(-f) = X^*(f)$. So, cumulant spectrum values in quadrants I (II) are equivalent to those estimates computed in quadrant III (IV). Consider only quadrants I and IV. See Figure 3.3.

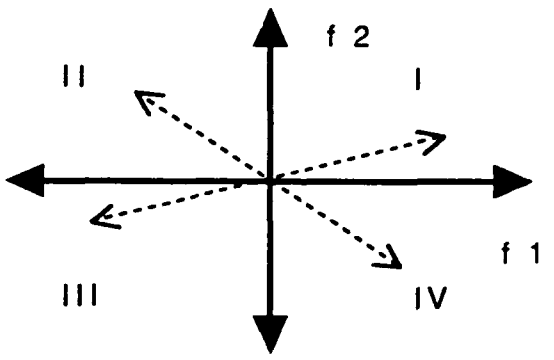

Figure 3.3: Real Second-Order Cumulant Spectrum Principal Domain (I)

Thus, the 2-CSPD for a real-valued process is:

$$\{f_1,f_2 : 0 \le f_1 \le \infty, -\infty \le f_2 \le \infty\}.$$

Now consider $\hat{Cum}S_{xx}(-f_2,-f_1)$:

$$\begin{aligned} Cum\hat{S}_{xx}(-f_2,-f_1) &= \frac{1}{T} E\{X^*(-f_2)\, X^*(-f_1)\} \\ &= \frac{1}{T} E\{X(f_1)\, X(f_2)\} \\ Cum\hat{S}_{xx}(-f_2,-f_1) &= Cum\hat{S}^*_{xx}(f_1,f_2). \end{aligned}$$

This property is due to the combination of the *permutation* and *conjugation* properties of the Fourier transform. It states that the 45° line in quadrant I and the $-45°$ line in quadrant IV are both lines of symmetry. Thus the original two frequency plane space (f_1,f_2) has been halved by the permutation property and then this half-space is split into halves again (see Figure 3.4).

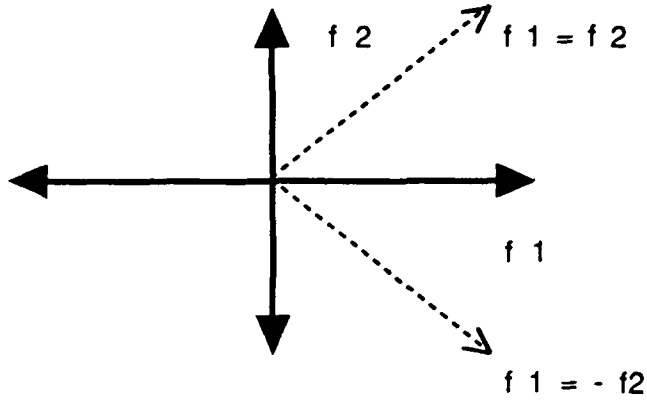

Figure 3.4: Real Second-Order Cumulant Spectrum Principal Domain (II)

Hence, both symmetry properties result in slicing the original planar region down into a quarter of its size and the reduced 2-CSPD for a real-valued **x** is now:

$$\{f_1,f_2 : 0 \le f_1 \le \infty, |f_2| \le f_1\}.$$

In actual implementation, the second-order cumulant spectrum is evaluated numerically through a digital signal processing scheme. Hence, to satisfy the well-known Nyquist sampling theorem, the stochastic process is bandlimited and sampled at of least twice the highest frequency component, f_c, to prevent aliasing. Consequently, when the auto second-order cumulant spectrum is computed, it is only necessary to compute estimates which reside in the triangular *discrete* 2-CSPD region (see Figure 3.5) defined by:

$$\{f_1, f_2 : 0 < |f_2| \leq f_1 \leq f_c\}.$$

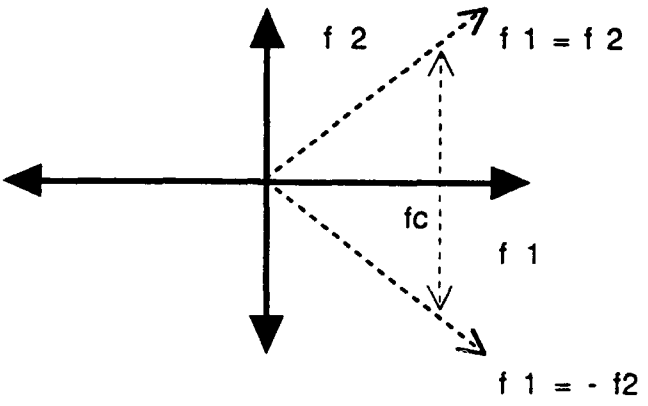

Figure 3.5: Discrete Second-Order Cumulant Spectrum Principal Domain

The same four step process can be applied to each succeedingly higher dimension. For the third-order cumulant spectrum:

$$Cum\, S\,(f_1, f_2, f_3\,) = \int_{-\infty}^{\infty}\int_{-\infty}^{\infty} c_3(t_1, t_2, t_3) e^{-j2\pi\,(\,t_1 f_1 \,+\, t_2 f_2 \,+\, t_3 f_3\,)}\, dt_1\, dt_2\, dt_3, \quad [39]$$

each estimated quantity is defined over the entire (f_1, f_2, f_3) cubic frequency space. However, estimates need only be computed in the *discrete* 3-CSPD region defined by:

$$\{f_1, f_2, f_3 \; : \; 0 < |f_3| \leq f_2 \leq f_1 \leq f_c\}.$$

The graphical depiction of principal domain regions in higher dimensions is more difficult. Fortunately, a picture is not required by the computer to calculate the estimates.

3.2.1.2 Estimation Procedure

This section describes the computational procedure to compute estimates for the second-order cumulant spectrum (2-CS) from the direct discrete Fourier transforms (DFTs) of finite record lengths. The procedure is basically an extension of procedures for computation of traditional power spectra and it will be shown that 2-CS estimates are computed from multiplying two discrete complex amplitude spectral density functions. The same procedure can be followed for computing estimates for the third-order cumulant spectrum (3-CS) except that three complex amplitude spectral density functions are multiplied and are computed over a different principal domain region.

Begin with [38] which expresses $\hat{CumS}_{xx}(f_1, f_2)$ in terms of expectations of two random complex amplitude functions: $X(f_1)$ and $X(f_2)$. Performing the expectation operation of random variables requires knowledge of an appropriate probability density function which in most experimental studies is unknown. Thus, ensemble averaging over a sequence of sample 2-CS is the approach for estimating

the expectation of the two complex random variables. Consider N identical independent trials or runs of an experiment. Each run yields an outcome denoted by $x_f^{(k)}(t)$, where $k = 1, 2, \ldots, N$. The collection of individual realizations defines the ensemble of a particular stochastic process. If it is impractical or too costly to gather a large number of realizations of a particular stochastic process by repeating the experiment N times, there is another way to obtain more samples. If the time duration of the original data record is long enough, it may be subdivided into individual frames of sufficient length to maintain independence and subsequently improve the quality of the estimates. Of extreme importance with processing time series data from periodic phenomena is definition of the frame length as an integral multiple of the fundamental rotational frequency of the process being studied. Also, another constraint when characterizing incipient faults is to capture at least two fundamental periods. This is the lower bound as frequency resolution of sampled estimates is given by $\nabla f = 1/T$ where T is the processed record length. Frame lengths defined in this manner will capture modulations of the specified periodic frequency which have been found to help characterize incipient wear states. No data windowing techniques are needed to reduce the effects of leakage if an integral number of periods or cycles are captured with the defined frame lengths.

So consider the set of N realizations or records for $\mathbf{x}$, each record being T seconds long. Each realization sampled with sampling interval t_s, and consists of $N = T/t_s$ samples. T and N are determined from considerations previously discussed. Let $\mathbf{x}^{(k)}[n]$ represent the k^{th} sampled realization and $X^{(k)}[l]$ the corresponding DFT of $\mathbf{x}^{(k)}[n]$. On the basis of [38], the appropriate estimate of the k^{th} sample 2-CS is:

$$CumS_{xx}(f_1, f_2) = \frac{1}{T} X_T^{(k)}(f_1) X_T^{(k)}(f_2). \qquad [40]$$

Consider the values of the CFTs at $f_l = l\nabla f$ where $\nabla f = 1/T$. Then [38] becomes:

$$CumS_{xx}(f_{l1}, f_{l2}) = \frac{1}{T} X_T^{(k)}(f_{l1}) X_T^{(k)}(f_{l2}).$$

Now, the sample values of the CFTs in terms of their respective DFTs are:

$$X_T^{(k)}(f_l) = \frac{X^{(k)}[\,l\,]}{\nabla f}, \qquad [41]$$

so expression of the continuous auto 2-CS in terms of its discrete auto 2-CS is:

$$CumS_{xx}^{(k)}(f_{l1}, f_{l2}) = \frac{CumS_{xx}^{k}[l_1, l_2]}{\nabla f^2}. \qquad [42]$$

Substituting [41] and [42] into [40] to obtain the sample discrete auto 2-CS:

$$\frac{CumS_{xx}^{(k)}[\,l_1, l_2\,]}{\nabla f^2} = \frac{1}{T} X_T^{(k)} \frac{l_1}{\nabla f} X_T^{(k)} \frac{l_2}{\nabla f}.$$

The final estimate of the discrete auto 2-CS is found by ensemble averaging over all N realizations of the stochastic process studied:

$$\hat{CumS}_{xx}[\,l_1, l_2\,] = \frac{1}{N} \sum_{k=1}^{N} CumS_{xx}^{(k)}[\,l_1, l_2\,]. \qquad [43]$$

Note that if $\mathbf{x} = \{x(t), t \in \mathbf{N}\}$ is in volts, then the 2-CS estimate has the dimensions of volts^2 and represents spectral components of two dimensional bandwidth centered at f_1 and f_2 contributing to the mean square value of the stochastic process.

It is important to mention that estimates of succeedingly higher orders of cumulant spectra are found by a procedure similar to the one described for the second-order case. The only difference is the number of DFTs being multiplied over a correspondingly dimensioned PD region. Pseudo-code for second-order cumulant estimation of cyclostationary time series is given below and the actual FORTRAN program is at Appendix A.

Procedure Second-Order Cumulant Estimation

Receive valid time series input parameters (# samples, sample rate, block length)

Load time series data into FFT work array

Calculate statistics (moments and cumulants) and subtract mean from data

While data blocks exist **do**

a) Subtract block mean from data
b) Perform DFT
c) Calculate Second-Order Cumulant Spectrum (double complex product)
d) Accumulate Chi-Squared Statistics over 2-CSPD

End Do

Output block summary statistics and correlations and Global Statistics

END

Valid parameters imply that sufficient working storage space is defined to handle the amount of samples in the time series and also the chosen block length is *at least twice* the fundamental frequency of the system. Two or more fundamental periods in a processed data block will calculate second-order cumulant es-

timates which correspond to intermodulation effects or nonstationary characteristics of the random fault mechanism. Breaking the entire time series record into proper block lengths is a method to increase estimation reliability by decreasing estimate variability.

3.2.1.3 Reliability of the Estimates

Because of inter-machine variability, time series estimates of the stochastic process under study are not perfect. Estimator quality is usually defined by its bias and variance. Bias, b, is the difference in expected value of the estimator and the "true" value:

$$b = E[\hat{\phi}] - \phi,$$

and so an estimator is unbiased if $E[\hat{\phi}] = \phi$. Variance is the spread in value about the expected value:

$$\begin{aligned} V[\phi] = \sigma^2 &= E[(\hat{\phi} - E[\hat{\phi}])^2] \\ &= E[\hat{\phi}^2 - 2\hat{\phi}E[\hat{\phi}] + E^2[\hat{\phi}]] \\ &= E[\hat{\phi}^2] - 2E[\hat{\phi}]E[\hat{\phi}] + E^2[\hat{\phi}] \\ &= E[\hat{\phi}^2] - E^2[\hat{\phi}]. \end{aligned}$$

So, estimator variance is equal to mean square value of the estimator minus the square of the mean of the estimate. Now, consider mean square error which is defined as the following and can be derived through expansion of the expectation operation:

$$\varepsilon^2 = E[(\hat{\phi} - \phi)^2] = \sigma^2 + b^2.$$

Assume that the realizations are independent and that the process is ergodic. Then with bar notation meaning expectation:

$$\begin{aligned}
\overline{Cum\hat{S}_{xx}[\, l_1, l_2\,]} &= \frac{1}{N}\sum_{k=1}^{N} \overline{CumS_{xx}^{(k)}[\, l_1, l_2\,]} \\
&= \frac{1}{N}\sum_{k=1}^{N} \overline{CumS_{xx}[\, l_1, l_2\,]} \\
&= \frac{1}{N} N CumS_{xx}[\, l_1, l_2\,] \\
&= CumS_{xx}[\, l_1, l_2\,].
\end{aligned}$$

and hence the estimator in [42] is unbiased. Also, [42] has a variance given by:

$$Var\{Cum\hat{S}_{xx}[\, l_1, l_2\,]\} = \frac{1}{N} CumS_{xx}^2[\, l_1, l_2\,],$$

so that the variance decreases with the number of realizations. This agrees with one's intuition that averaging of more realizations of random processes creates better estimators.

Chapter 4

HOS Feature Extraction

4.1 Introduction

A feature extraction algorithm is developed to exploit the additional information provided by the power spectrum and the HOS transformations of raw time series data. Several thousands of spectral estimates are usually generated for a particular time series analysis application so a finite subset of the spectral estimates, or features, are chosen from the entire collection of spectral measurements to provide "optimum" classification results. There are three reasons for investigating alternative estimation and feature extraction methods and evaluating their classification results rather than using only one type of spectral analysis approach. *First*, there is a cost for performing many different types of spectral estimation procedures and their subsequent feature extraction. Actual computing time to perform HOS estimation is *not* the most prohibitive factor; it is the feature extraction process and subsequent classification that takes time and additional computing. It is possible that power spectrum estimation and feature extraction may provide sufficient classification performance for a particular application. However, performing HOS estimation and feature extraction can be worthwhile if it *improves* the overall classification performance of the power spectrum-based approach. Proper HOS transformations of the raw time series can lead to more effective decision surfaces because of the more accurate representation of the

stochastic process structure being studied. *Second*, reducing the dimensionality of the feature space eliminates redundancy as variables which do not add to the classification accuracy are not included in the final decision rules. *Third*, a lower misclassification rate is sometimes achieved by using fewer feature variables. Further discussion of this topic is in the next section. The significant outcome of the feature extraction process is the exposure of the individual spectral feature variables and their *combinations* in measuring differences of multivariate populations. Thus, the HOS feature extraction approach is not only *multivariate*, but also *multispectral*.

4.2 Features and Their Relationship to Misclassification Rate

Previous pattern recognition research observed for a given design set, increasing the number of feature variables, d, causes classification performance to initially improve, but then to deteriorate (Hand, 1981). This occurs because the decision surface better fits the design set with increasing d but generalizes less well to new samples since the design set became more sparsely distributed and less representative of the class-conditional pdfs. Hand (1981) explains this phenomenon using Hotelling's T^2 statistic.

Hotelling's T^2 statistic, the distance between two sample means relative to the dispersion within the samples is:

$$T^2 = \frac{n_1 n_2}{n} (\bar{x}_1 - \bar{x}_2)' V^{-1} (\bar{x}_1 - \bar{x}_2) = \frac{n_1 n_2}{n} D^2,$$

where $\bar{x}_i$ is the mean for class ω_i, V is the assumed common variance-covariance matrix, and D^2 is the squared Mahalanobis distance measure defined in the background chapter. To investigate multivariate population differences, the question asked is how often is T^2 observed as large or larger than the T^2 estimated from the samples if the two populations are identical? The statistical criterion value defined by:

$$J = \frac{n-1-d}{(n-2)d} T^2$$

is compared with the F distribution with d and (n-1-d) degrees of freedom. If the probability of a large T^2 is sufficiently low, one can conclude, with a certain risk of error, that the populations are distinct.

Now, T^2 changes as d, number of measurement or feature variables, increases (Liddell, 1977). Consider each feature variable as independent of every other feature variable and the standardized difference between the sample means is some constant, k , for each variable. This allows $D^2 = k^2 d$ and thus:

$$J = (n-1-d)n_1 n_2 k^2 d/(n-2)dn$$

$$= \frac{(n-1)n_1 n_2 k^2}{(n-2)n} - d\frac{n_1 n_2 k^2}{(n-2)n}. \qquad [44]$$

[44] is a linear function of d, *decreasing* as d *increases*.

Van Ness and Simpson (1976) and Van Ness (1979) studied the rate at which D^2 must increase as d increases in order to maintain a constant or decreasing error rate. They analyzed data from normal populations and compared three parametric and two non-parametric classification algorithms. For each classifier,

they produced plots to determine the discriminatory power lost by increasing d with D^2 fixed, and how much D^2 must increase in order to justify increasing d. Their results showed that the non-parametric algorithms were quite stable at high dimensions, and also outperformed the parametric algorithms at smaller dimensions. Nevertheless, feature extraction is necessary to "squeeze" the most information from a stochastic process with the least amount of variables. Some existing feature extraction approaches were examined for use in this work.

4.3 Existing Feature Extraction Approaches

Algorithmic approaches for finding a feature space spanned by a subset of the original measurement space are categorized into two major areas: selection and transformation. Feature variable selection is appropriate if cost or other factors present prevent all of the original set of features to be measured and used; it is a combinatorial analysis problem. When all the variables can be measured, variable transformation is performed but increased reliability occurs if a lower dimensional space is used. Variable transformation approaches include linear and non-linear techniques. Both approach categories assume the number of potential features is much less than the number of training samples. This was not the case with experimental time series cases analyzed in this research. Consequently, a *hybrid* approach was developed in this work. Before describing this hybrid approach, existing selection and transformation methods are given as some of their aspects are incorporated in the HOS feature extraction process.

Selection of a subset from the complete set of variables is approached with exhaustive search, branch and bound, and stepwise methods. Exhaustive

search methods are only feasible when d is quite small. The major problem with exhaustive search methods is how to test the many possible sets without the large number of tests invalidating the significance level of each test. Branch and bound algorithms accelerate the search of all variable sets but do not explicitly evaluate all of them. Branch and bound is usually used on problems where the number of possibilities evaluated increases exponentially with some fundamental parameter of the problem. Unfortunately, even though branch and bound techniques slow down the growth rate of possibilities, it remains exponential. Thus, suboptimal search methods such as sequential forward selection and backward elimination approaches are also used. Kittler (1978) gives empirical comparisons of these two stepwise methods and extensions such as his generalized plus l-take away r selection algorithm. This approach finds the particular l-dimensional subset of those variables not yet added which, when combined with the current set, leads to the greatest J statistic [44]. Then each step examines the selected set to identify those r variables, when discarded, reduce J by the least. His general conclusions were that selection and backward selection methods which select/reject several variables simultaneously were better than methods which select/reject one variable at a time. Additionally, forward selection of two variables and backward deletion of one variable gave the best results and was computationally favorable with branch and bound methods. Since stepwise methods could continue indefinitely if computation time is not a constraint, stopping criteria such as a test statistic given by Rao (1970) tests whether an extra $(d - d')$ variables makes a significant contribution to the discrimination task.

Variable transformation methods include canonical discriminant analysis (CDA) which finds a set of axes spanning a subspace of the complete space where

class separability is maximized. CDA is done in a similar fashion as principal component analysis (PCA) for summarizing total variation. But, with PCA, only one data set is analyzed, while CDA analyzes at least two data sets. PCA also subtracts means so it is an analysis of variance/ covariance. CDA also does a PCA of class variable means. Variables used for canonical discriminant computation need to have an approximate multivariate normal distribution within each class and a common covariance matrix. However, a linear discriminant boundary may be determined by a least squares argument without the assumption of normality and common dispersions of the two parent distributions (Kendall et al., 1983). If it is the case that the multivariate normality assumption is unjustified, non-linear feature extraction methods have also been developed (Fukunaga and Ando, 1977).

4.4 New Hybrid Approach

When the number of potential feature variables is much greater than the sample size, a hybrid approach that attacks such problems in stages is necessary (Jain and Dubes, 1978). The HOS feature extraction algorithm is composed of three stages. *First*, visual plots of ensemble averaged spectra and their differences between groups are generated after each respective spectral estimation process to obtain a rough idea of which estimates to use as possible feature variables. This is the *graphical variable selection* stage. Hinich and Clay (1968) describe the general procedures followed for frequency domain estimation of a time series record. The statistical tests of linearity and Gaussianity of a time series (Hinich, 1982) are extended for use with second-order cumulant spectrum estimates. The modulus

of the second-order cumulant spectrum and bispectrum estimates are statistically transformed to chi-square values for subsequent use as feature measurements. Hinich (1989) describes the statistical transformation process for bispectra moduli. All types of spectral estimates are ensemble averaged for the frequency variates of the particular spectral function after estimation of all time series records used for training function computation is performed. *Second*, univariate analyses of variance are performed and the resulting F-statistics are plotted for the corresponding frequency principal domains of each spectra type to confirm visual differences seen in the ensemble averaged plots. Spectral variables shown to be good candidates for the feature set are selected based on their F value. Only the top ten of each spectra type are chosen as potential feature variables. This second stage is a *dimension reduction* step to reduce each individual spectral space to representative variables. *Third*, a conventional variable selection algorithm, stepwise selection of variables available in SAS 6.0,[1] a statistical analysis software package, is applied using the thirty spectral variables identified from the second stage. Stepwise discriminant analyses are performed to obtain the best linear (power spectrum) discriminators, the best nonstationary (second-order cumulant spectrum), the best quadratic (bispectrum) discriminators, the best linear and nonstationary discriminators, etc., so the important relationships of the *reduced* and *combined* spectral feature space are considered. The "optimum" individual spectral feature sets composed of ten potential feature variables, either power spectrum, bispectrum, or second-order cumulant spectrum feature sets, are found to be average discriminators by themselves. However, when the different spectral

[1] SAS is a registered trademark of the SAS Institute, Inc.

feature sets are combined according to certain statistical criteria, their *discrimination* and *classification* power significantly increase (see Chapter 5).

This hybrid feature extraction approach generates ensemble averaged plots, F-test plots, and "optimum" feature sets. Once feature extraction for the various types and combinations of spectra is complete, marginal and sensitivity studies are conducted on simulated and actual time series to test and evaluate the different approaches.

Before the HOS feature sets are presented and discussed for the simulated and actual experimental data, statistical test results of raw time series from the *actual* wear database are given. Bispectrum statistical tests are employed to investigate if the observed time series records are consistent with the hypothesis that the underlying stochastic process has a Gaussian distribution, and whether the process contains evidence of nonlinearity in the underlying physical mechanisms generating the observed vibrations. The sample bispectrum is the two dimensional Fourier transform of the expected value of the vibration signal at three time points, and should be a standardized normal random variable if the process is stationary, linear, and Gaussian (Hinich, 1982). Shown at Table 4.1 on page 92 and Table 4.2 on page 92 are the results from applying the Hinich linearity and gaussianity tests to the two bit classes for each stack/load time series.

Table 4.1

Gaussianity and Linearity Test Statistic Results For New Bits--Actual Wear Experiment. The Z statistic is a normal approximation of the central chi-squared variate with large degrees of freedom. It is a N(0,1) random variable under the null hypotheses of a Gaussian and a linear process.

Time Series (Stack/Load)	Gaussianity Statistic (Z) Mean	Std	Linearity Statistic (Z) Mean	Std
NIP/3	54.2	39.7	54.8	42.4
NIP/4	356.4	212.9	367.2	216.2
6S2P/3	40.8	32.1	40.2	35.8
6S2P/4	186.9	183.9	192.4	189.4

Table 4.2

Gaussianity and Linearity Test Statistic Results For Slightly Used Bits--Actual Wear Experiment. The Z statistic is a normal approximation of the central chi-squared variate with large degrees of freedom. It is a N(0,1) random variable under the null hypotheses of a Gaussian and a linear process.

Time Series (Stack/Load)	Gaussianity Statistic (Z) Mean	Std	Linearity Statistic (Z) Mean	Std
NIP/3	105.4	67.4	108.4	69.3
NIP/4	358.7	326.1	367.0	332.4
6S2P/3	56.8	43.9	56.5	47.9
6S2P/4	237.3	229.3	229.9	192.8

These global test statistics show that the drill spindle vibration time series for the Z accelerometer are definitely *non-Gaussian* and *nonlinear* for both new and slightly used drill bits. Also, the ensemble averages and standard deviations of both statistical measures are higher for slightly used bits than new bits. Possibly, the increased nonlinear and non-Gaussian structure of slightly used bit spindle

vibrations are due to bit wear mechanisms such as flank or rake wear changing the geometry of the bit cutting surface and causing the thrust forces to increase. Possibly incipient bit wear causes more significant frequency coherence at certain frequency components. Also Table 4.1 on page 92 and Table 4.2 on page 92 reveal as more panel stack material is cut with each revolution of the drill (4 mil/rev versus 3 mil/rev), higher statistical values are obtained which correspond to the increased "strength" of the interacting frequency components. Thus, these *global* statistical measures are corresponding to the actual physics of the circuit card cutting process.

4.5 Results

Even though the global Hinich statistical measures are indicative of class distinguishability, feature extraction emphasis is on the statistical selection of *particular* linear, nonstationary, and nonlinear spectrum estimates for subsequent input to an efficient classification algorithm. The ultimate aim is to reveal features of a consistent relationship that have good classification performance. The selected features can then potentially provide a deeper understanding of the physics of a particular physical process under study. Hence, the desired properties of extracted features in order of priority are:

1. consistent classification performance,
2. physically interpretable with some correspondence to the physics of the stochastic process, and
3. good visual discrimination ability.

Feature extraction results are given generally for the simulation scenarios and then details for all the database partitions of the actual experiment are given in tabular format. (The simulated and actual wear experiments are described in Chapter 5). Feature extraction results will confirm the research hypothesis that HOS features, and particularly estimates of the second-order cumulant spectrum *not* part of the purely periodic support grid within the 2-CSPD region provide better features for incipient wear characterization.

Simulation feature extraction results for all the scenarios (see Table 5.1 on page 115) are summarized as particular frequency values do not have any physical meaning. The final HOS extracted feature sets for all simulated scenarios were composed of twenty-eight power spectrum, fifty-one bispectrum, and twenty-five cumulant spectrum feature variables. For each particular scenario, the number of HOS features was larger than the number of power spectrum features and had a higher statistical significance level. Most significantly, *twenty-one* of the twenty-five, or 84 percent, of the second-order cumulant spectrum variables were off the pure cyclostationary support grid in the 2-CSPD. These features were also in the middle to highest ranges of statistical significance with relation to the other features selected. Thus, evidence from simulations weighs in favor that incipient wear characterization is enhanced by performing cumulant spectrum estimation and feature extraction. The *real* test of the hypothesis will be examination of feature extraction results from actual wear data.

Visual inspection of each type of ensemble averaged spectral plots for the two classes of drill bits give a preliminary look of which frequency variates are bit class distinguishable. See Figure 4.1 on page 96 and Figure 4.2 on page 97 for ensemble averaged power spectrum plots and ensemble averaged bispectrum

chloropleth plots for *new* drill bits for a particular case of the actual wear data described in Chapter 5. Also, see Figure 4.3 on page 98 and Figure 4.4 on page 99 for ensemble averaged power spectrum and ensemble averaged bispectrum plots for *slightly used* drill bits of the same case.

These individual plots, Figure 4.1 on page 96 and Figure 4.3 on page 98, and Figure 4.2 on page 97 and Figure 4.4 on page 99, of the different drill bits are combined so that differences in spectrum estimates for the two groups are more visually apparent. See Figure 4.5 on page 100 and Figure 4.6 on page 101 for representations of the differences in ensemble averaged power spectrum and ensemble averaged bispectrum.

Overlaying the representations of the two ensemble power spectrums and their variability serves its purpose as a preliminary look at what *range* of frequencies are bit class distinguishable. Differences in ensemble averaged power spectrum plots for all four stack/chip load cases were quite similar as that shown in Figure 4.5 on page 100. Power spectra exhibited the presence of strong spectrum peaks at frequencies below 5 kHz. These peaks occurred at the shaft spindle rotational frequency, f_o, and its harmonics, $2f_o$ and $4f_o$, and reflect the periodic cutting forces due to hardness differences of the glass and epoxy material in the circuit card layers. Most of the signal content occurs at the harmonic frequencies and do not appear useful as outstanding wear indicators. However, there are two frequency ranges which *visually* appear useful as potential wear indicators: frequency values near one-half the fundamental rotational frequency of the drill spindle, $.5f_o$, and between 14-14.5 kHz. Other researchers have noted this subharmonic structure with journal bearings in high-speed turbomachinery, sometimes referring to it as a *whirl* frequency (Braun, 1986). This may be due to less

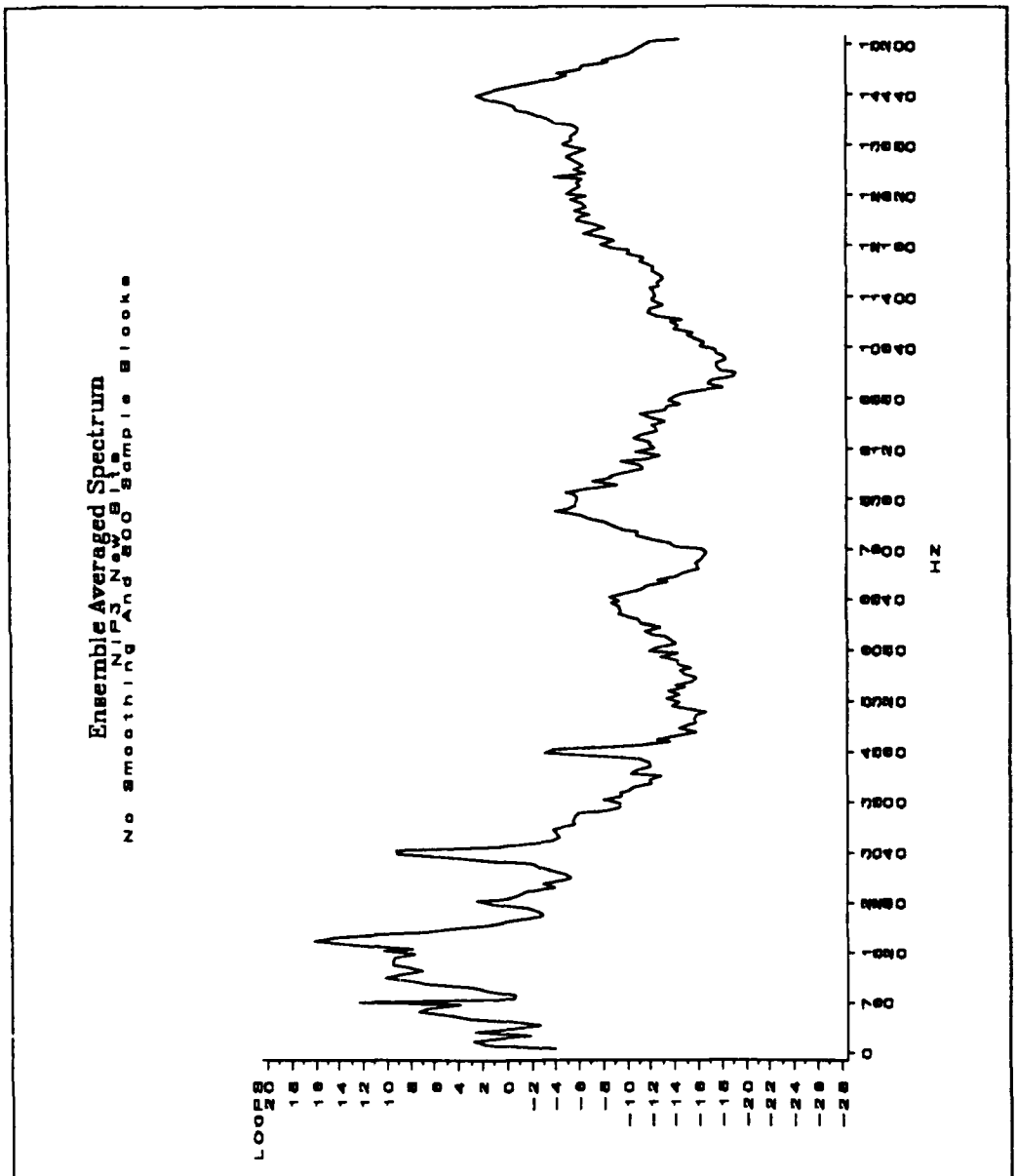

Figure 4.1: Ensemble Averaged Power Spectrum--NIP3 Case (New Drills). No smoothing performed with a block size of 800 samples.

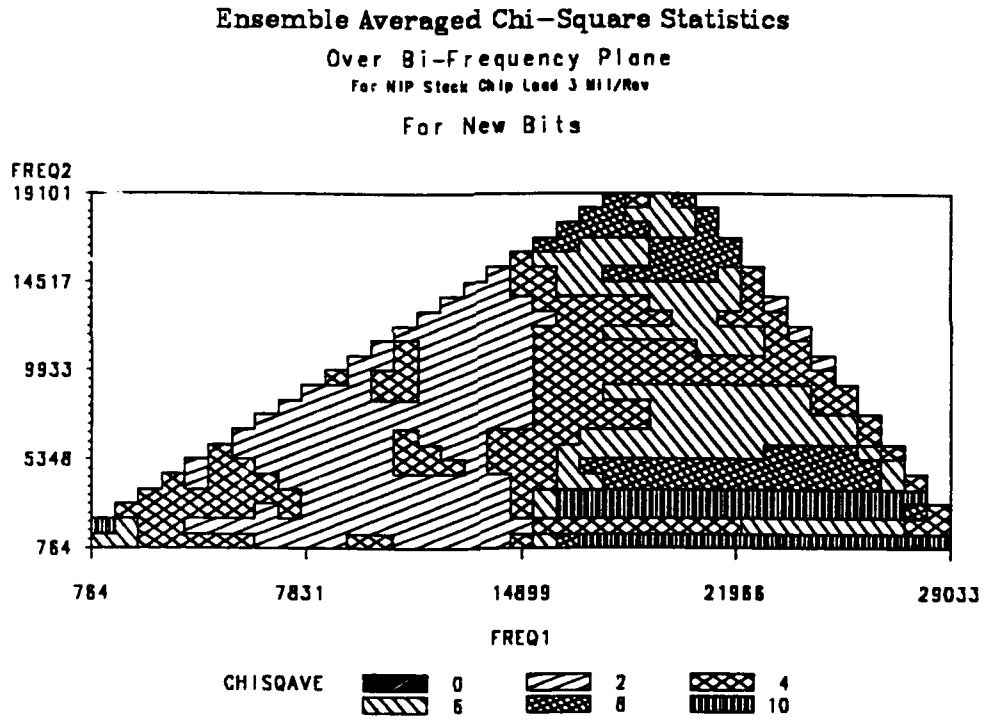

Figure 4.2: Ensemble Averaged Bispectrum--NIP3 Case (New Drills). Ensemble averaged chi-square statistical measures are transformations of bispectra moduli or squared gain. Legend defined shows the magnitude of the chi-square statistic denoting frequency interaction strength. No smoothing performed with a sample block size required to capture *two* integral periods of the process.

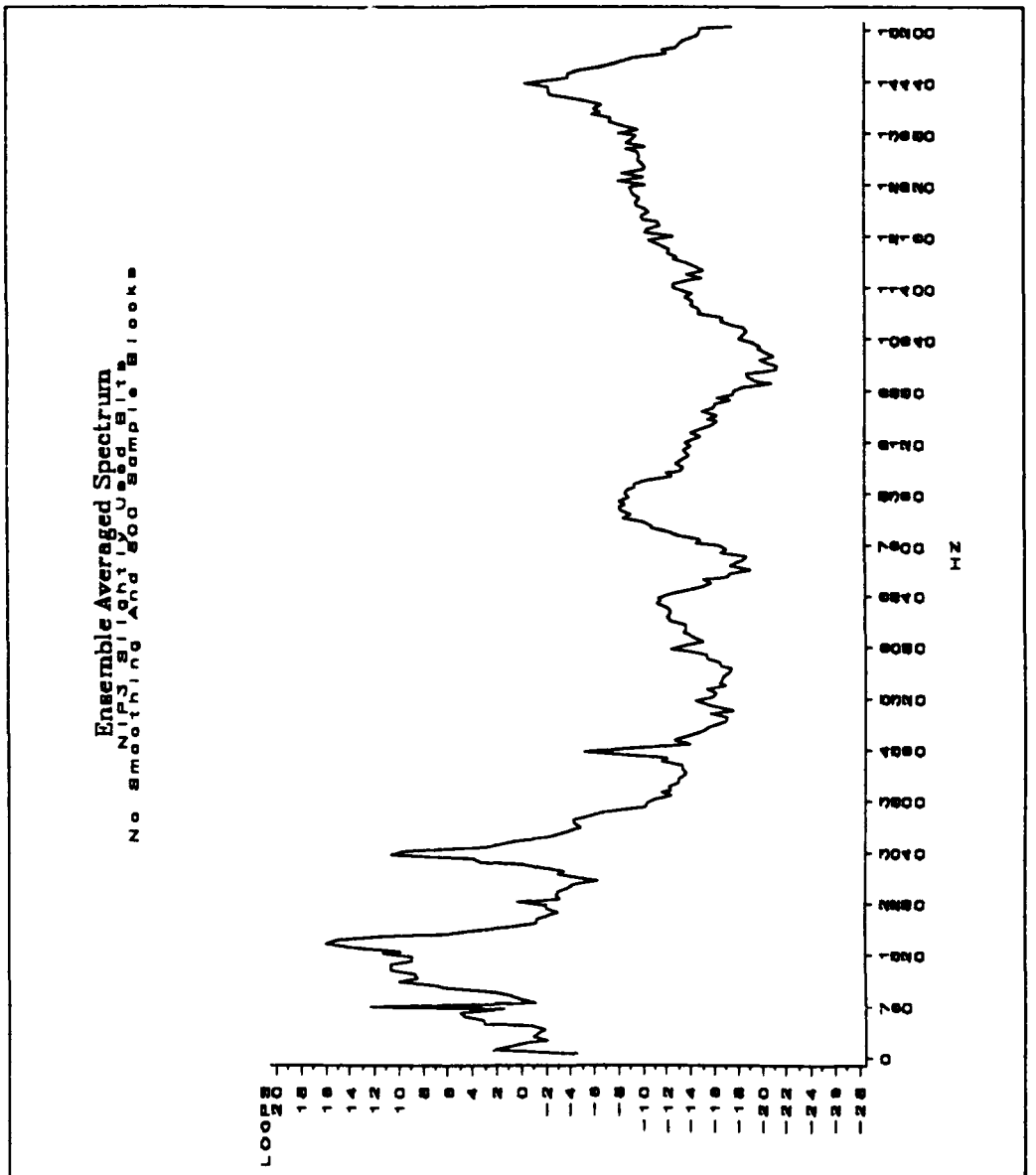

Figure 4.3: Ensemble Averaged Power Spectrum-NIP3 Case(Slightly Used Drills). No smoothing performed with a block size of 800 samples.

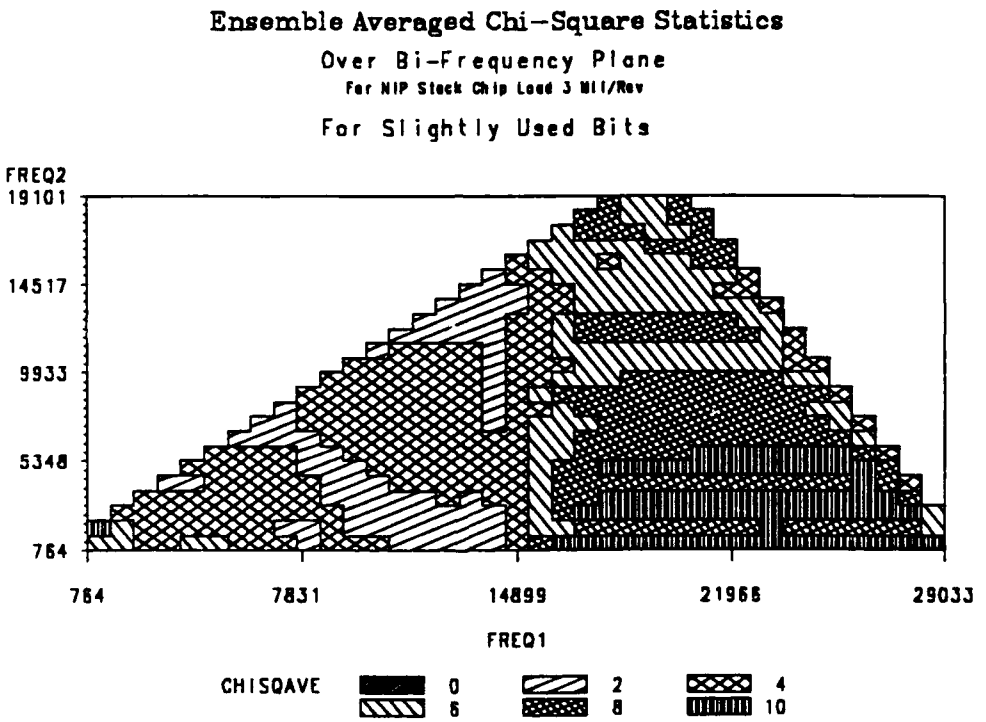

Figure 4.4: Ensemble Averaged Bispectrum--NIP3 Case (Slightly Used Drills). Ensemble averaged chi-square statistical measures are transformations of bispectra moduli or squared gain. Legend defined shows the magnitude of the chi-square statistic denoting frequency interaction strength. No smoothing performed with a sample block size required to capture *two* integral periods of the process.

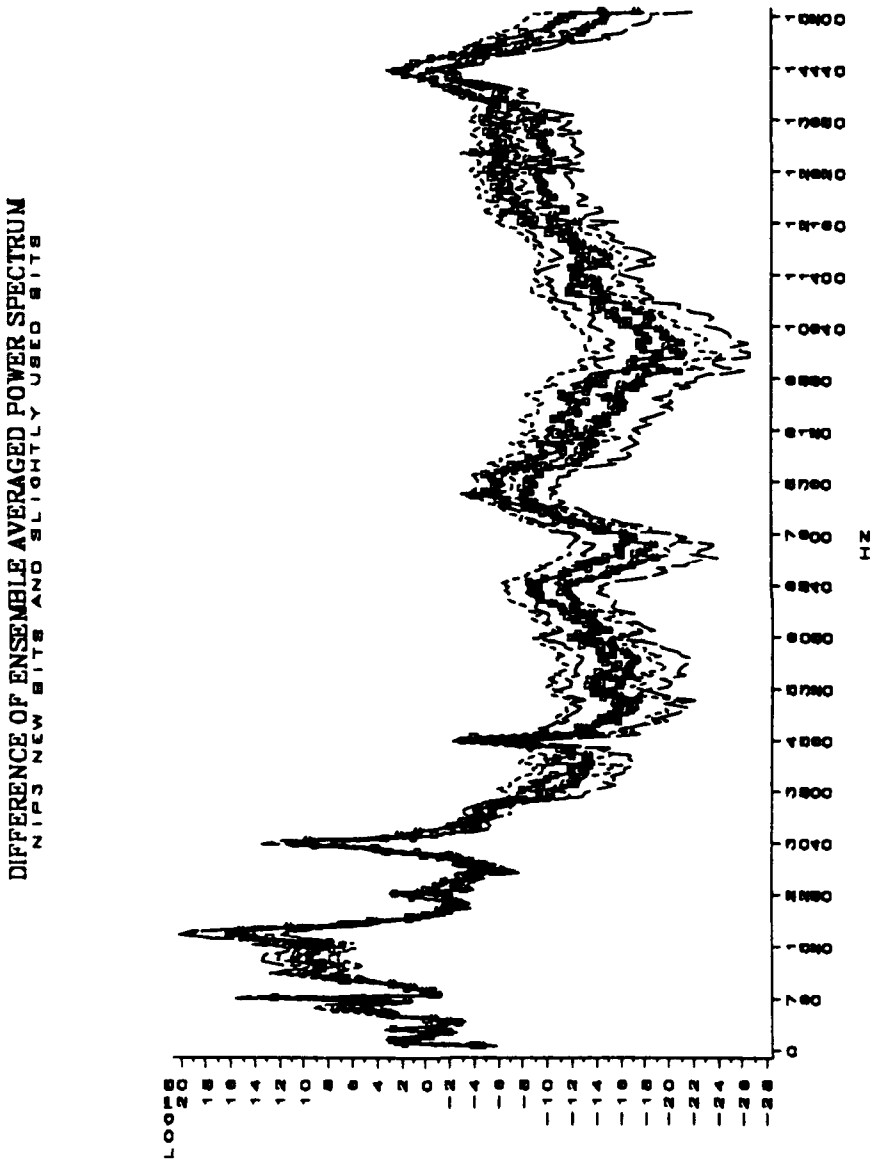

Figure 4.5: Ensemble Averaged Power Spectrum Differences--NIP3 Case. New bit ensemble average is denoted by squares and slightly used bit ensemble average by circles. Small dashes are 95 percent confidence limits for new and larger dashes are those for slightly used. No smoothing performed with a block size of 800 samples.

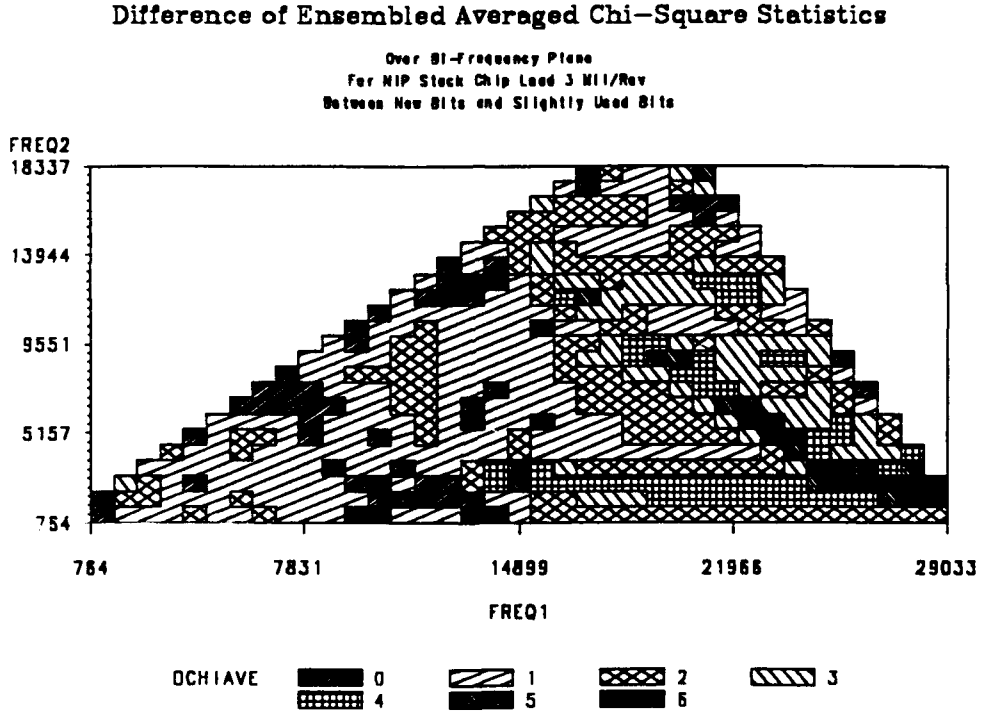

Figure 4.6: Ensemble Averaged Bispectrum Differences--NIP3 Case. Differences in ensemble averaged chi-square statistical measures are transformations of bispectra moduli or squared gain. Legend defined shows the magnitude of the chi-square statistical differences of frequency interactions. No smoothing performed with a sample block size required to capture *two* integral periods of the process.

frictional forces of a slightly worn drill bit. The higher range of frequency values are near a *torsional resonant* frequency of the drill spindle. As the top portion of the spindle rotates in one direction, its body rotates the opposite direction (see Figure 5.3 on page 127). The spindle rotation causes the drill bit to *slightly* go up and down during the drilling process. It appears the spindle torsional mode is more strongly excited by new drills than slightly worn drills. A decaying torsional oscillation excited by contact of worn cutting surfaces of the drill is physically intuitive.

The bispectrum difference chloropleth plots *clearly* show the general regions and the particular frequency interaction *pairs* that are class distinguishable. Differences in ensemble averaged bispectrum chloropleth plots for all four stack/chip load cases are similar to Figure 4.6 on page 101. Differences of ensemble bispectrum chi-square values first show drill class distinguishability in frequency interaction regions composed of *first* through the *eighth* harmonics of the fundamental rotational frequency of the drill spindle with frequencies greater than 14 kHz. A portion of this significant different frequency structure may be due to parametric coupling of the torsional resonant frequency with each of its lower harmonics. This fact is *significant* as Ramirez (1991) discovered from his analysis of *extended* drill wear data that the fifth through the eighth *power spectrum* harmonics of the same accelerometer (Z or thrust axis) are the most sensitive drill wear indicators. Thus, a *predictive* capability may have been demonstrated with bispectrum analysis of the incipient wear data. Also significant is that for all the stack/load cases, bispectrum estimates are most significantly different in the outer triangle (OT) region of the bispectrum principal domain. This was evidence and motivation for further investigation with cumulant spectrum estimation and fea-

ture extraction as it meant the existence of a nonstationary generating source in the stochastic process (Hinich, 1989).

Extracted second-order cumulant spectrum features were consistently not on the pure cyclostationary support grid in the 2-CSPD which confirms the major theoretical proposition stated in Chapter 3. Furthermore, they were *always* the most significant feature variables for all but one of the eight actual wear database partition cases (NIP4). Significantly, the NIP4 is the only database partition where no overall marginal improvement in discrimination and classification power was obtained by incorporating HOS feature information. This fact adds further evidence that better incipient wear characterization is provided with 2-CSPD estimates *off* the cyclostationary support grid. Consider the following physical explanation why these statistical correlations discovered by the feature extraction algorithm are most important. Cards were manufactured in the same facility with the same resin system but had *different* glass cloth and layer thicknesses. See Figure 4.7 on page 104 for two examples of card construction. Because the glass fibers (oval disks in diagram) cut during each hole are not uniformly configured in the card layers, the vibration signals will have periodic and *aperiodic* characteristics and reflect the effects of many different cutting geometries randomly encountered by the drill. So the cutting forces and energy represented by the vibration measurements change within a certain layer of the card and also for each revolution of the drill. Vibration measurements carrying wear information of the drill cutting edges will thus be more sensitive to spectral correlations that are *not* integer multiples of the fundamental rotation of the drill spindle. Extracted features shown in the following tables reveal the importance of second-order cumulant estimation.

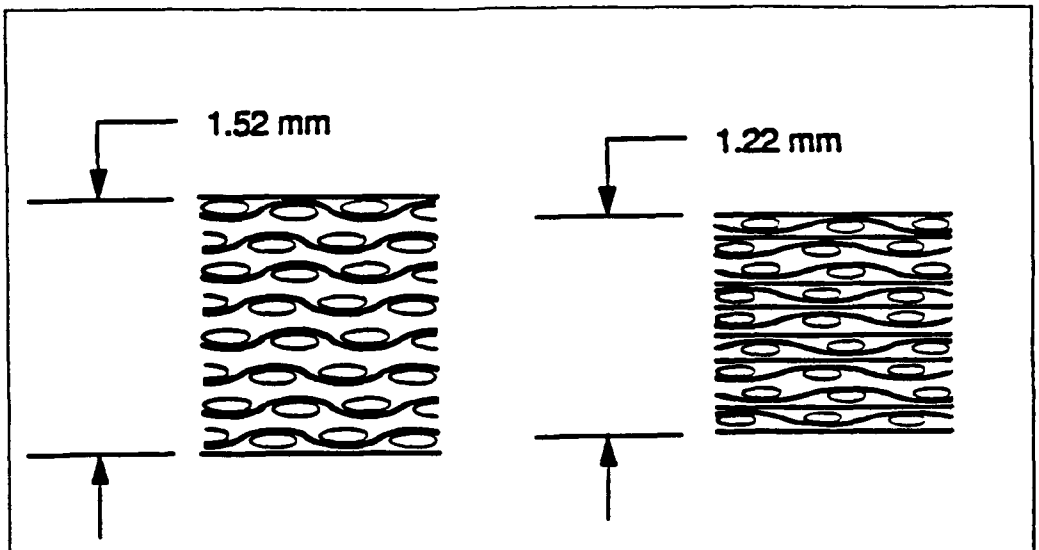

Figure 4.7: Circuit Card Construction

Table 4.3

Actual Experiment Feature Extraction--NIP/3 Case. Scum denotes the second-order cumulant spectrum, Bisp denotes the bispectrum, and Spec denotes the power spectrum. Feature variables are listed in the order entered by the SAS variable selection algorithm. Cyclic frequency of the drill spindle is 764 Hz.

Frequency Value (Hz)	Spectrum Type	F-Stat Value	Off 2-CSPD Periodic Grid?
9550,1910	Scum	16	yes
12224,1528	Scum	13	no
6876,8404	Bisp	8.5	n/a
14520	Spec	7.6	no
764,11460	Bisp	5.4	n/a
1528,15281	Bisp	6.7	n/a
8608	Spec	7.9	yes
13290	Spec	3.0	yes
13190	Spec	4.2	yes

Table 4.4

Actual Experiment Feature Extraction--6S2P/3 Case. Scum denotes the second-order cumulant spectrum, Bisp denotes the bispectrum, and Spec denotes the power spectrum. Feature variables are listed in the order entered by the SAS variable selection algorithm. Cyclic frequency of the drill spindle is 764 Hz.

Frequency Value (Hz)	Spectrum Type	F-Stat Value	Off 2-CSPD Periodic Grid?
8404,1910	Scum	17.3	yes
8786,1528	Scum	9.3	yes
4584,15281	Bisp	6.4	n/a
13520	Spec	5.8	yes
13060	Spec	4.6	yes
3056,25213	Bisp	3.1	n/a
5425	Spec	3.9	yes
4508	Spec	6.8	yes
9168,22157	Bisp	4.0	n/a
12988,1146	Scum	3.4	yes

Table 4.5

Actual Experiment Feature Extraction--NIP/4 Case. Scum denotes the second-order cumulant spectrum, Bisp denotes the bispectrum, and Spec denotes the power spectrum. Feature variables are listed in the order entered by the SAS variable selection algorithm. Cyclic frequency of the drill spindle is 588 Hz.

Frequency Value (Hz)	Spectrum Type	F-Stat Value	Off 2-CSPD Periodic Grid?
12936,1176	Scum	15	no
11466,588	Scum	10	yes
14700,2058	Scum	10	yes
2353,12354	Bisp	6	n/a
1765.8236	Bisp	6	n/a
4706,11766	Bisp	4	n/a

Table 4.6

Actual Experiment Feature Extraction--6S2P/4 Case. Scum denotes the second-order cumulant spectrum, Bisp denotes the bispectrum, and Spec denotes the power spectrum. Feature variables are listed in the order entered by the SAS variable selection algorithm. Cyclic frequency of the drill spindle is 588 Hz.

Frequency Value (Hz)	Spectrum Type	F-Stat Value	Off 2-CSPD Periodic Grid?
6468,1470	Scum	9.1	yes
9413,10589	Bisp	7.7	n/a
12870	Spec	3.6	yes
2574	Spec	4.3	yes
14494,2352	Scum	4.5	yes
6471,8824	Bisp	6.2	n/a
12642,1764	Scum	3.2	yes
9702,1470	Scum	4.0	yes

Table 4.7

Actual Experiment Feature Extraction--Combined Load 3 Case. Scum denotes the second-order cumulant spectrum, Bisp denotes the bispectrum, and Spec denotes the power spectrum. Feature variables are listed in the order entered by the SAS variable selection algorithm. Cyclic frequency of the drill spindle is 764 Hz.

Frequency Value (Hz)	Spectrum Type	F-Stat Value	Off 2-CSPD Periodic Grid?
8404,1910	Scum	36	yes
13370,12988	Scum	11	yes
3056,9932	Bisp	6.0	n/a
14870	Spec	4.5	yes
6876,11460	Bisp	5.4	n/a
6112,12988	Bisp	4.4	n/a
1528,1528	Bisp	3.6	n/a
8455	Spec	4.4	yes
9550,1910	Scum	11	yes

Table 4.8

Actual Experiment Feature Extraction--Combined Load 4 Case. Scum denotes the second-order cumulant spectrum, Bisp denotes the bispectrum, and Spec denotes the power spectrum. Feature variables are listed in the order entered by the SAS variable selection algorithm. Cyclic frequency of the drill spindle is 588 Hz.

Frequency Value (Hz)	Spectrum Type	F-Stat Value	Off 2-CSPD Periodic Grid?
9702,2646	Scum	13.5	yes
4410,1176	Scum	8.5	yes
12642,1764	Scum	4.9	yes
7060,11178	Bisp	5.0	n/a
9702,294	Scum	4.2	yes
8236,11178	Bisp	5.0	n/a
14494,2352	Scum	5.3	yes
9354	Spec	4.4	yes
10589,13531	Bisp	5.3	n/a
7648,12354	Bisp	2.8	n/a

Table 4.9

Actual Experiment Feature Extraction--Combined Stack NIP Case. Scum denotes the second-order cumulant spectrum, Bisp denotes the bispectrum, and Spec denotes the power spectrum. Feature variables are listed in the order entered by the SAS variable selection algorithm. Cyclic frequency of the drill spindle is 588 Hz and 764 Hz.

Frequency Value (Hz)	Spectrum Type	F-Stat Value	Off 2-CSPD Periodic Grid?
9408,2058	Scum	7.2	yes
9413,17061	Bisp	5.9	n/a
588,6471	Bisp	3.6	n/a
7060,15296	Bisp	3.5	n/a
12348,1470	Scum	3.5	yes
13530	Spec	3.8	no

Table 4.10

Actual Experiment Feature Extraction--Combined Stack 6S2P Case. Scum denotes the second-order cumulant spectrum, Bisp denotes the bispectrum, and Spec denotes the power spectrum. Feature variables are listed in the order entered by the SAS variable selection algorithm. Cyclic frequency of the drill spindle is 588 Hz and 764 Hz.

Frequency Value (Hz)	Spectrum Type	F-Stat Value	Off 2-CSPD Periodic Grid?
8232,2058	Scum	36.0	yes
8820,1470	Scum	20.0	yes
2941,7648	Bisp	13.5	n/a
12642,2352	Scum	10.5	yes
1765,8236	Bisp	10.4	n/a
588,13531	Bisp	8.4	n/a
8236,10589	Bisp	5.6	n/a
13160	Spec	5.3	yes
4706,16472	Bisp	5.0	n/a
12870	Spec	4.6	yes
12936,1176	Scum	4.4	no
13240	Spec	3.7	yes

The evidence of HOS feature extraction of actual incipient wear data clearly supports that HOS features are significant in the feature sets extracted to define class differences. Additionally, the theoretical proposition of second-order cumulant spectrum estimates *off* the periodic support grid as those which better characterize incipient faults of cyclostationary processes is confirmed. Now, what remains is an investigation of the impact of the extracted HOS features on classification performance, using various multivariate classifiers under different process conditions, to test the robustness of the new incipient fault detection approach.

Chapter 5

Evaluation of HOS Approach

5.1 Introduction

Performing discrimination and classification tasks on *simulated* and *actual* time series data generated from processes that have cyclostationary characteristics comprises the test and evaluation of the new HOS incipient fault detection approach. Factorial designs, data collected, and principles behind the experiments are described and then the discrimination and classification results using different feature extraction sets are given. Probability of false alarm and probability of detection are the measures of effectiveness used to evaluate the relative merit of the various approaches.

5.2 Simulated Wear Experiment

Modulation theory describes how a pure deterministic signal emitted by a periodic force is transformed into a signal actually measured by a condition monitoring system. Consider modulation as a mapping of the driving force signal space to the measurement signal space. Some possible mapping factors are : (1) internally and externally generated noise, (2) structural propagation, (3) change in process state, and (4) change in process environment. The transformation of an original driving force signal is equivalent to a translation of spectra. A pure sine

wave tone is a delta function or a single spike in spectral representation. A change in process *environment* (i.e. cutting forces required to cut through various strengths and types of material) will cause variation in frequency and amplitude, but the spectral components which specify the cutting force process dynamics are translated without any change to their relative energy distribution--the peak magnitude is decreased but the sidebands correspondingly increase to compensate the energy loss. However, a change in process *state* will cause variation or modulation of phase which will generate *new* frequencies with a different energy distribution of the signature signal spectral components. Parameters of the simulation experiment emphasized changes in phase, rather than changes in amplitude, and its impact on classification/feature extraction performance for several sets of process state and process environment parameters.

When the driving force of a physical system is periodical (eg., in rotating machinery), the signature signal emitted by the process and received by sensors may be represented by a harmonic process (Priestley, 1986). Consider a rotating drill machine and the process of cutting holes in electronic circuit cards which is the actual wear experiment analyzed later in this chapter. Assume the signature signal is a vibration time series sensed by accelerometers. The harmonic process model (HPM) in this case is:

$$V_c(t) = \sum_{n=0}^{k} A_n \cos(2\pi n f_c t + \phi_n) + n(t) \qquad [45]$$

where $V_c(t)$ is the voltage of the cosine wave carrier signal; A and ϕ are the amplitude and phase terms of the driving force mechanism (drill rotation) or carrier signal; f_c is the fundamental carrier frequency determined by the period of the

driving force function and vibration characteristics of the machine system; and $n(t)$ is the corrupting noise generated by other vibratory sources and distortional effects. Noise is assumed Gaussian and independent to the emitted vibration signal and k is the number of interacting sinusoids. Thus, the observed periodic voltage time series record is described by sums of sine and cosine waves whose amplitudes and phases are chosen to give the best fit to the observational data. The decomposition of the periodic time signal is found by obtaining the Fourier series of the time series record.

If $\{\phi_n,\ n = 0, 1, 2, \ldots\}$ are identical and independent uniformly distributed variables on $(-\pi, \pi)$, $\{V_c(t), t \geq 0\}$ is stationary no matter what frequency and amplitudes are selected to represent the voltage time series. Furthermore, both the autocorrelation and autocovariance functions of a HPM consist of a sum of cosine terms and therefore never die out in contrast to moving average (MA) and autoregressive (AR) processes. Thus, finite dependence or finite memory where joint random variables are highly correlated when the time instants are close together, and low correlation when the time instants are widely separated, is *not* applicable to a HPM representation of stochastic processes. (see Appendix B for stationarity of HPM and inapplicability of finite memory).

In this discussion, consider the cosine-wave carrier signal as referring to [45]. Its amplitudes, A_n, and phases, ϕ_n, can be varied according to modulating or information signals representing physical wear processes. The cosine-wave carrier signal is amplitude and phase modulated once the rotating drill begins to wear due to its drilling holes in electronic panels. The inherent energy will fluctuate, or be *amplitude* modulated, due to the change in drill bit surface contact pressure and force at each cutting revolution because of differences in hardness

and thickness of panel materials. Additionally, as more holes are drilled over time, the drill bit cutting edges will wear and cause *phase* modulation of the baseline or reference (no wear) voltage signal. Consider the situation where k is just 1.

The cosine-wave carrier signal, [45], or the inherent energy of the rotating drill spindle is amplitude modulated due to its periodic nature. A cosine wave with fluctuating amplitude is also known as the phenomenon of *beats*. By superimposing two cosine waves with nearly equal frequencies, $\omega \pm \delta\omega$, the result is:

$$\cos(\omega + \delta\omega)t + \cos(\omega - \delta\omega)t = 2\cos\omega t \cos\delta\omega t.$$

This oscillates at the average frequency, $\omega = 2\pi f_c$, but the amplitude changes slowly according to the modulating function, $2\cos\delta\omega t$. So the amplitude modulated version of [45] where the time reference is chosen so the carrier phase angle is zero is:

$$V_{am}(t) = k[1 + mf(t)]\cos(\omega_c t) + n(t).$$

Multiplying $f(t) = 2\cos\delta\omega t$ by $\cos(\omega_c t)$ causes a spectrum shift up to a range of frequencies surrounding the carrier frequency, f_c, and the addition of the carrier term provides a discrete spectral line at frequency f_c. These range of frequencies are sometimes called the lower and upper sidebands where each sideband contains amplitude and phase information of the original sinusoidal signal. Amplitude modulation is not the only method of modulating a cosine-wave carrier.

Consider a frequency modulated system in which the frequency of the carrier is caused to vary in accordance with some type of information-carrying signal. This could be variations in the bit cutting forces due to rake and flank wear and minor speed fluctuations of the drill spindle as it wears over time. The

frequency of the sine wave carrier is $\omega_c + kf(t)$ with $f(t)$ representing the phase modulating signal and k is a system constant. Expressing the more general frequency modulated carrier in mathematical terms is difficult because one can define the frequency of a sine wave only when the frequency is a constant. Strictly speaking, there is only the sine or cosine of an angle. However, if the angle varies linearly over time, one can interpret the frequency as the derivative of the angle:

$$f_c(t) = \cos\theta(t) = \cos(\omega_c t + \theta_o).$$

If $\theta(t)$ does not vary linearly, the instantaneous radian frequency ω_i is the derivative of the angle as a function of time:

$$f_c(t) = \cos\theta(t); w_i = \frac{d\theta}{dt}.$$

This now agrees with the usual use of frequency if $\theta = \omega_c t + \theta_o$.

Hence, the rotating drill spindle does not generate a signal that is a pure harmonic tone, $\cos 2\pi f_c t = \cos\omega_c t$, but rather is an amplitude and phase modulation representation of [45]:

$$V_{ampm}(t) = k[1 + m_a f(t)]\cos(\omega_c t + \phi_c + m_p g(t)) + n(t) \qquad [46]$$

where $V_{ampm}(t)$ is the amplitude and phase modulated cosine-wave carrier signal, m_a is the amplitude modulation index, $f(t)$ is the amplitude modulating signal, ϕ_c is the carrier signal phase, m_p is the phase modulation index, and $g(t)$ is the phase modulating signal. Now, $f(t) = \cos\omega_a t$ and $g(t) = \cos\omega_p t$ with f_a and f_p being the frequency of the amplitude and phase modulating wave, respectively.

Consider both amplitude and phase modulations modeled by:

$$V_{ampm}(t) = \sum_{k=0}^{N-1} A_k e^{i2\pi ft}.$$

Hence, a zero-mean random fluctuation vibration signal made up of a sum of N complex sinusoids with each frequency being described by complex amplitude A has zero complex mean when there is no modulation. Once wear progresses, these complex amplitude signals contain both random amplitude and phase modulations which result in broadening of their bandwidth or a correction to the pure line spectrum, and A becomes a nonzero complex random variable. If $m_a f(t)$ and $m_p g(t)$ are zero mean, stationary, and statistically independent, the power spectral density of $V_{ampm}(t)$ can be derived to show how the presence of random amplitude and phase modulations produce bandwidth broadening (see Appendix C). The primary interest for incipient fault detection is classifying changes in the phase modulation index parameter of the signature signal that corresponds to the degree of wear or developing failure in a rotating machine process. Details of the simulation experiments are given next.

Two hundred and fifty independent classification runs using three alternative feature extraction methods for fourteen treatments, or incipient failure cases, were performed. Three simulation parameters or factors are changed in a most deliberate fashion to represent fourteen very difficult discrimination/classification problems. These parameters are amplitude and phase modulation indice values, and standard deviation of an independent Gaussian noise term. The fourteen treatments can be logically categorized as seven scenarios shown at Table 5.1 on page 115. Each scenario has two treatments with a correspondingly increased value in phase modulation associated with a fixed

level of amplitude modulation and independent Gaussian noise standard deviation. Thus, each treatment entry of Table 5.1 on page 115 is a discrimination and classification problem of two classes of two hundred and fifty simulated time series.

Table 5.1

Seven Incipient Fault Detection Scenarios--Simulated Wear Data. Each scenario has two discrimination/classification cases. Numbers in parentheses are the simulation parameters: amplitude modulation index, phase modulation index, and standard deviation of Gaussian noise.

Scenario Number	Classification Treatment
1A	(.3,.7,.4) vs (.3,.71,.4)
1B	(.3,.7,.4) vs (.3,.72,.4)
2A	(.3,.7,.8) vs (.3,.71,.8)
2B	(.3,.7,.8) vs (.3,.72,.8)
3A	(.3,.7,1.4) vs (.3,.71,1.4)
3B	(.3,.7,1.4) vs (.3,.72,1.4)
4A	(.3,.4,.4) vs (.3,.41,.4)
4B	(.3,.4,.4) vs (.3,.42,.4)
5A	(.3,.4,.8) vs (.3,.41,.8)
5B	(.3,.4,.8) vs (.3,.42,.8)
6A	(.3,.4,1.4) vs (.3,.41,1.4)
6B	(.3,.4,1.4) vs (.3,.42,1.4)
7A	(.5,.7,.4) vs (.5,.71,.4)
7B	(.5,.7,.4) vs (.5,.72,.4)

Standard International Mathematical Statistical Library (IMSL) routines were used to generate Gaussian noise and deterministic phase. Levels for amplitude modulation were considered fixed as it represents more of a change in environment rather than a change in process state; however, amplitude modulation was

changed for sensitivity and verification purposes. There were three phase modulation levels, .7 was chosen as the base reference to represent a new process/object condition, and .71 and .72 represented an increasingly worn condition. Note that zero values for the modulation indices represent the pure cosine wave carrier frequency. It is important to emphasize that parameter selection was not an arbitrary process, but rather required an *iterative* parameter verification process to ensure the simulated spectral structure represented incipient fault problem situations. See Figure 5.1 on page 117 and Figure 5.2 on page 118 for examples of the simulated raw time series for two discrimination/classification treatments of one incipient fault scenario.

In summary, the simulation experiments generated time series data for marginal analyses to determine if there is additional discrimination power and classification performance using features provided by more involved spectrum estimation procedures such as the bispectrum and second-order cumulant spectrum. Sensitivity analyses also are conducted to determine the impact of slight increases in phase modulation and varying levels of noise on each of the feature extraction method's classification performance.

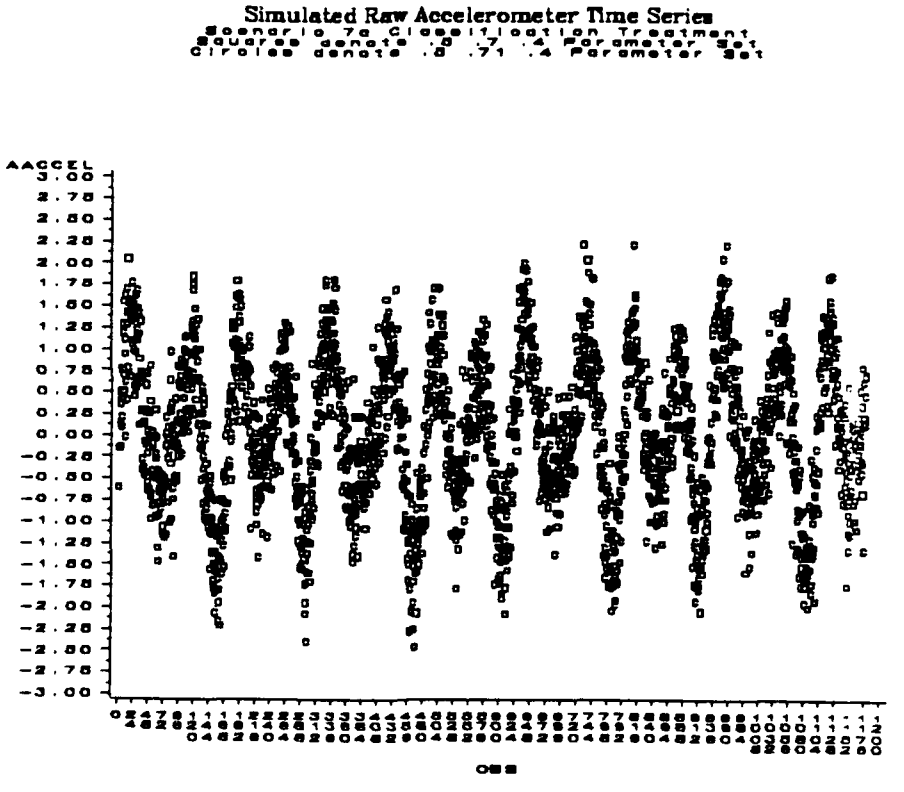

Figure 5.1: Simulation Scenario 7A Incipient Failure Representation. Squares are used for the .5 .70 .4 parameter set and circles are used for the .5 .71 .4 parameter set.

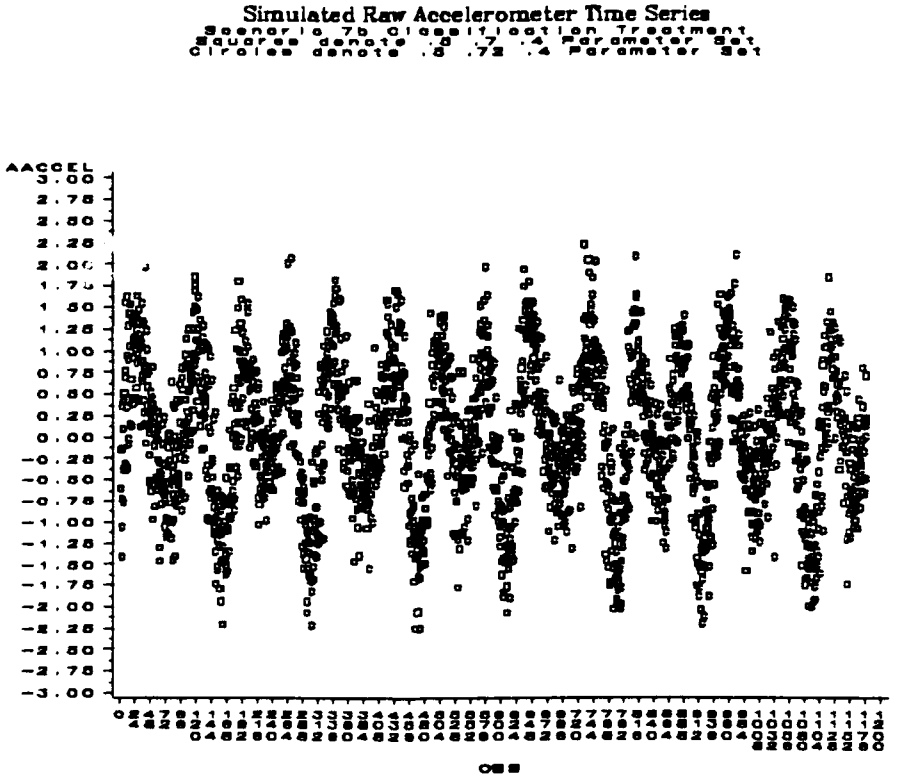

Figure 5.2: Simulation Scenario 7B Incipient Failure Representation. Squares are used for the .5 .70 .4 parameter set and circles are used for the .5 .72 .4 parameter set.

5.2.1 Experimental Design

The experimental design is a randomized complete block. To eliminate bias in the measurement of the two major response variables, probability of false alarm and probability of detection, four strategies were employed. First, since classification performance is directly related to the trained discriminant rule or function, ten different training functions were calculated for each classification treatment. Each of the training rules were constructed from a random sample of thirty out of a two hundred and fifty signal ensemble for each class. Second, a jacknife error estimation process described in the Chapter 2 was followed for computing classification results for a particular classification run. Third, as an additional safety measure to properly and fairly compare feature extraction methods, a paired comparison T-test analysis approach was followed to eliminate any classification performance variability due to different capabilities of the ten training discriminant rules. Lastly, in addition to training classification, *test* classification was conducted to obtain estimates of *actual* classification performance. Parameters of each generated time series were the following: 1178 time samples, .020 seconds for total record length, 58 kilohertz sampling frequency, 760 hertz carrier frequency, 380 hertz amplitude modulating frequency, and 190 hertz phase modulating frequency. For each simulation treatment or incipient failure case, three spectral estimation and feature extraction methods were performed for subsequent input to a linear classifier.

5.2.2 Results

As described in the background chapter concerning measuring differences in multivariate populations, Wilks' lambda and averaged square canonical correlation statistics are used as discrimination effectiveness measures for the training or discriminant rules constructed from thirty random samples for each class drawn from the 250 signal ensemble groups. However, since classification is the major objective in many applications of discriminant analysis, alternative spectral feature extraction approaches are best compared by examining two major classification performance components which define the rate of correct classification: probability of detection and probability of false alarm. These classification performance measures are reported as relative comparisons via paired t-tests for each scenario/classification treatment. The classification treatments are specified as blocks of simulation parameter triads (amplitude modulation index, phase modulation index, and Gaussian noise standard deviation). These simulation parameter blocks defined the time series class. Two types of classification performance are reported: discriminant or *training* classification and *test* classification. Classification results revealed no significant statistical difference in classification performance between the alternative feature extraction methods for the four treatments with a high (1.4) level of noise standard deviation. However, for the ten other treatments or five scenarios listed in Table 5.1 on page 115, some interesting results were obtained.

5.2.2.1 Discrimination

The marginal discrimination benefit of combining second-order cumulant spectra features to power spectra features is shown in Table 5.2.

Table 5.2

Marginal Discrimination Benefit of Combining Power Spectrum With Second Cumulant Spectrum Features--Simulated Wear Data. Both effectiveness measures represent relative discriminating power of a specific discriminating function computed on a random selection of thirty time series of each simulated class. Power spectra is denoted by 'PS' and second-order cumulant spectra is denoted by 'SCUM'.

Classification Treatment	Wilks' Lambda		Squared Canonical Corr	
	PS	PS & SCUM	PS	PS & SCUM
(.3,.7,.4) vs (.3,.71,.4)	.499	.374	.500	.604
(.3,.7,.4) vs (.3,.72,.4)	.660	.424	.339	.637
(.3,.7,.8) vs (.3,.71,.8)	.553	.499	.446	.500
(.3,.7,.8) vs (.3,.72,.8)	.506	.262	.493	.737
(.3,.4,.4) vs (.3,.41,.4)	.593	.309	.406	.690
(.3,.4,.4) vs (.3,.42,.4)	.640	.355	.359	.644
(.3,.4,.8) vs (.3,.41,.8)	.489	.344	.510	.655
(.3,.4,.8) vs (.3,.42,.8)	.340	.306	.659	.693
(.5,.7,.4) vs (.5,.71,.4)	.486	.272	.513	.727
(.5,.7,.4) vs (.5,.72,.4)	.552	.372	.447	.627

Both the Wilks' lambda statistical criterion (lower is better) and the averaged square canonical correlation improved significantly when nonstationary feature information is combined with power spectra feature information. Furthermore, combining nonlinear or bispectra feature information to the already constructed HOS feature set provides additional increases in the discriminant effectiveness

measures. Discrimination measures with this HOS feature composition compared to only power spectra feature sets are shown in Table 5.3.

Table 5.3

Marginal Discrimination Benefit for Combining Bispectrum and Second-order Cumulant Spectrum with Power Spectrum Features--Simulated Wear Data. Both effectiveness measures represent relative discriminating power of a specific discriminating function computed on a random selection of thirty time series of each simulated class. Power spectra is denoted by 'PS', second-order cumulant spectra is denoted by 'SCUM', and bispectra is denoted by 'B'.

Classification Treatment	Wilks' Lamb.a		Squared Canonical Corr	
	PS	PS,SCUM,B	PS	PS,SCUM,B
(.3,.7,.4) vs (.3,.71,.4)	.499	.205	.500	.834
(.3,.7,.4) vs (.3,.72,.4)	.660	.172	.339	.867
(.3,.7,.8) vs (.3,.71,.8)	.553	.195	.446	.804
(.3,.7,.8) vs (.3,.72,.8)	.506	.131	.493	.868
(.3,.4,.4) vs (.3,.41,.4)	.593	.128	.406	.871
(.3,.4,.4) vs (.3,.42,.4)	.640	.172	.359	.828
(.3,.4,.8) vs (.3,.41,.8)	.489	.198	.510	.801
(.3,.4,.8) vs (.3,.42,.8)	.340	.122	.659	.878
(.5,.7,.4) vs (.5,.71,.4)	.486	.232	.513	.767
(.5,.7,.4) vs (.5,.72,.4)	.552	.210	.417	.789

Significantly, inspection of the ten discriminant functions constructed for each simulation treatment using stepwise discriminant procedures revealed the most statistically significant and more plentiful variables were of the HOS variety. Although not shown in either Table 5.2 on page 121 or Table 5.3, results showed with regard to discriminating power, one type of feature extraction vector by itself (power spectra, bispectra, or second-order cumulant spectra) was not as powerful as combination of feature types. In summary, HOS estimation and feature extraction methods provide a substantial improvement in these two discriminating

effectiveness measures for the simulated incipient fault scenarios, and appears worthwhile to pursue even though in some of the treatments diminishing marginal benefits are apparent. In addition to measures of discrimination power, measures of classifying power are helpful in the comparison of the feature extraction methods.

5.2.2.2 Classification

The marginal contribution results of combining second-order cumulant spectra features to power spectra features, and also combining bispectra features to second-order cumulant and power spectra features, with regards to *training* classification are shown within Table 5.4.

Table 5.4

Training Classification Performance of HOS Features versus Power Spectrum Features--Simulated Wear Data. Numbers represent relative performance difference of ten discriminant rules over 30 classification runs. Alpha is the statistical significance level for rejecting equal performance means.

Feature Extraction Method	False Alarm Performance Prob	Alpha	Detection Performance Prob	Alpha
PS & SCUM vs PS	-4.9	.0004	+4.8	.0018
PS, SCUM,B vs PS	-10.4	.0001	+11.5	.0001

Clearly, combining nonstationary feature information to stationary features improves both false alarm probability and detection probability with extremely high levels of statistical significance. Furthermore, the inclusion of nonlinear information gives better training classification performance with an additional higher level of statistical confidence.

Evidence is clear that combining HOS features with power spectrum features improves *training* classification of the simulated scenario data. More important to the evaluation of the feature extraction methods is an estimate of the *actual* or *test* classification error rate. This measures a feature extraction method's capability to classify *future* time series samples. Hence, Table 5.5 and Table 5.6 on page 125, respectively show the marginal contribution to *test* classification performance by combining second-order cumulant spectra features with power spectra features, and combining bispectra features to second-order and power spectra features.

Table 5.5

Second-order Cumulant Spectra & Power Spectra vs Power Spectra Feature Extraction Test Classification--Simulated Wear Data. Numbers represent relative performance difference over 250 runs per classification problem. Alpha is the statistical significance level for rejecting equal performance means.

Classification Treatment	False Alarm Performance Prob	Alpha	Detection Performance Prob	Alpha
(.3,.7,.4) vs (.3,.71,.4)	-0.3	.85	+2.7	.0001
(.3,.7,.4) vs (.3,.72,.4)	-4.5	.0001	+4.6	.0001
(.3,.7,.8) vs (.3,.71,.8)	+2.7	.01	+2.7	.01
(.3,.7,.8) vs (.3,.72,.8)	+1.2	.21	+3.5	.0006
(.3,.4,.4) vs (.3,.41,.4)	-0.1	.90	+2.8	.002
(.3,.4,.4) vs (.3,.42,.4)	-3.1	.006	+4.5	.01
(.3,.4,.8) vs (.3,.41,.8)	+3.6	.01	+3.6	.01
(.3,.4,.8) vs (.3,.42,.8)	+0.2	.97	+2.4	.003
(.5,.7,.4) vs (.5,.71,.4)	+1.5	.16	+3.1	.0001
(.5,.7,.4) vs (.5,.72,.4)	+0.8	.45	+5.9	.02

Table 5.6

Bispectra, Second-order Cumulant Spectra, & Power Spectra vs Power Spectra Feature Extraction Test Classification--Simulated Wear Data. Numbers represent relative performance difference over 250 runs per classification problem. Alpha is the statistical significance level for rejecting equal performance means.

Classification Treatment	False Alarm Performance Prob	Alpha	Detection Performance Prob	Alpha
(.3,.7,.4) vs (.3,.71,.4)	-1.0	.45	+3.4	.0001
(.3,.7,.4) vs (.3,.72,.4)	-4.9	.0001	+6.8	.0001
(.3,.7,.8) vs (.3,.71,.8)	-0.2	.88	+0.3	.81
(.3,.7,.8) vs (.3,.72,.8)	+1.2	.30	+3.9	.001
(.3,.4,.4) vs (.3,.41,.4)	-1.5	.32	+1.8	.002
(.3,.4,.4) vs (.3,.42,.4)	-6.5	.0001	+6.2	.002
(.3,.4,.8) vs (.3,.41,.8)	+3.0	.005	+3.0	.005
(.3,.4,.8) vs (.3,.42,.8)	+0.07	.01	+1.0	.0009
(.5,.7,.4) vs (.5,.71,.4)	-0.4	.73	+4.6	.0001
(.5,.7,.4) vs (.5,.72,.4)	-0.5	.69	+7.0	.004

When the feature information set includes both stationary (power spectrum) and nonstationary (second-order cumulant spectrum) components, better test classification performance is obtained. Significantly, detection performance is increased for all treatments. Additionally, within each pair of treatments, or scenario, a greater change in the phase modulation index parameter is accompanied with an *increased* false alarm and detection capability. Thus, HOS features appear sensitive to greater changes in phase modulation which implies they have an increasing ability to detect more severe wear condition states. Noise does impact classification performance, but the HOS approach still maintains its superiority over the power spectrum approach. Combining nonlinear (bispectrum) feature information further improves test classification performance. Thus, there

is an increasing marginal benefit for conducting HOS estimation for subsequent feature extraction.

5.3 Actual Wear Experiment Description

Electronic circuit card construction begins with sandwiched layers of very thin copper and epoxy-glass composite material. Holes are drilled through these layers to provide pathways for interconnections between the copper conductor layers and sites for solder attachment of electronic components. A typical electronic panel consists of 1000 to 5000 holes with diameters of .5 mm to 2.5 mm. High-speed machines (20,000 to 200,000 RPM) can drill 1 to 5 holes per second with either single or multiple drill spindles. The drilling machine used by IBM in their experimental study has a drilling capability of up to 75,000 RPM and is shown in Figure 5.3 on page 127. Ramirez (1991) gives a complete description of the mechanics of the machine structure.

Most circuit card manufacturing defects can be traced to problems in the drilling process (Block, 1989). Problems caused partly by worn or damaged bits include rough hole surfaces due to glass fiber tearing, smearing of epoxy from high bit temperatures, and poor hole location and variation in hole diameter because of drill wander. Thus, there are three major reasons for IBM and others in industry to investigate drill bit wear monitoring methods: (1) to improve the quality of finished electronic panels by reducing incidence of poor quality holes; (2) to reduce panel scrap costs by reducing incidence of badly damaged holes; and (3) to reduce bit replacement costs by using as much of its useful life as possible. Clearly, panel quality is a function of hole quality, which in turn, is a function of

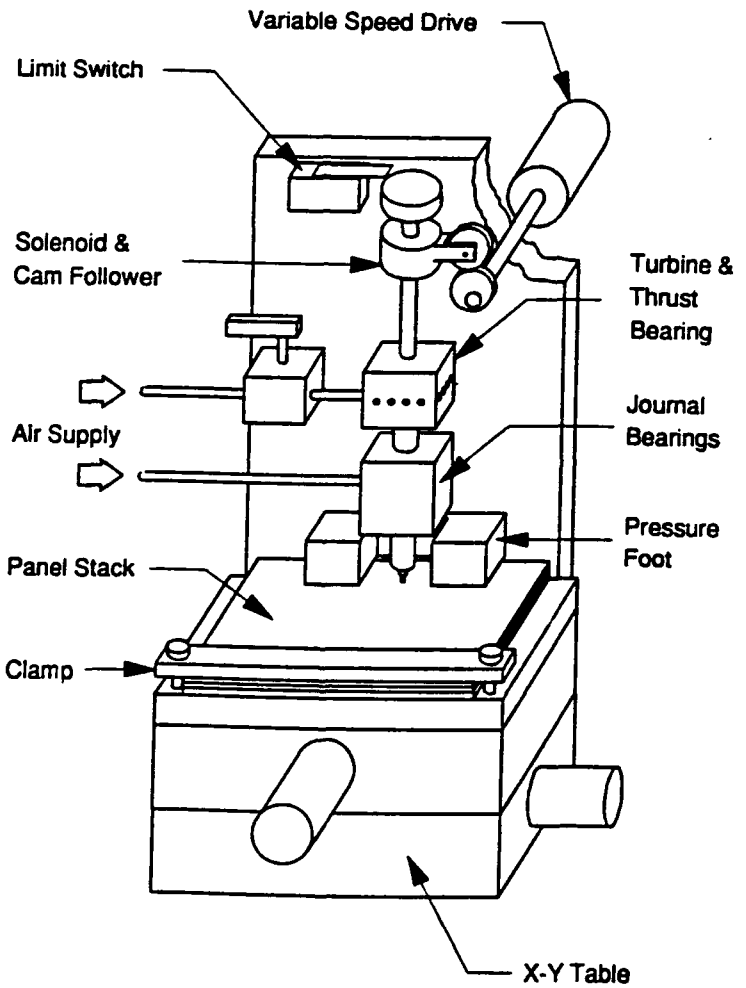

Figure 5.3: Drilling Machine used for IBM Wear Experiment

drill bit condition and engineers in this particular manufacturing application agree that there is some point that hole quality degrades as drills wear, necessitating a bit replacement strategy. Presently, drill bit replacement strategy is conservatively based on the shortest observed useful life since there is no effective wear monitoring system implemented in the industrial environment. Actual wear varies with lot-to-lot changes in the workpiece, drilling rate, condition of drilling machine, and type of drill bit. Drill bits characteristically exhibit large variances in tool life.

IBM experiment instrumentation included X (lateral), Y (translational), and Z (vertical) accelerometers, a magnetic reluctance probe, and X and Y capacitance probes (see Figure 5.4 on page 129). This study focused on the accelerometer signal data. Two accelerometers (X and Y) were bonded to the journal bearing block to measure lateral acceleration transmitted from the drill spindle to the machine structure. The Z accelerometer was mounted to the thrust bearing block which moved with the spindle.

5.3.1 Experimental Design

A factorial experimental design with three factors was employed: age of bit, material stack type, and chip load. Chip load is the amount of axial distance travelled by the drill bit tip in a single revolution or rotation. There were two levels for bit age (new or no holes drilled, and slightly used or 8000 holes drilled), three levels of stack type (NIP, 6S2P, and short NIP), and two levels for chip load (3 mil/revolution and 4 mil/revolution). A 1.09 mm diameter drill with a spindle speed of 47,000 RPM and nominal chip load of .076 mil/revolution was used.

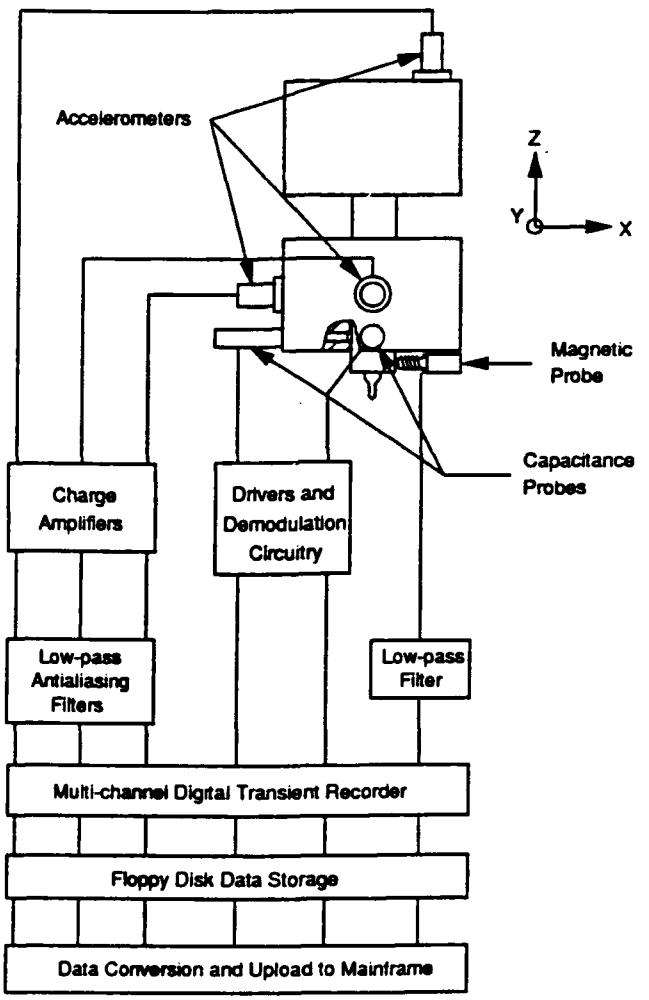

Figure 5.4: Instrumentation of Drill Spindle

5.3.2 Collected Data

Vibration time series for each of the three accelerometers were analyzed for two types of drill bits, new and slightly used. Ten bits of each type were randomly selected and optically verified for wear condition. Figure 5.5 contains magnified pictures of a typical new and slightly used drill bit. New and slightly used bit data were obtained for both chip loads and two of the three stack types. Shown at Figure 5.6 on page 132 and Figure 5.7 on page 133 are raw accelerometer time series for a typical new and slightly used drill bit for one of the stack material/chip load cases. There were three replications, or runs, for all eighty bits in the experimental database which produced 720 time series records. Preliminary estimation, feature extraction, and classification analyses consistently showed the best sensor site for bit class discrimination was the vertical or Z accelerometer. This conclusion was confirmed in a physical sense as the thrust forces are additive rather than subtractive, and had better signal-noise characteristics than either the X or Y accelerometers. Thus, results presented in this report are only for the Z accelerometer. For computational purposes, each 3 mil/rev (4 mil/rev) time series is divided into appropriate record lengths as given the respective 760 Hz (587 Hz) harmonic frequency of the drill spindle, an integer number of signal periods was necessary to avoid the effects of leakage when performing spectral estimation procedures. Power spectrum, cumulant spectrum, and bispectrum estimates are computed over blocks within each time series record. All spectral estimates are averaged over appropriate block lengths, and then incorporated into the ensemble averaging of all samples of its particular class.

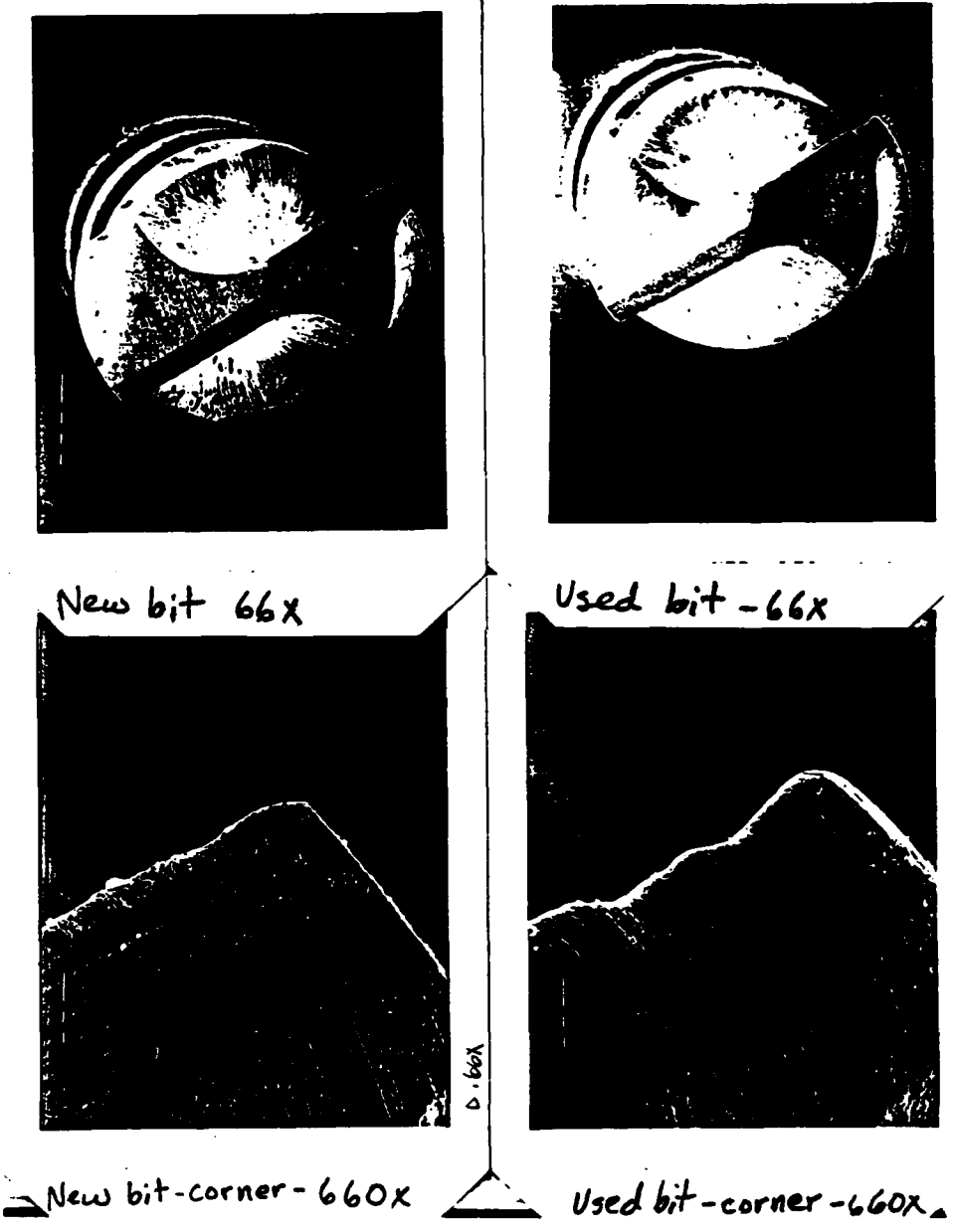

Figure 5.5: Magnified Photos of New and Slightly Used Drill Bit

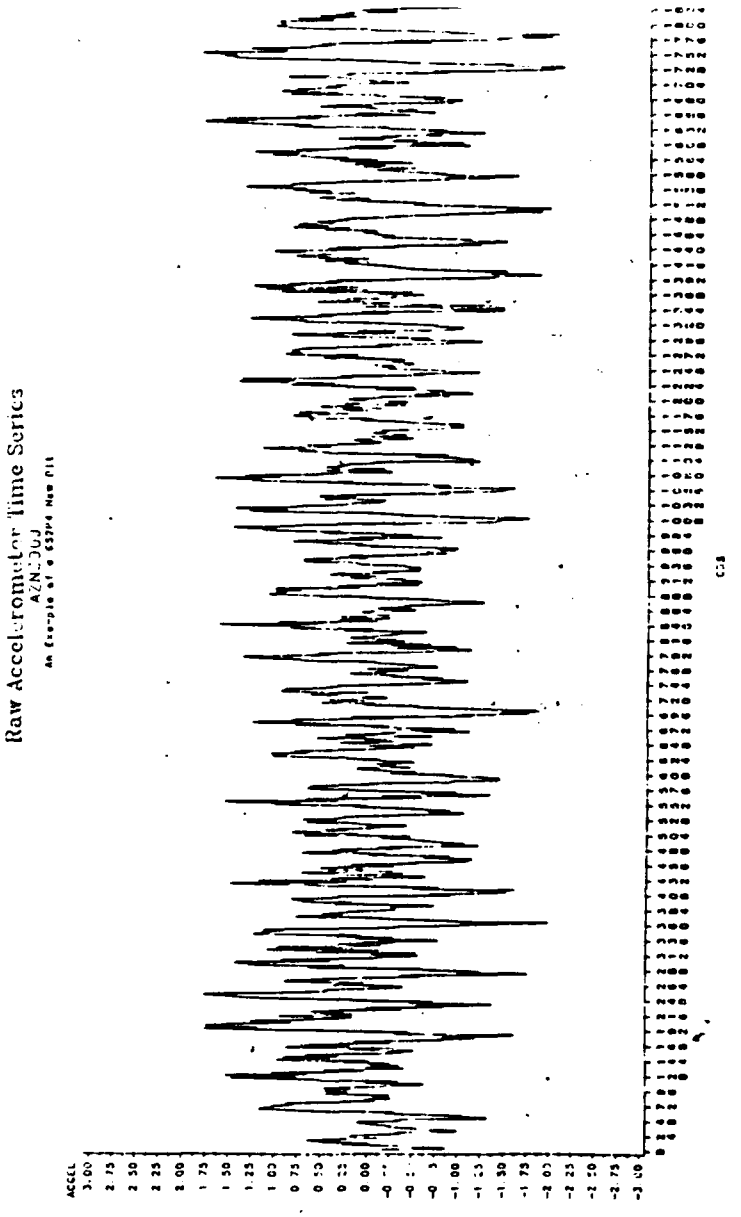

Figure 5.6: Raw Accelerometer Time Series--6S2P/4 Case (New Drill). One sample time series of an ensemble from the Z accelerometer.

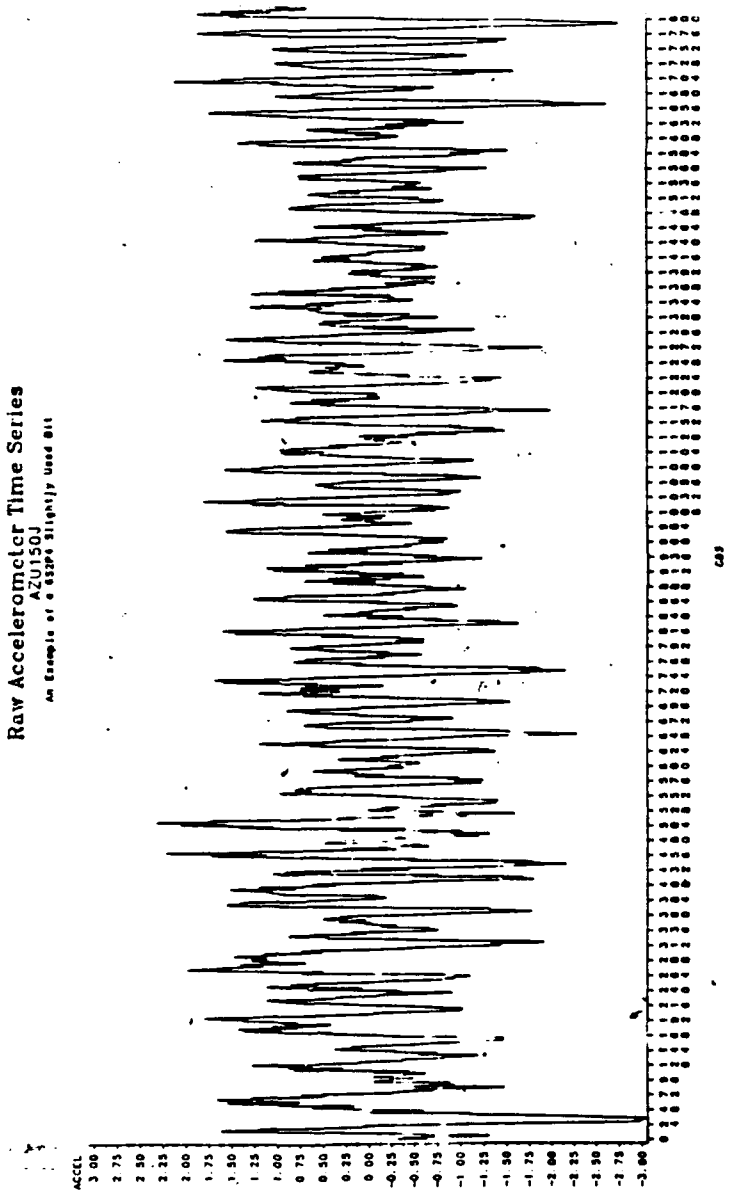

Figure 5.7: Raw Accelerometer Time Series--6S2P/4 Case (Slightly Used Drill). One sample time series of an ensemble from the Z accelerometer.

5.3.3 Results

Performance results are given as two separate but related categories, discrimination and classification. Both performance categories are reported by individual stack material and chip load case, combined chip load, combined stack material, and corresponding averaged values. Performance results obtained for combined data address the impact of drilling process parameter variation such as stack type and cutting conditions on the feature extraction methodology. It is desirable from a monitoring system implementation perspective that the feature extraction and classification methodology should not be severely impacted by process parameter variation. There are various statistical measures to compare the discriminating power of the feature extraction methods. In this study, the approach is to first report Wilks' lambda and squared canonical correlation measures for the training or discriminant rules constructed from the number of existing samples in the experimental database for the data partition types. However, since classification is the major objective in many applications of discriminant analysis, alternative spectrum feature extraction approaches are also compared by examining two major classification performance components which define the rate of correct classification: probability of detection and probability of false alarm.

5.3.3.1 Discrimination

Shown in Table 5.7 on page 136 is the marginal benefit of combining HOS feature sets with power spectrum features for discrimination effectiveness. Both the Wilks' lambda statistical criterion (smaller is better) and the averaged

square canonical correlation measures had significant marginal improvement in six of the eight partition database types. For the two cases of no overall marginal improvement, NIP4 and NIP, differences are not significantly different from a full HOS feature approach (spectrum, cumulant spectrum, and bispectrum) versus just power spectrum features. Recall from Chapter 4 that the most significant second-order cumulant feature for the NIP4 case was on, rather than off, the 2-CSPD diagonal spectral support line. Significant marginal improvement for the other six cases is obtained by combining cumulant spectrum (nonstationary) features to power spectrum (stationary) features, and for combining bispectrum (nonlinear) to stationary and nonstationary feature sets. Additionally, marginal improvement is gained by combining nonlinear feature information for all database partitions, and particularly for the two cases of no overall marginal improvement between HOS and power spectrum feature extraction discrimination effectiveness, a large marginal improvement with nonlinear features was gained.

Table 5.7

Marginal Discrimination Benefit of HOS Features versus Only Power Spectrum Features--Actual Wear Data. Both effectiveness measures represent relative discriminating power of a specific discriminating function computed on thirty vibration time series of each bit class, new and slightly used. Power spectrum is denoted by 'PS', second-order cumulant spectrum is denoted by '2C', and bispectrum is denoted by 'B'.

Discrimination Case	Wilks' Lambda			Squared Canonical Corr		
	PS	PS&2C	PS,2C&B	PS	PS&2C	PS,2C&B
NIP/3	.429	.561	.295	.570	.438	.704
NIP/4	.379	.462	.430	.620	.537	.569
6S2P/3	.510	.370	.299	.489	.629	.700
6S2P/4	.555	.530	.392	.444	.470	.607
Stack/Load Average	.468	.480	.354	.530	.518	.645
Chip Load 3	.609	.600	.530	.390	.399	.469
Chip Load 4	.736	.525	.353	.263	.474	.646
Load Average	.673	.562	.441	.327	.437	.558
NIP Stack	.399	.656	.456	.600	.343	.543
6S2P Stack	.684	.536	.446	.315	.463	.553
Stack Average	.541	.596	.451	.458	.403	.548

Inspection of the HOS discriminant functions constructed for each database partition type using stepwise discriminant procedures revealed the more statistically significant and number of variables were of the HOS variety rather than the power spectrum. Although not shown in Table 5.7, results did show from the standpoint of discriminating power, one type of spectrum feature extraction vector by itself (power spectrum, bispectrum, or second-order cumulant spectrum) is not

as powerful as the combination of feature types. In summary, HOS estimation and feature extraction methods provide a substantial improvement in these two discriminating effectiveness measures for the drill bit wear data and appears useful.

5.3.3.2 Classification

Combining HOS features to power spectrum features clearly improves discrimination power. Equally important to an evaluation of the feature extraction methods is an estimate of the *expected actual* classification error rate. Results are given with tables identified by the applied multivariate classification algorithm, two parametric approaches (linear and quadratic discriminant or LDF and QDF) and one non-parametric approach (k-nearest neighbor). Results are stated in the following manner: (1) within a classification algorithm, a direct one-to-one comparison of the feature extraction methods for stack/load and also for the combined process parameters (cutting condition and stack material) classification cases; and (2) a comparison of feature extraction method performance across classification algorithms for all classification cases. Comparison of the feature extraction methods in this fashion allows an evaluation of each approach for its sensitivity to stochastic process conditions and also to the classification algorithm.

The contribution of combining HOS features to power spectrum features using a linear classifier is shown in Table 5.8 on page 139. LDF classification results demonstrate the marginal benefit of performing HOS estimation and feature extraction for all classification cases. Averaged classification performance measures (stack/load, load, and stack) reveal combining HOS features with power

spectrum features obtains an increasing marginal benefit in terms of overall classification accuracy. False alarm rates may be higher in some cases, but the marginal increase in detection capability makes up for the difference in lost capability. This performance result is significant as a higher detection capability is more desirable than a lower false alarm rate in most industrial manufacturing situations. For each of the feature extraction approaches, better performance is obtained with databases which are the most homogeneous. Also, they all have better classification ability with the combined stack material database than the combined cutting (load) database. Thus, there is less sensitivity to cutting (chip load) variation than stack material variation which agrees with a major finding of Ramirez (1991) that variations in circuit card construction can mask the effects of wear. Significantly though with the more heterogeneous data (combined load and combined stack), the performance of the HOS approaches is *not* degraded as much as the purely power spectrum approach.

Table 5.8

HOS Feature Extraction versus Solely Power Spectrum Feature Extraction Classification Using LDF Algorithm--Actual Wear Data. Numbers represent percent of thirty slightly used drill bits incorrectly classified as new, or false alarm rate, and percent of thirty drill bits correctly classified as slightly used, or detection rate. Power spectrum is denoted by 'PS', second-order cumulant spectrum is denoted by '2C', and bispectrum is denoted by 'B'.

Classification Case	False Alarm Probability			Detection Probability		
	PS	PS&2C	PS,2C&B	PS	PS&2C	PS,2C&B
NIP/3	.133	.366	.200	.850	.966	.933
NIP/4	.133	.250	.233	.933	1.00	.966
6S2P/3	.150	.166	.100	.862	.933	.896
6S2P/4	.283	.350	.150	.816	.933	.916
Stack/Load Average	.175	.283	.170	.865	.958	.927
Chip Load 3	.150	.316	.300	.728	.850	.816
Chip Load 4	.258	.300	.233	.675	.866	.850
Load Average	.204	.308	.266	.701	.858	.833
6S2P Stack	.250	.316	.200	.661	.950	.933
NIP Stack	.183	.333	.250	.933	1.00	.900
Stack Average	.216	.324	.225	.797	.975	.917

Shown in Table 5.9 on page 140 is the marginal contribution of combining HOS features to power spectrum features using a quadratic classifier. Similar marginal benefit results with HOS information are obtained as with a linear classifier, but the more difficult parametric classification, quadratic rather than a linear function, is *not* beneficial for the power spectrum feature extraction approach.

Table 5.9

HOS Feature Extraction versus Solely Power Spectrum Feature Extraction Classification Using QDF Algorithm--Actual Wear Data. Numbers represent percent of thirty slightly used drill bits incorrectly classified as new, or false alarm rate, and percent of thirty drill bits correctly classified as slightly used, or detection rate. Power spectrum is denoted by 'PS', second-order cumulant spectrum is denoted by '2C', and bispectrum is denoted by 'B'.

Classification Case	False Alarm Probability			Detection Probability		
	PS	PS&2C	PS,2C&B	PS	PS&2C	PS,2C&B
NIP/3	.183	.366	.333	.833	1.00	1.00
NIP/4	.183	.166	.200	.833	.966	.966
6S2P/3	.150	.200	.100	.810	.966	.931
6S2P/4	.300	.300	.250	.700	.816	.883
Stack/Load Average	.200	.258	.220	.794	.937	.945
Chip Load 3	.175	.366	.266	.737	.916	.950
Chip Load 4	.258	.266	.116	.675	.833	.900
Load Average	.216	.316	.191	.706	.874	.925
6S2P Stack	.241	.266	.133	.635	.933	.933
NIP Stack	.108	.400	.333	.933	1.00	1.00
Stack Average	.175	.333	.233	.784	.967	.967

Average stack/load classification is degraded with power spectrum features and has no consequential impact on either averaged load or stack classification. However, the impact on averaged total classification accuracy using HOS features is: -1.5 percent for stack/load, +8.3 percent for combined load, and +2.1 percent for combined stack. For the stack/load case, false alarm rate increased more than the corresponding increase in detection capability so there was a slight decrease

in overall QDF classification performance for this database partition. However, the masking of wear effects due to variations in card construction is not as great with HOS features and QDF classification. The major disadvantage of a power spectrum approach is almost overcome. Significantly, *detection* capability was the major component of the increase in the LDF classification accuracy of HOS features using a QDF approach.

The marginal contribution of combining HOS features to power spectrum features with a non-parametric classifier (k-nearest neighbor with $k = 4$) is shown in Table 5.10 on page 142. Direct comparisons of these classification results clearly show the increased *overall* classification power of the HOS feature extraction approach. There are increases in both false alarm and detection capability with HOS features. Additionally, increasingly marginal benefits are evident as more spectral feature types are combined. Nearest neighbor classification makes no difference or degrades previous parametric classification results with solely power spectrum features due to increases in false alarm probabilities. However, the amount of increased total classification accuracy due to the non-parametric method ranges, in an absolute sense, from 3 to 8 percent, with combined HOS and power spectrum feature sets. Additionally, combined chip load classification with power spectrum and cumulant spectrum features is only slightly degraded with the change in card material. There is no doubt non-parametric classification (4-nearest neighbors) is the best classification approach with this incipient drill wear database.

Table 5.10

HOS Feature Extraction versus Solely Power Spectrum Feature Extraction Classification Using 4-Nearest Neighbor Algorithm--Actual Wear Data. Numbers represent percent of thirty slightly used drill bits incorrectly classified as new, or false alarm rate, and percent of thirty drill bits correctly classified as slightly used, or detection rate. Power spectrum is denoted by 'PS', second-order cumulant spectrum is denoted by '2C', and bispectrum is denoted by 'B'.

Classification Case	False Alarm Probability			Detection Probability		
	PS	PS&2C	PS,2C&B	PS	PS&2C	PS,2C&B
NIP/3	.150	.266	.133	.850	.936	.983
NIP/4	.100	.166	.133	.933	1.00	.966
6S2P/3	.366	.300	.133	.844	1.00	1.00
6S2P/4	.183	.216	.200	.850	.933	.966
Stack/Load Average	.200	.230	.150	.869	.966	.962
Chip Load 3	.408	.183	.316	.822	.933	.933
Chip Load 4	.175	.266	.200	.775	.933	.950
Load Average	.291	.224	.258	.798	.933	.941
6S2P Stack	.516	.183	.166	.745	.966	.983
NIP Stack	.266	.233	.250	.900	.866	.933
Stack Average	.391	.208	.208	.822	.916	.958

Usefulness of combining HOS feature sets with power spectrum feature sets is clearly demonstrated with the results gathered from simulated and actual wear experiments. A HOS approach for incipient fault detection has increased discrimination and classification power and is less sensitive to process and noise conditions than solely a power spectrum approach. Conclusions of the study are stated in the next chapter.

Chapter 6

Conclusions and Further Research

Inferences from the data analyses of the conducted experiments are stated in general and specific form. This research focused on cyclostationary processes represented by simulations of single-tone amplitude and phase modulated carrier signals which primarily emphasized phase modulation changes and new and slightly worn high-speed drills in the "manufacturing environment". The evidence clearly advocates for the adoption of a HOS feature fusion approach in a condition monitoring scheme for rotating systems. Whether the HOS approach can create actual economic savings in an industrial setting is a question left for further research.

Two important general conclusions are drawn from the results of this study:

1. Incipient fault detection capability of multivariate classifiers significantly improve with HOS feature information.
2. Better operations and maintenance decisions to discontinue/service rotating systems are possible if the condition monitoring method incorporates the HOS feature fusion approach.

Five secondary research questions supported these general conclusions: (1) What is the impact of combining HOS features with power spectrum features upon discrimination and classification of incipient faults? (2) What is the impact of a changing process environment upon classification? (3) What is the impact of applied classifier algorithm upon classification? (4) What is the impact of a

slight change in phase modulation upon discrimination and classification? (5) What is the impact of increasing noise in the signal environment upon discrimination and classification? Results from the modulated signal simulations answered all secondary research questions except for the third one while results from the actual experiment answered the first three questions.

In the simulation experiments, when the feature information set included HOS features better discrimination power was obtained (see Table 5.2 on page 121 and Table 5.3 on page 122). Additionally, when the feature information set included both power spectrum and second-order cumulant spectrum features, better *training* and *test* classification performance was obtained than with just a power spectrum feature set (see Table 5.4 on page 123 and Table 5.5 on page 124). Further improvement in *training* and *test* classification performance was obtained when bispectrum features were combined with second-order cumulant and power spectrum features (see Table 5.4 on page 123 and Table 5.6 on page 125). Thus, HOS estimation for subsequent feature extraction provided an increasing marginal benefit for a linear classifier. HOS features were sensitive to very slight changes in phase modulation which implied the ability to detect incipient faults and a greater potential capability to detect more severe wear condition states of rotating machinery. Finally, noise impacted classification performance whether with or without HOS information. However, with moderate or even high levels of noise in the signal environment, HOS approaches were still better at detecting different simulated signal classes with very high levels of statistical confidence (see Table 5.5 on page 124 and Table 5.6 on page 125).

In the actual experiment, when the feature information set included power spectrum and second-order cumulant spectrum features, better discrimination

power was obtained than a feature set based only on the power spectrum. Further discriminatory power was obtained by combining bispectrum features with cumulant spectrum and power spectrum feature sets (see Table 5.7 on page 136). This same marginal beneficial trend was demonstrated with classification results. When power spectrum and second-order cumulant spectrum features were combined, classification performance increased from that of a power spectrum feature set. The classification performance further improved for all three applied multivariate classifiers when bispectrum features were combined with cumulant spectrum and power spectrum feature sets (see Table 5.8 on page 139, Table 5.9 on page 140, and Table 5.10 on page 142).

Actual wear classification results presented in the tables of Chapter 5 are now condensed as *total* classification averages (see Table 6.1 on page 146). All feature extraction methods were sensitive to changes in process parameters. However, HOS feature extraction was *less* sensitive than solely power spectrum feature extraction. Specifically, variations in card construction significantly masked the effects of wear when power spectrum features were used for all classification approaches. Also, chip load variation masked the effects of wear when power spectrum features were used with two of the three classifiers. However, variations in card construction and chip load only slightly masked the effects of wear when power spectrum and cumulant spectrum features were used with the 4-nearest neighbor classifier. Furthermore, variations in card construction and chip load had *no* wear masking effect when full HOS feature sets were used with a quadratic classifier. By selecting and combining HOS features which captured the nonstationary and nonlinear characteristics of the cutting forces as the drill

bit penetrates the circuit card layers, total classification capability was definitely enhanced.

Table 6.1

Actual Incipient Wear Total Classification Averages. Combined load database tested the impact of stack variation, combined stack tested the impact of load variation, and load/stack was the most homogeneous database partition with no variation of drilling process parameters. 'PS' represents power spectrum, '2C' represents second-order cumulant spectrum, and 'B' represents bispectrum. 'LDF' and 'QDF' denotes linear and quadratic parametric classification, and 'NN' denotes the nearest neighbor non-parametric classification.

Features and Classification	Combined DataBases		Homogeneous DataBase
	Comb Load	Comb Stack	Load and Stack
PS & LDF	75.1	79.1	84.5
PS, 2C & LDF	77.9	82.6	83.8
PS, 2C, B & LDF	78.3	84.6	87.8
PS & QDF	74.5	80.5	79.7
PS, 2C & QDF	77.9	81.7	84.0
PS, 2C, B & QDF	86.7	86.7	86.3
PS & NN	75.4	71.6	83.5
PS, 2C & NN	85.4	85.4	86.8
PS, 2C, B & NN	84.1	87.5	90.6

Thus, results of all five secondary research questions revealed that a condition monitoring approach based on power spectrum characteristics was more sensitive to external noise and stochastic process parameter variation than that which incorporated HOS information. These results provided statistical evidence for the two general conclusions of the study and *clearly* demonstrated the benefits

of HOS estimation and feature extraction as preprocessing steps for a multivariate classifier.

6.1 Areas of Further Research

Further studies are possible in both the applications and methodology areas. *First*, analysis of IBM extended drill wear data, already gathered and obtained, is needed so more than two classes of drills can be examined. Hence, testing the ability of classifiers with and without HOS features to detect different levels of drill wear can be investigated. The particular HOS feature sets selected from analyses of the incipient wear factorial experiment can be further examined for their predictive ability of advancing drill wear. It is already known that the fifth through the eighth harmonics of the Z acceleration power spectrum were most sensitive to advanced drill wear (Ramirez,1991). These particular power spectrum responses steadily increased as drill wear progressed, and rapidly increased when drill wear-out was achieved. Quite significantly, the bispectrum chloropleth difference plots of each case of the incipient wear data revealed these same harmonic frequencies interacting with higher frequencies to be among the most significantly different frequency interactions between classes! It is possible that bispectrum analysis can be used as a predictive tool of advancing wear. *Second*, a large database of pump and fan failure data obtained from TRACOR (Austin) can be studied for applicability to other rotating machinery besides high-speed drills. The TRACOR data is already analyzed by some of the vibration analysis techniques mentioned in Chapter 2. Results from the HOS analytical approach could be compared with the results of these other techniques. *Third*,

other classification algorithms such as neural networks could be applied to investigate whether trends identified in this research continue to hold. Obtaining the right type of information required for proper further investigation of the HOS approach is tedious, difficult, and expensive. The hard work of obtaining excellent experimental data is done as both rotating machine failure databases are available from the author. Some ideas of expanding on the methodological work is given next.

First, third-order cumulant estimation and feature extraction can be performed for the experiments described in this work. This is extremely important to investigate as the contribution from this cumulant spectrum measure will probably be more significant than the second-order cumulant. *Second*, more involved and complicated simulation experiments such as testing with differing levels of the experimental parameters and also multiple-tone simulations are needed. *Third*, more investigation with regard to the correspondence of the statistical findings of this research to the actual physics of wear processes occurring in high-speed drilling of composite circuit card materials is a good research project for a mechanical systems graduate student. *Finally*, depiction of how the statistically significant features change and move through spectral principal domain regions over multiple conditions of the machine is another area for methodological research.

6.2 Summary

This research study was significant in many respects. This is the *first* work to provide a rigorous study of the HOS approach in detecting incipient

faults. Moreover, this is the first work to address the nonstationary aspects of random fault mechanisms. Most incipient fault detection methods are usually tested against one specific application or machine system. Due to the inherent stochastic nature of the systems under study, a statistical and experimental design framework is necessary to thoroughly investigate a particular monitoring approach. Deriving statistical conclusions which show consistency with both simulated and actual time series signals gives validity for the new HOS monitoring approach. Understanding the necessity to investigate and justify structural assumptions such as linearity, Gaussianity, and stationarity of time series data is one of the major lessons learned in this study. This research explains the procedures for manipulating such time series data so that other rotating machinery situations can be properly analyzed. Because the research approach provides the tools for investigating and exploiting a wider potential range of time series characteristics generated by random fault mechanisms of cyclostationary processes, improved executive decisions in both the maintenance and operational environments of rotating machinery are possible.

Appendices

Appendix A

Second-Order Cumulant Spectrum Estimation Program

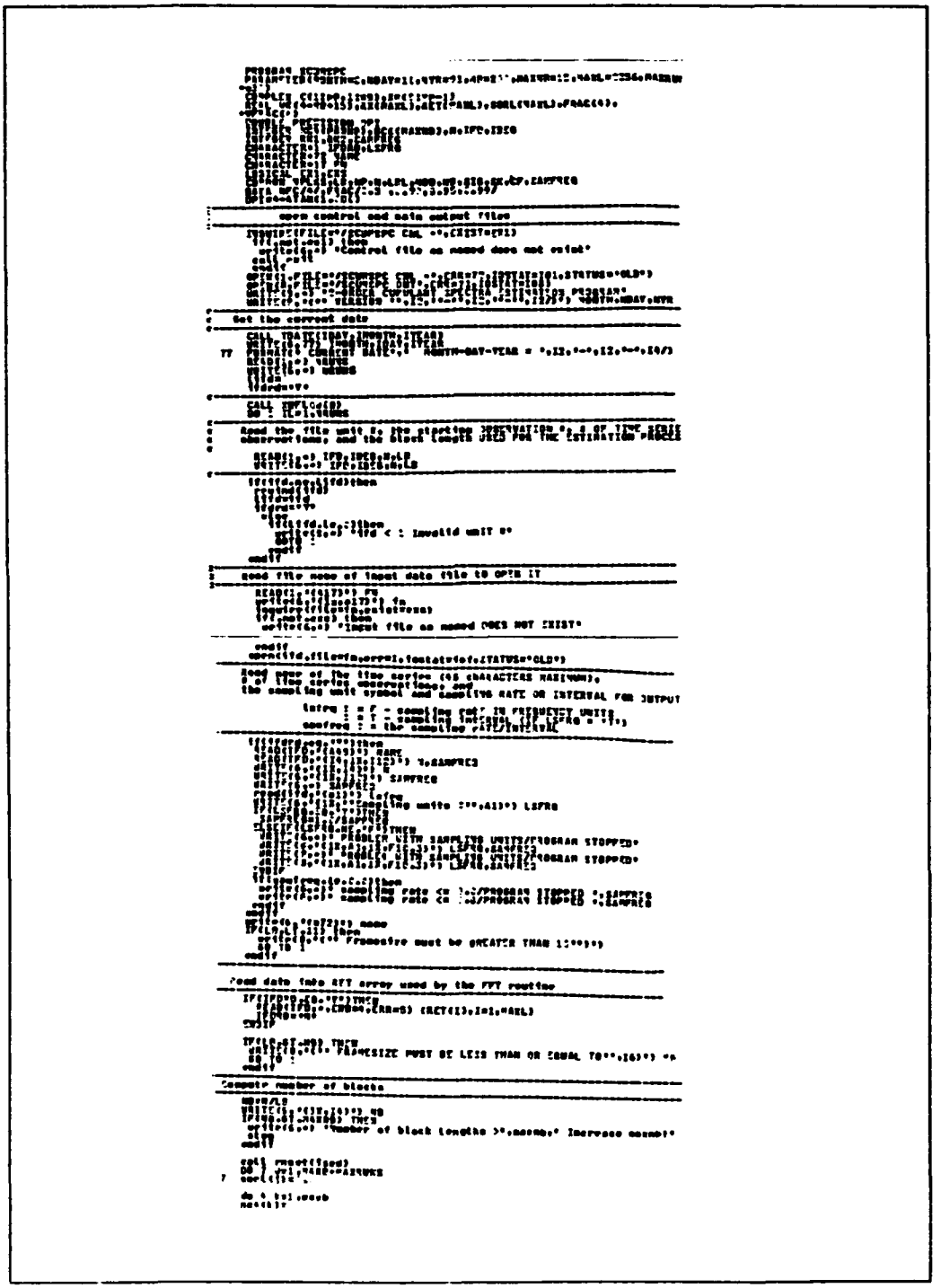

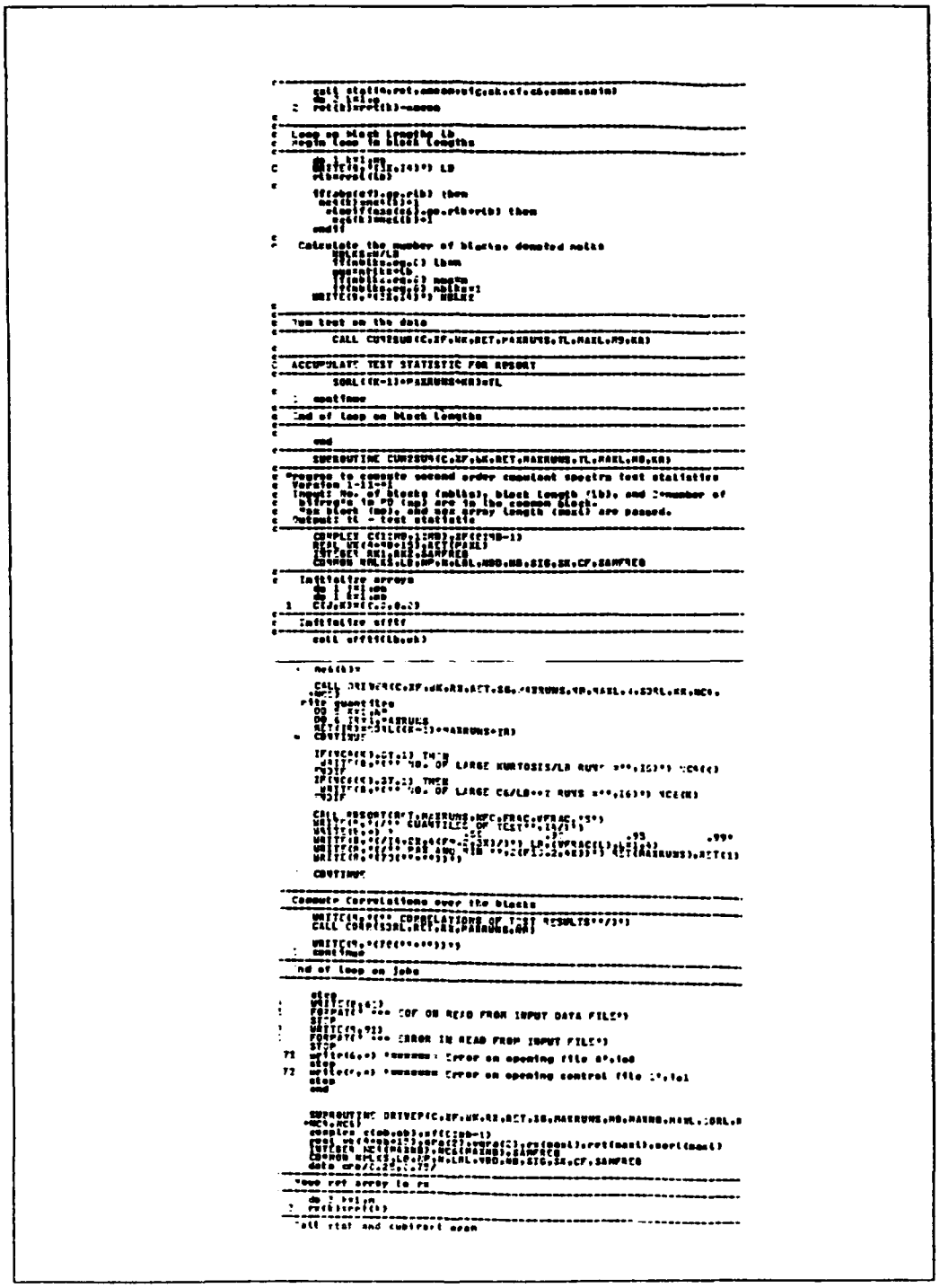

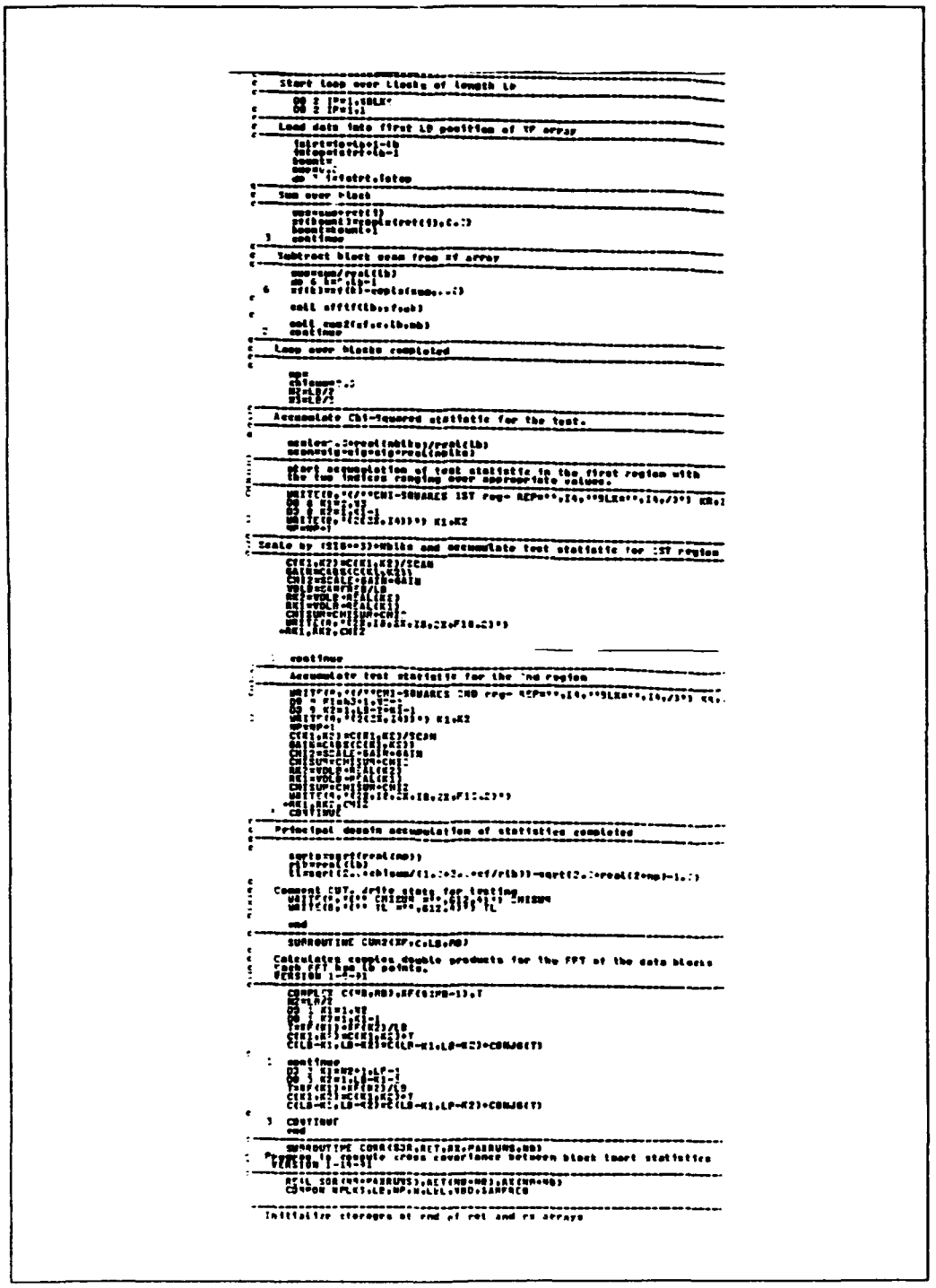

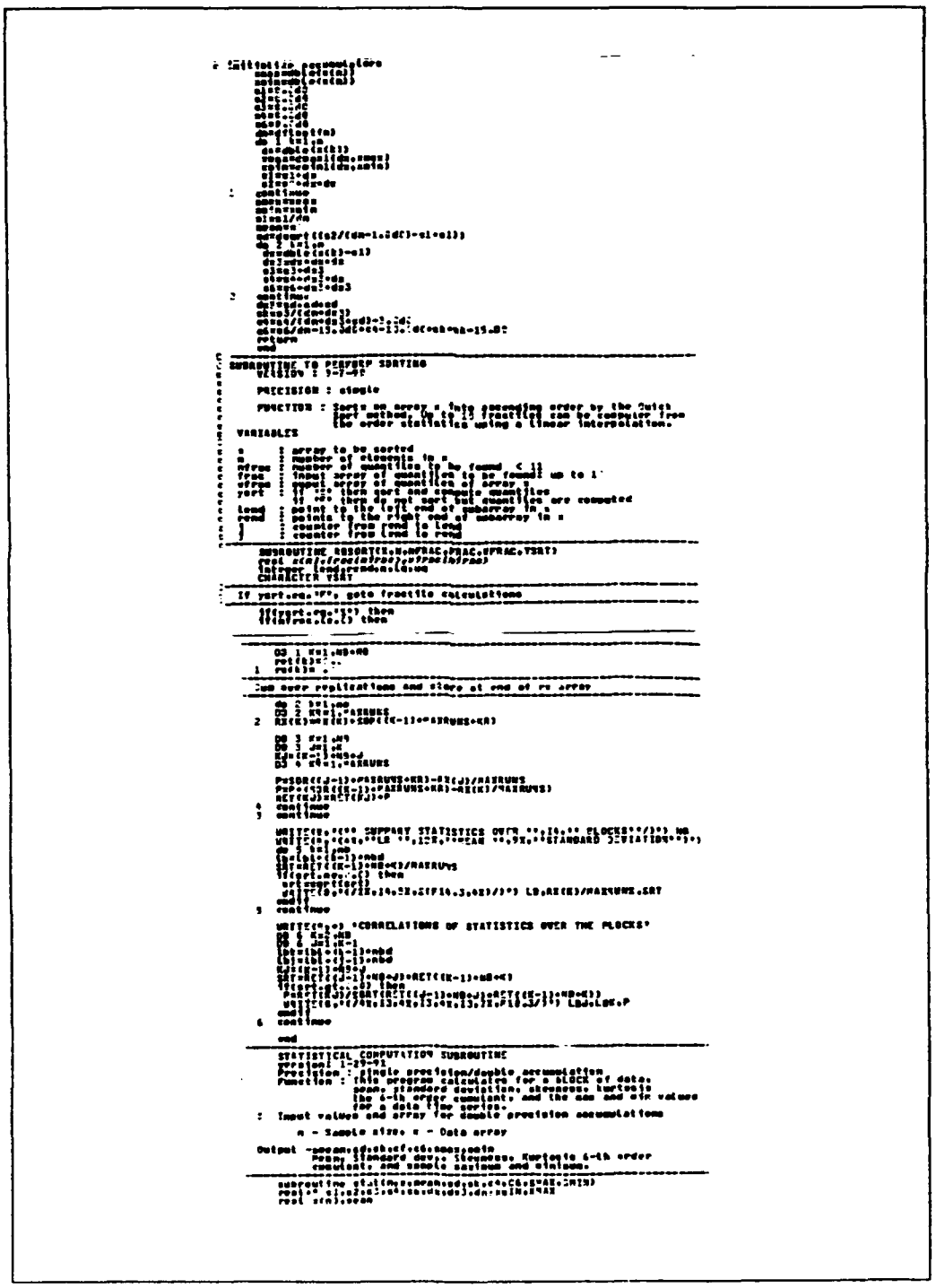

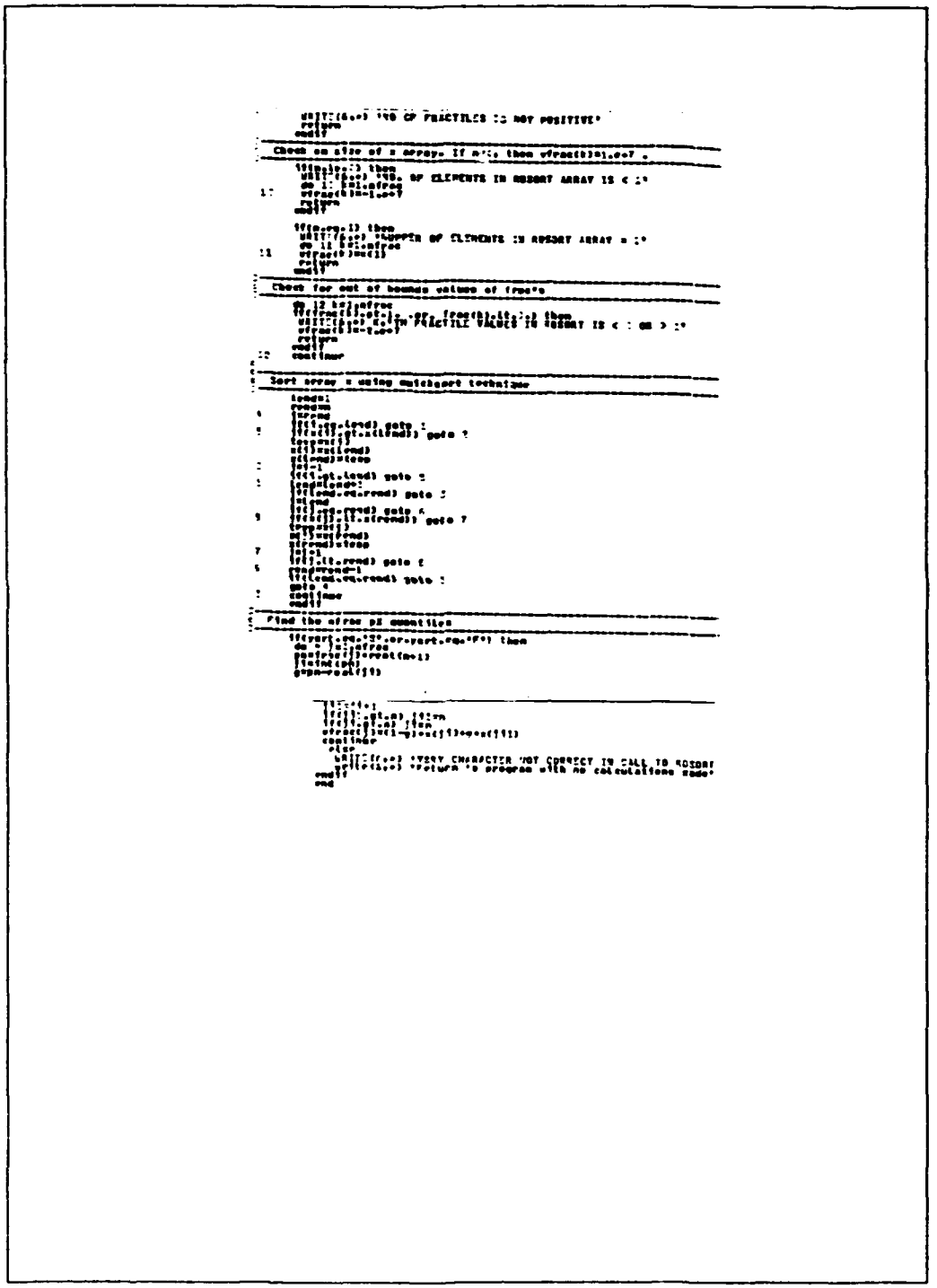

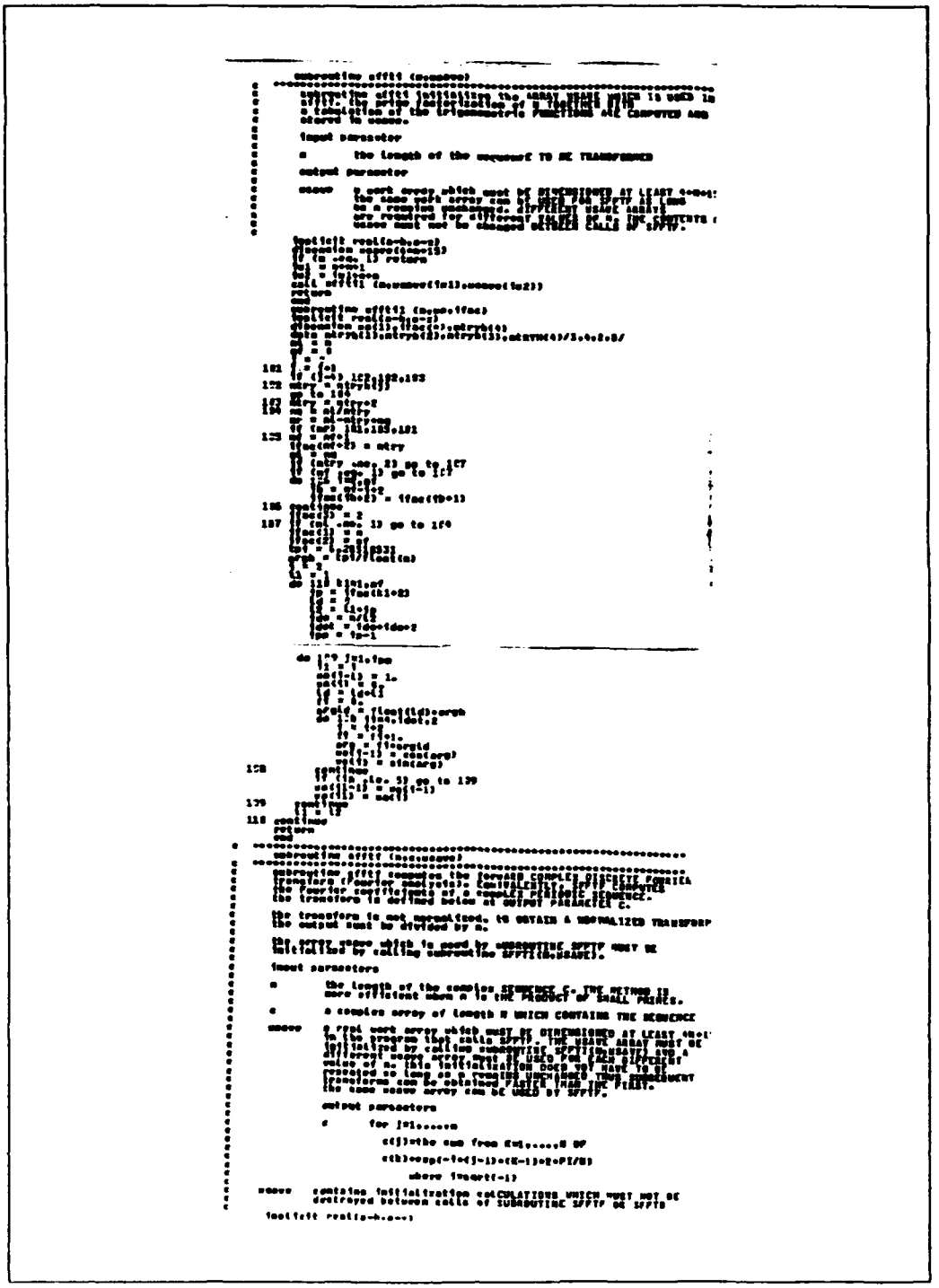

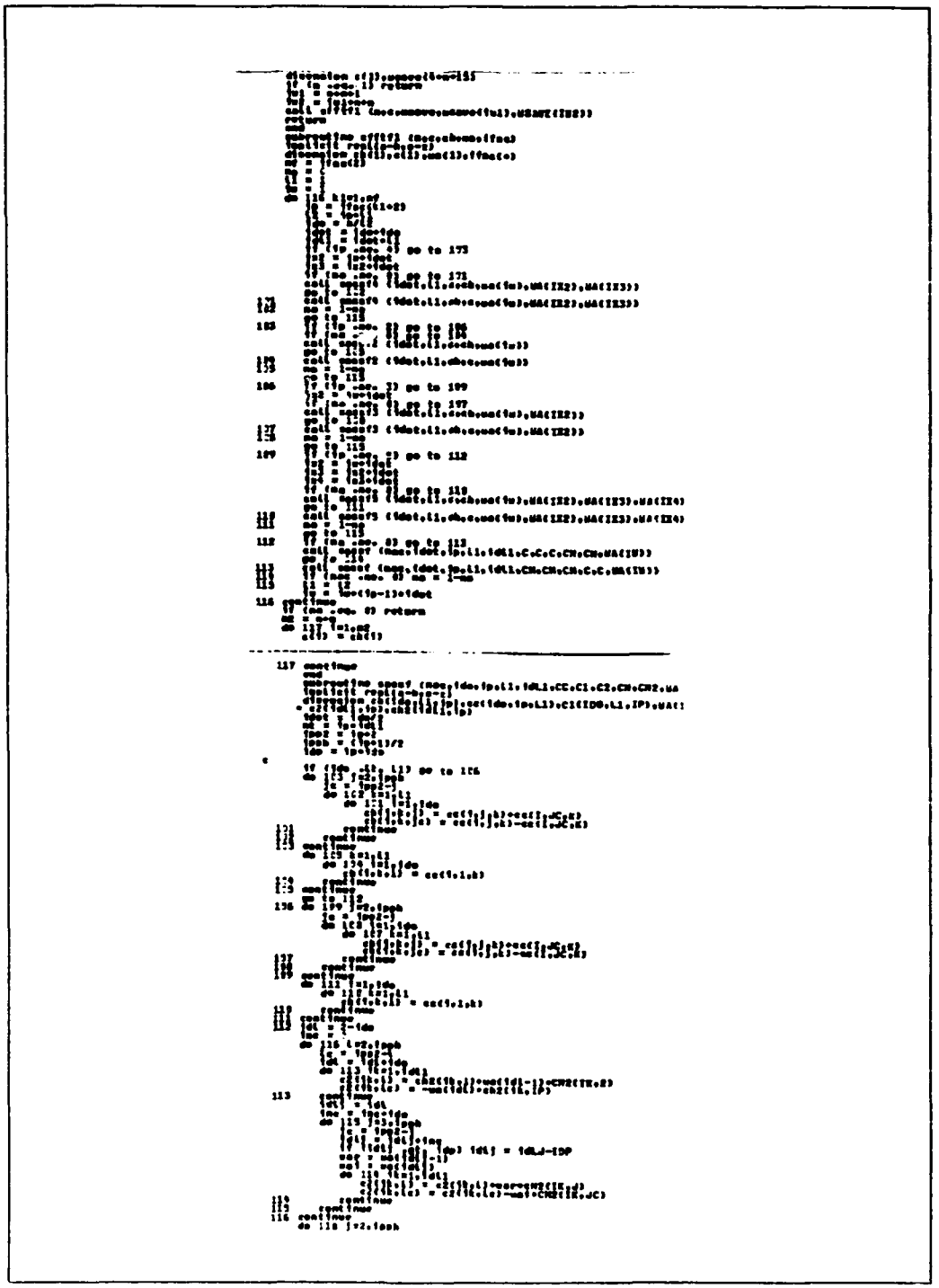

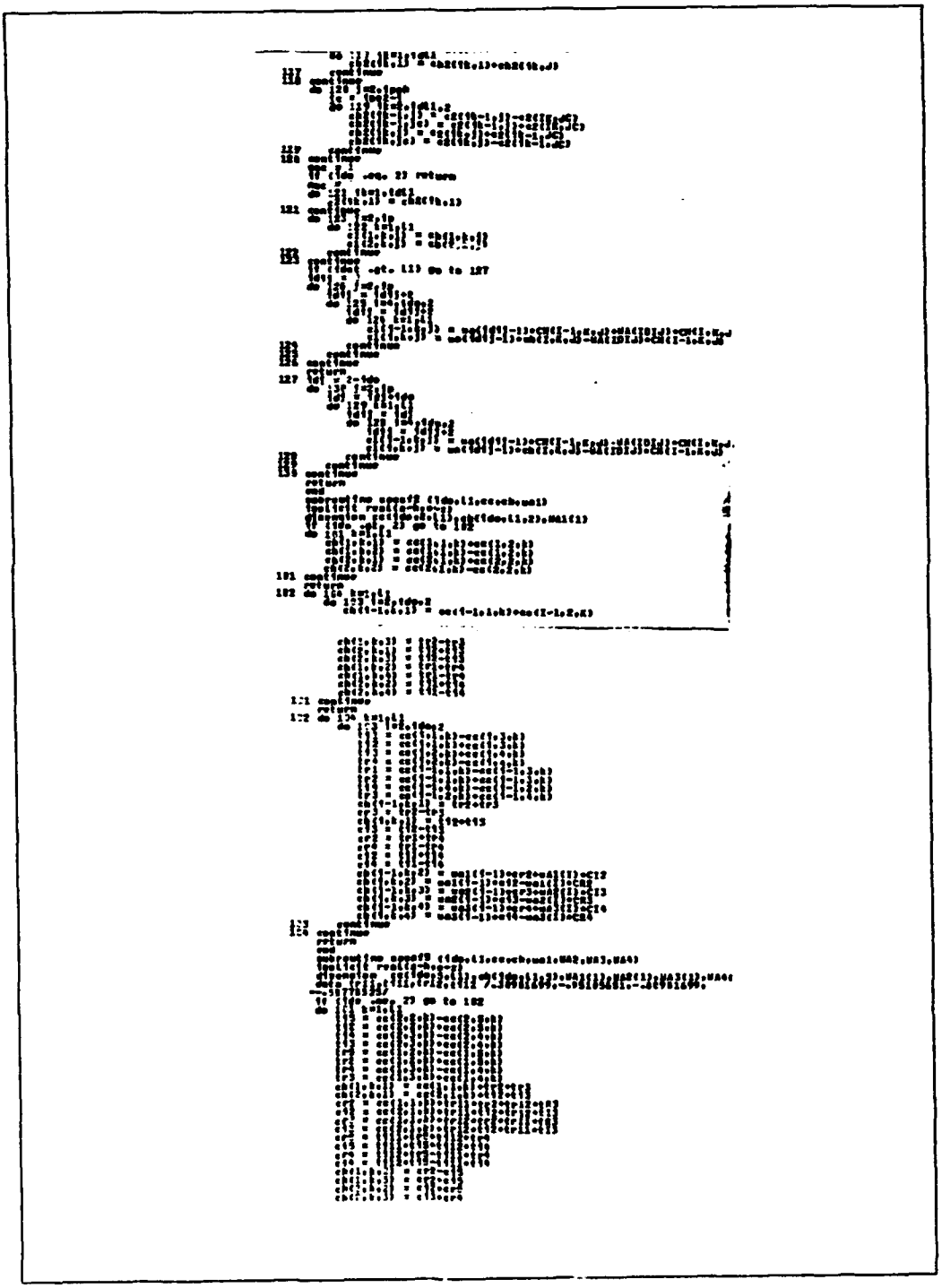

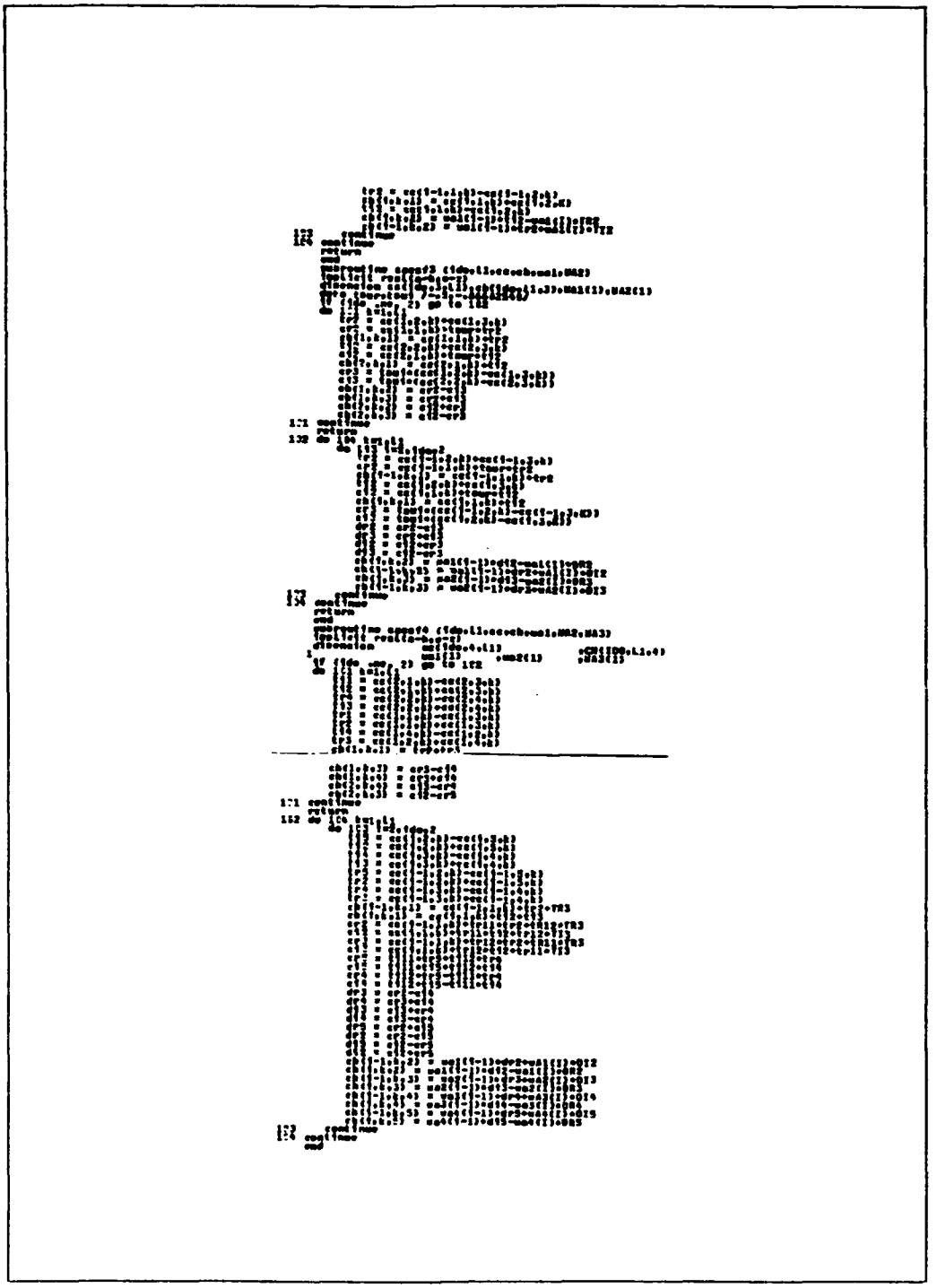

Appendix B

Harmonic Process Model Stationarity and Finite Memory

Harmonic Process Model (HPM) Stationarity and Finite Memory

When ϕ_n are independent uniformly distibruted random variables, V(t) is always stationary irrespective of A_n and ω_n values. There are two conditions for stationarity:

$$E[V_t] = 0 \text{ for all t} \qquad [B-1]$$

and

$$Cov(V_1, V_2) = Cov(\tau) = R_{xx}(\tau) \qquad [B-2]$$

where τ is the time shift or lag parameter.

B-1 is easily shown first and consider B-2 for the n = 1 case. The argument shown is easily extended to the general case. Because of the given information the expected value of V (t) is:

$$E[V(t)] = \frac{a}{2\pi}\int_{-\infty}^{\infty} \cos(\omega_c t + \phi)d\phi$$

$$= \frac{a}{2\pi}[\sin(\omega_c t) + \phi]\Big]_{-\pi}^{\pi} = 0 \quad \text{for all t}$$

Now for the second condition for stationarity.

$$
\begin{aligned}
Cov(V_1, V_2) &= E\{V(t)\}\{V(t+\tau)\} \quad \tau = 0, \pm 1, \pm 2, \ldots \\
&= \frac{a}{2}\pi\int_{-\infty}^{\infty} \cos(\omega_c t + \phi)d\phi \, \frac{a}{2}\pi\int_{-\infty}^{\infty} \cos\{\omega_c(t+\tau) + \phi\}d\phi \\
&= \frac{a^2}{4\pi}\int_{-\infty}^{\infty} \cos(\omega t + \phi)\cos(\omega(t+\tau) + \phi)d\phi \\
&= \frac{a^2}{4\pi}\int_{-\infty}^{\infty} [\cos\{(2\omega t + \omega\tau) + 2\phi\} + \cos\omega\tau]d\phi \\
&= \frac{a^2}{4\pi}\int_{-\infty}^{\infty} (\cos\omega\tau)d\phi = \frac{a^2}{4\pi}\phi\cos\omega\tau\Big]_{-\infty}^{\infty} \\
&= \frac{a^2}{4\pi}[\pi\cos\omega\tau - (-\pi)\cos\omega\tau] \\
&= \frac{a^2}{4\pi}(2\pi\cos\omega\tau) = \frac{a^2}{2}\cos(\omega\tau).
\end{aligned}
$$

For the general case :

$$
R(\tau) = \sum_{n=0}^{\infty} \frac{a_n^2}{2}\cos\omega_n\tau
$$

Thus, the autocorrelation function $\rho(\tau)$:

$$
\begin{aligned}
\frac{R(\tau)}{R(0)} &= \frac{\sum_{n=0}^{\infty} a_n^2\cos\omega_n\tau}{\sum_{n=0}^{\infty} a_n^2\cos\omega_n(0)} \\
&= \sum_{n=0}^{\infty}\cos\omega_n\tau
\end{aligned}
$$

So, both the autocorrelation and autocovariance functions of a harmonic process consist of a sum of cosine terms and thus never die out. This is in contrast to MA and AR processes and so the finite dependence assumption, or finite memory, is not applicable for HPM. Stationarity is applicable no matter what choice is made of the amplitude and frequency terms.

Appendix C

Power Spectrum Broadening

Cosine-Wave Carrier Signal Spectrum Broadening

Signals generated from rotating machinery not yet performing a particular machining process produce a *pure* harmonic tone due to its periodic driving force mechanism: $\cos 2\pi f_c t = \cos \omega_c t$. However, once machining is performed, the generated signal is:

$$V_{ampm}(t) = k[1 + m_a f(t)] \cos(\omega_c t + \phi_c + m_p g(t)) + n(t)$$

Notation described in the report text is repeated in this appendix but is condensed for ease of presentation. In the text, $V_{ampm}(t)$ is the amplitude and phase modulated cosine-wave carrier signal, m_a is the amplitude modulation index, $f(t)$ is the amplitude modulating signal, ϕ_c is the carrier signal phase, m_p is the phase modulation index, and $g(t)$ is the phase modulating signal. Now, $f(t) = \cos \omega_a t$ and $g(t) = \cos \omega_p t$ with f_a and f_p are the frequency of the amplitude and phase modulating wave, respectively. Briefer notation for this appendix is the following:

$$V_{ampm}(t) = k[1 + m(t)] \cos(\omega_c t + \phi(t) + \theta)$$

where random amplitude and phase modulations are represented by $m(t)$ and $\phi(t)$ respectively, and θ is the random carrier phase variable that is independent of both the random amplitude and phase modulation variables and has the same uniform pdf. If $m(t)$ and $\phi(t)$ are zero mean, stationary, and statistically independent random variables, the power spectral density of $V_{ampm}(t)$ is now derived.

First, the autocovariance ($R_V = [V(t)V(t')]$) is computed:

$$R_V = E[(1+m)(1+m')]\,E[\cos(\rho+\phi+\theta)\cos(\rho'+\phi'+\theta)] \quad [C-1]$$

where $m' \equiv m(t')$, $\phi' \equiv \phi(t')$, $\rho = \omega_c t$, and $\rho' = \omega_c t'$. Also the shortened notation of $CC \equiv E[\cos(\rho+\phi+\theta)\cos(\rho'+\phi'+\theta)]$ will be utilized. The first ensemble average of C-1 is

$$E[(1+m)(1+m')] = 1 + R_m(\tau), \quad [C-2]$$

where $\tau = t' - t$, $R_m \equiv E[m(t)m(t')]$, and the ensemble averages of m and m' vanish because m is a zero-mean random variable. The second ensemble average of C-1 is more work to calculate. Derivation uses the trigonometric identity for cos (a + b) and the fact that ϕ and θ are statistically independent:

$$\begin{aligned} CC &= E[\cos(\rho+\phi)\cos(\rho'+\phi')]E[\cos^2\theta] + E[\sin(\rho+\phi)\sin(\rho'+\phi')]\,E[\sin^2\theta] \\ &\quad - \{[\sin(\rho+\phi)\cos(\rho'+\phi')] + [\cos(\rho+\phi)\sin(\rho'+\phi')]\}E[\sin\theta\cos\theta] \\ &= \frac{1}{2}E[\cos(\rho-\rho'+\phi-\phi')] \\ &= \frac{1}{2}\cos(\rho-\rho')E[\cos(\phi-\phi')] - \frac{1}{2}\sin(\rho-\rho')E[\sin(\phi-\phi')]. \end{aligned} \quad [C-3]$$

Because $|\phi|$ is very small in comparison with unity, Taylor series expansions of $\sin(\phi-\phi')$ and $\cos(\phi-\phi')$ are used to give:

$$\begin{aligned} CC \simeq \frac{1}{2}\cos(\rho-\rho')\left[1 - \frac{1}{2}E[(\phi-\phi')^2] + \cdots\right] \\ + \frac{1}{12}\sin(\rho-\rho')\left[E[(\phi-\phi')^3] + \cdots\right]. \end{aligned} \quad [C-4]$$

Ignoring terms of third-order and higher, and substitution for ρ and ρ' C-4 is then:

$$CC = \frac{1}{2}\cos(\omega_c\tau)\,[1 - R_\phi(0) + R_\phi(\tau)\,]. \qquad [C-5]$$

Finally, substitution of C-4 and C-2 into C-1 yields:

$$\begin{aligned} R_s(\tau) &\simeq \frac{1}{2}\,[1 + R_m(\tau)][1 - R_\phi(0) + R_\phi(\tau)]\cos\omega_c\tau \\ &\simeq \frac{1}{2}\,[1 - R_\phi(0) + R_m(\tau) + R_\phi(\tau)]\cos\omega_c\tau, \end{aligned} \qquad [C-6]$$

where terms proportional to R_mR_ϕ are ignored due to their higher order in the smaller quantities m and ϕ.

The power spectral density is obtained by using C-6 in the standard definition of the power spectrum as shown:

$$P(f) = \int_{-\infty}^{\infty} R(\tau)e^{(-i2\pi f\tau)}d\tau.$$

The result is:

$$
\begin{aligned}
P(f) = {} & \frac{1}{4}(1-\sigma_\phi^2)\int_{-\infty}^{\infty} e^{-i\,2\,\pi(f-f_c)\tau}\,d\tau \\
& + \frac{1}{4}(1-\sigma_\phi^2)\int_{-\infty}^{\infty} e^{-i\,2\,\pi(f+f_c)\tau}\,d\tau \\
& + \frac{1}{4}\int_{-\infty}^{\infty} R_m(\tau)e^{-i\,2\,\pi(f-f_c)\tau}\,d\tau \\
& + \frac{1}{4}\int_{-\infty}^{\infty} R_m(\tau)e^{-i\,2\,\pi(f+f_c)\tau}\,d\tau \\
& + \frac{1}{4}\int_{-\infty}^{\infty} R_\phi(\tau)e^{-i\,2\,\pi(f-f_c)\tau}\,d\tau \\
& + \frac{1}{4}\int_{-\infty}^{\infty} R_\phi(\tau)e^{-i\,2\,\pi(f+f_c)\tau}\,d\tau
\end{aligned}
\qquad [C-7]
$$

Using the definitions of Dirac delta functions and the power spectrum C-7 becomes:

$$
\begin{aligned}
P(f) = {} & \frac{1}{4}(1-\sigma_\phi^2)[\delta(f-f_c)+\delta(f+f_c)] + \\
& \frac{1}{4}[P_m(f-f_c)+P_m(f+f_c)+P_\phi(f-f_c)+P_\phi(f+f_c)],
\end{aligned}
\qquad [C-8]
$$

where $\sigma_\phi^2 \equiv R_\phi(0)$. From C-8 it is seen how the discrete spectral lines are broadened by both amplitude, P_m, and phase modulations, P_ϕ.

_____. "Computation and Interpretation of Kth Order Spectra." In *Spectral Analysis of Time Series*, edited by B. Harris. New York: John Wiley, 1967b.

Brockett, P. L., Hinich, M. J. and Patterson, D. "Bispectral-Based Tests for the Detection of Gaussianity and Linearity in Time Series." *Journal of the American Statistical Association*, Vol 83, No. 403 (1988), 657-664.

Brockett, P. L., Hinich, M. J. and Wilson, G. R. "Nonlinear and Non-Gaussian Ocean Noise." *Journal of the Acoustical Society of America*, 82 (1987), 1386-1399.

Cramer, H. "On Some Classes of Nonstationary Stochastic Processes." . *Proceedings of the Fourth Berkeley Symposium on Statistics and Applied Probability*, II (1960), 57-78.

Dan, L. and Mathew, J. "Tool Wear and Failure Monitoring Techniques for Turning - A Review." *International Journal of Machine Tools and Manufacture*, 30 (4) (1990), 179-189.

Darlow, M. S. and Badgley, R. H. "Applications for Early Detection of Rolling-Element Bearing Failures Using the High-Frequency Resonance Technique." *ASME,*, 75-DET-46.

Drago, R. J. "Incipient Failure Detection." *Power Transmission Design*, February (1979), 40.

Dyer, D. and Stewart, R. M. "Detection of Rolling Element Bearing Damage by Statistical Vibration Analysis." *Trans. ASME, J. Mech. Design*, 100 (2) (1978), 229-235.

Elbestawi, M., Marks, J. and Papazafiriou, A. "Process Monitoring in Milling by Pattern Recognition." *Mechanical Systems and Signal Processing*, 3 (3) (1989), 305-315.

Fukunaga, K. and Ando, S. "The Optimum Nonlinear Features For a Scatter Criterion in Discriminant Analysis." *IEEE Transactions on Information Theory*, IT-23 (1977), 453-459.

Gardner, W. A. and Franks, L.E. "Characterization of Cyclostationary Random Signal Processes." *IEEE Trans. Inform. Theory*, IT-21 (1) (1975), 4-14.

Gardner, W. A. *Introduction to Random Processes with Applications to Signals and Systems*, New York: McGraw Hill, 1989.

Georgel, B. *Proceedings of International Signal Processing Workshop on Higher-Order Statistics*, Chamrousse, France, July, 1991.

Gersch, W. "Two Applications of Parametric Times Series Modelling Methods." In *Mechanical Signature Analyis*, edited by S. Braun. London: Academic Press, 1986.

Gladyshev, E. G. "Periodically Correlated Random Sequences." *Sov. Math.*, 2 (1961), 385-388.

Hand, D. J. *Discrimination and Classification.* New York: John Wiley, 1981.

Hasselman, K., Munk, W. and Macdonald G. "Bispectra of Ocean Waves." In *Time Series Analysis*, edited by M. Rosenblatt. New York: John Wiley, 1963.

Helland, K., Lii, K. and Rosenblatt, M. "Bispectra and Energy Transfer in Grid-Generated Turbulence." In *Developments in Statistics (Vol 2)*, edited by P. Krishnaiah. New York: Academic Press, 1979.

Hills, M. "Allocation Rules and their Error Rates." *J. Roy. Stat. Soc.*, B28 (1966), 1.

Hinich, M. J. "Testing for Gaussianity and Linearity of a Stationary Time Series." *Journal of Time Series Analysis*, 3 (1982), 169-176.

Hinich, M. J. "Detecting a Transient Signal by Bispectral Analysis." *Technical Paper ARL-TP-88-99*, Applied Research Laboratories of the University of Texas, Austin, TX, 1989.

Hinich, M. J. and Clay, C. S. "The Application of the Discrete Fourie r Transform in the Estimation of Power Spectra, Coherence and Bispectra of Geophysical Data." *Review of Geophysics*, 6 (1968), 347-363.

Hinich, M. J. and Wolinsky, M. A. "A Test for Aliasing Using Bispectral Analysis." *Journal of the American Statistical Association*, Vol. 83, No. 402 (1988), 499-502.

Hinich, M. J. and Patterson, D. M. "Evidence of Nonlinearity in the Trade-by-Trade Stock Market Return Generating Process." *Economic Complexity, Chaos, Sunspots, Bubbles, and Nonlinearity*, edited by Barnett, Gewcke, and Shell, New York: Cambridge University Press, 1989.

Hurd, H. L. "An Investigation of Periodically Correlated Stochastic Processes." *Ph.D. Thesis*, Duke University, Durham, NC, 1969.

_____. "Nonparametric Time Series Analysis for Periodically Correlated Processes." *IEEE Trans. Inform. Theory*, 35 (2) (1989), 350-359.

_____. "Represenation of Stongly Harmonizable Periodically Correlated Processes and Their Covariances." *Journal of Mulitvariate Analysis*, 29 (1989), 53-67.

Jain, A. K. and Dubes, R. "Feature Definition in Pattern Recognition With Small Sample Size," *Pattern Recognition*, 10 (1978), 85-97.

Jetly, S. "Measuring Cutting Tool Wear On-Line: Some Practical Considerations." *Manufacturing Engineering*, July (1984), 55-60.

Kendall, M. G. and Stuart, A. *The Advanced Theory of Statistics.* London: Griffin, 1958.

Kendall, M. G. and Stuart, A. and Ord, J. K. *The Advanced Theory of Statistics.* Vol. 3, 4th Edition, New York: MacMillan, 1983.

Kim, Y. and Powers, E. J. "Digital Bispectral Analysis of Self-Excite d Fluctuation Spectra." *The Physics of Fluids*, 21 (1978), 1452-1453.

Kittler, J. "Feature Set Search Algorithms." In *Pattern Recognition and Signal Processing*, edited by C. Chen, The Netherlands: Sijthoff and Noordhoff.

Kullback, S. *Information Theory and Statistics.* New York: Wiley, 1959.

Lachenbruch, P. A. *Discriminant Analysis.* New York: Hafner Press, 1975.

Leonev, V. P. and Shiryaev, A. N. "On a Method of Calculation of Semi-Invariants." *Theory of Prob. Appl.*, Vol. 4, No. 3 (1959), 319-329.

Liddell, D. "Multivariate Respons in More Than One Sample." *The Statistician*, 26 (1977), 1-15.

Lii, K., Rosenblatt, M. and Van Atta C. "Bispectral Measurements in Turbulence." *Journal of Fluid Mechanics*, 77 (1976), 45-62.

Liu, T. I. and Wu, S. M. "On-Line Detection of Drill Wear." *ASME Journal of Engineering for Industry*, 112 (1990), 299-302.

Micheletti, G. F., Koenig, W. and Victor, H. R. "In Process Tool Wear Sensors for Cutting Operations." *Annals of the CIRP*, 25 (2) (1976), 483-496.

Milner, G. M. "Feasibility of Vibration Monitoring of Small Rotating Machines for the Environmental Control and Life Support Systems (ECLSS) of the NASA Advance Space Craft." *Proceedings of the 41st Meeting of Mechanical Failures Prevention Group*, edited by T. Shives and L. Mertaugh, New York: Cambridge University Press, 1988.

_____. *Personal interview.* TRACOR Applied Sciences site visit, Austin, Texas, 1990.

Nikias, C. L. and Raghuveer, M. R. "Bispectrum Estimation: A Digital Signal Processing Framework." *Proceedings of the IEEE*, Vol. 75, No. 7 (1987), 869-891.

Nikias, C. L. and Mendel, J. M. "Workshop on Higher-Order Spectral Analysis." *IEEE Societies: Control Systems, Geoscience and Remote Sensing, Acoustics, and Speech and Signal Processing.* Vail, CO., 1989.

Nolte, L. W. "Adaptive Optimum Detection: Synchronous-Recurrent Transients." *The Journal of the Acoustical Society of America*, 44 (1) (1968), 224-239.

Ogura, H. "Spectral Representation of Periodic Nonstationary Random Processes." *IEEE Trans. Inform. Theory*, IT-17 (1971), 143-149.

Owsley, N. L. and Quazi, A. H. "Performance of Selected Transient Signal Detectors." *U.S. Navy Journal of Underwater Acoustics*, 20 (3) (1970), 589-599.

Paul, L. F. "An Adaptive Signal Classification Procedure-Application to Aircraft Engine Condition Monitoring." *Pattern Recognition*,9 (1977), 121-130.

Priestley, M. *Spectral Analysis and Time Series*, New York: Academic Press, 1981.

Ramirez, C. N. "On-Line Drill Condition Monitoring By Measurement of Drill Spindle Vibration and Dynamics." *Ph.D. Thesis*, The University of Texas at Austin, May 1991.

Randall, R. B. "A New Method of Modelling Gear Faults." *Trans. ASME J. Mech. Design*, 102 (2) (1982), 259-267.

Rangwala, S. and Dornfeld, D. "Sensor Integration Using Neural Networks for Intelligent Tool Condition Monitoring." *ASME Journal of Engineering for Industry*, 112 (1990), 219-228.

Rao, C. R. "Inference on Discrimination Function Coefficients." In *Essays in Probability and Statistics*, edited by R. Bose et al., Chapel Hill, The University of North Carolina Press, 1970, 587-602.

Rosenblatt, M."Remarks on Some Nonparametric Estimates of a Density Function." *Ann. Math. Stat.*, 27 (1956), 832-835.

_____. "Cumulants and Cumulant Spectra." In *Handbook of Statistics (Vol 3)*, edited by D. Brillinger and P. Krishnaiah. Amsterdam: North-Holland, 1983.

Rosenblatt, M. and Van Ness, J. W. "Estimation of the Bispectrum." *Annals of Mathematic Statistics*, 36 (1965), 1120-1136.

Sato, T., Sasaki, K. and Nakamura Y. "Real-Time Bispectral Analysis of Gear Noise and Its Application to Contactless Diagnosis." *Journal of Acoustical Society of America*, 62 (1977), 382-387.

Shaman, P. "Large-Sample Approximations to the First and Second-Order Moments of Bispectral Estimates." New York University, 1965.

Shiryaev, A. N. "Some Problems in the Spectral Theory of Higher-order Moments." *I. Theor. Prob. Appl.*, 5 (1960), 265-284.

Shives, T. R. and Mertaugh, L. J. (editors) *Detection, Diagnosis and Prognosis of Rotating Machinery to Improve Reliability, Maintainability, and Readiness through the Application of New and Innovative Techniques*, Cambridge: Cambridge Univeristy Press, 1986.

Shumway, R. H. "Discriminant Analysis for Time Series." In *Hdbk of Statistics (Vol. 2) Classification, Pattern Recognition, and Reduction of Dimensionality* edited by Krishnaiah and Kanal, Amsterdam: North-Holland, 1982.

Smith, C. M. "A description of the Hardware and Software of the Power Spectral Density Recognition (PSDREC) Continuous On-Line Reactor Surveillance System." *ORNL/TM-8862/VI*, October, 1983.

Subba Rao, T. and Gabr, M. "A Test for Linearity of Stationary Time Series." *Journal of Time Series Analysis*, 1 (1980), 145-158.

Tatsuoka, M. M. *Multivariate Analysis: Techniques for Educational and Psychological Research*, New York: John Wiley, 1971.

Van Atta, C. "Inertial Range Bispectra in Turbulence." *The Physics of Fluids*, 22 (1979), 1440-1442.

Van Ness, J. W. "On The Effects of Dimension in Discriminant Analysis For Unequal Covariance Populations." *Technometrics*, 21 (1979), 119-127.

Van Ness, J. W. and Simpson, C. "On the Effects of Dimension in Discriminant Analysis." *Technometrics*, 18 (1976), 175-187.

Wiener, N. and Masani, P. "The Prediction Theory of Multivariate Stochastic Processes." *Acta Mat.*, 98 (1957), 111-150.

Wilks, S. S. *Mathematical Statistics*. London: Wiley, 1963.

Wold, H. *A Study in the Analysis of Stationary Time Series*, Stockholm: Almqvist & Wiksell, 1954.

Wu, S. M. "Dynamic Data System: A New Modeling Approach.", *ASME Journal of Engineering for Industry*, August (1977), 709.

Yao, Y., Fang, D., and Arndt, G. "Comprehensive Tool Wear Estimation in Finish-Machining via Multivariate Time-Series Analysis of 3-D Cutting Forces." *Annals of the CIRP*, 39 (1) (1990), 57-60.